Effectively Applying Maritime Fuel Cell Systems Operating on Alternative Fuels

MSc Thesis Report

Daan Berk

Delft University of Technology

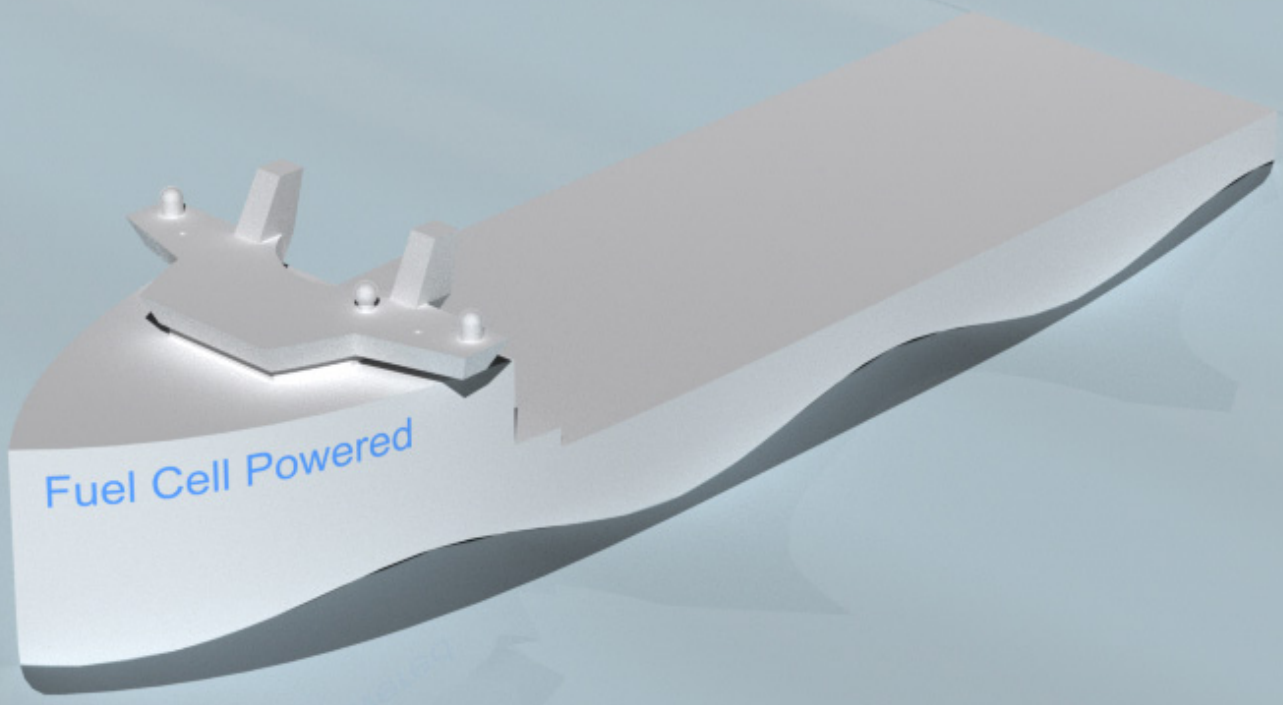

TU Delft

C-JOB
DEDICATED NAVAL ARCHITECTS

Effectively Applying Maritime Fuel Cell Systems Operating on Alternative Fuels

by

Daan Berk

Performed at

C-Job Naval Architects

to obtain the degree of Master of Science in the specialization of Marine Engineering
at the Delft University of Technology,
to be defended publicly on Tuesday May 28, 2024 at 15:00.

Thesis number:	MT.23/24.26.M	
Student number:	4922077	
Project duration:	September 4, 2023 – May 28, 2024	
Thesis committee:	Dr. Ir. L. van Biert,	TU Delft, supervisor & chairman
	Dr. Ir. P. de Vos,	TU Delft, committee member
	B. Grenko MSc,	TU Delft, supervisor
	Ir. N. de Vries,	C-Job Naval Architects, supervisor

An electronic version of this thesis is available at `http://repository.tudelft.nl/`.

TU Delft

C-JOB DEDICATED NAVAL ARCHITECTS

Preface

This report was written to finish my MSc thesis. Over the past years at the TU Delft, I have learned much about ships and the maritime industry. As my studies progressed, my desire to contribute to solving the problems of climate change and air pollution increased. My interest in fuel cells and alternative fuels brought me to this topic.

I had the wonderful opportunity to perform my research in collaboration with C-Job Naval Architects. This opportunity was given to me by Niels de Vries, who is also a committee member for the thesis. Niels, thank you for your time and efforts in helping me to improve my thesis. I would like to thank everyone at C-Job for providing me with support during my thesis. Furthermore, I would like to thank Joël van Duijn and Peter Lankreijer for the help and advice they have given me.

In addition to the previously mentioned people, I am also grateful for the help from Lindert van Biert, my TU Delft supervisor. Lindert, thank you for your help and guidance during courses in the master's and during my thesis. Also, I received a lot of support from Bojan Grenko. Bojan, thank you very much for all your advice and for motivating me during my thesis. Our coffee moments are very much appreciated!

Furthermore, I would like to thank my friends, both at the TU Delft and elsewhere, for their support during my thesis. In particular, I would like to thank Stijn Vervoordeldonk for reading my thesis and providing me with valuable comments on my work. Lastly, I would like to thank my parents and my brother for always believing in me and supporting me.

Daan Berk
Delft, May 2024

Summary

The primary objective of this thesis is to compare the application of various alternative fuels in combination with fuel cells in maritime environments, aiming to reduce harmful emissions in marine transportation. These emissions are partly caused by the chemical composition of maritime fuels and partly by combustion processes in internal combustion engines and fuel cells. The application of fuel cells and alternative fuels has the potential to mitigate these emissions.

Other research has considered the application of alternative fuels and fuel cells onboard ships, but the difference between using these various fuels in combination with fuel cells has not yet been researched in great detail. This study compares various alternative fuels in combination with fuel cells onboard ships by performing a case study where fuel cells and alternative fuels are integrated onboard an offshore vessel.

This thesis includes a review of existing literature on fuel cells, fuel processing, fuel storage technology, and maritime applications to select the most suitable technology for implementation onboard ships.

First, the most suitable fuel cell type for maritime applications is selected based on efficiency, durability, and operational requirements. Proton exchange membrane fuel cells (PEMFCs) and solid oxide fuel cells (SOFCs) are considered suitable fuel cell types for maritime applications; low-temperature PEMFCs are the most suitable of these two.

Next, techniques for fuel conversion and purification, such as methanol reforming, ammonia decomposition, and carbon monoxide removal, are analyzed. These processes consume mass and volume onboard the vessel, reduce the power system's efficiency, and reduce the transient response capabilities of maritime fuel cell systems.

After this, liquid hydrogen, ammonia, and methanol are investigated as alternative fuels in this report. The physical properties of these fuels result in different storage conditions for each fuel. In addition, the health and safety aspects result in additional rules and regulations for storing and using these fuels onboard ships.

To perform the case study, the vessel's operational profile is used to calculate the required power and energy for the vessel to conduct its operations. Next, the required power for auxiliary components to support the power and energy storage systems is calculated. Using these power and energy requirements and the losses occurring in the systems, the components of the power and energy storage systems are sized.

The case study showed that liquid hydrogen storage in combination with PEMFCs consumes the least volume onboard ships for lower autonomies. For higher autonomies, ammonia or methanol-fueled PEMFC systems consume less volume. In all cases, the PEMFC-fuelled systems, in combination with alternative fuels, require more volume onboard the vessel than internal combustion engine-based systems operating on marine diesel oil. The trends for mass and volume requirements by the power and energy storage systems are expected to remain similar for other vessels.

Besides the differences in mass and volume between the designed systems operating on alternative fuels, this thesis concludes that integrating fuel cell technology in maritime vessels is theoretically possible. However, it also points out the need for further research, development, and practical experience regarding the installation and operation of fuel cell systems and alternative fuel storage onboard ships. In addition, it is important to consider energy losses caused by auxiliary power consumers.

This thesis compared maritime fuel cell systems operating on alternative fuels from a technical perspective. For purposes where costs are also an important indicator when comparing various fuels, it is recommended that further research into the economic feasibility of installing and operating fuel cell systems and alternative fuels onboard ships is performed.

Contents

List of Figures

List of Tables

Nomenclature

The abbreviations and variables used in this report are listed below.

Greek variables

η	Efficiency	%
γ	Heat capacity ratio	-
ζ	System resistance	-

Chemical Definitions

CH_3OH	Methanol
CH_4	Methane
CO_2	Carbon Dioxide
CO	Carbon Monoxide
C	Carbon
e^-	Electron
H^+	Proton
H_2O	Water
H_2S	Hydrogen Sulfide
H_2	Hydrogen (molecule)
LH_2	Liquid hydrogen
N_2	Nitrogen (molecule)
NH_3	Ammonia
NOx	Nitrogen Oxides
O_2	Oxygen (molecule)
SOx	Sulfur Oxides
S	Sulfur

Abbreviations

AC	Alternating Current
AD	Ammonia Decomposition
AFC	Alkaline Fuel Cell
BoP	Balance of Plant
BP	Bipolar Plate
CCS	Carbon Capture and Storage

COGR	Cathode Off-Gas Recirculation	
DC	Direct Current	
DMFC	Direct Methanol Fuel Cell	
EMS	Electrochemical Membrane Separation	
GDL	Gas Diffusion Layer	
GT	Gas Turbine	
ICE	Internal Combustion Engine	
LNG	Liquefied Natural Gas	
MCFC	Molten Carbonate Fuel Cell	
MD	Methanol Decomposition	
MEA	Membrane Electrode Assembly	
MS	Membrane Separation	
PAFC	Phosphoric Acid Fuel Cell	
PEMFC	Proton Exchange Membrane Fuel Cell	
PM	Particle Matter	
PrOx	Preferential Oxidation	
PSA	Pressure Swing Adsorption	
SCR	Selective Catalytic Reduction	
SMET	Selective Methanation	
SMR	Steam Methanol Reforming	
SOFC	Solid Oxide Fuel Cell	
TCS	Tank Connection Space	
TEG	Thermoelectric Generator	
TRL	Technological Readyness Level	
TSA	Temperature Swing Adsorption	
UHC	Unburnt Hydrocarbons	
WGS	Water Gas Shift	

Prefixes

e	Electric	
HT	High Temperature	
LT	Low Temperature	

Roman variables

ΔH^0_{298K}	Enthalpy Change of Reaction at 298 K	kJ/mol
a	Process air flow factor	-

c_p	Specific heat capacity at constant pressure	$kJ/(kg \cdot K)$
g	Gravitational acceleration	m/s^2
H	Enthalpy	J
h	Specific enthalpy	J/kg
LHV	Lower heating value	J/kg
M	Molar mass	g/mol
m	Mass	kg
P	Power	W
p	Pressure	Pa
PR	Pressure ratio	-
Q	Heat	J
T	Temperature	K
V	Volume	m^3
v	Velocity	m/s
W	Work	J
X_{O2}	Oxygen mass fraction of outside air	-
z	Relative height	m

1 Introduction

Over the past centuries, ships have polluted the atmosphere. This air pollution has contributed to climate change, and it has contributed to health damage to humans and animals [1, 2]. The exhaust gases from ships (used to) contain harmful emissions such as carbon dioxide (CO_2), carbon monoxide (CO), nitrous oxides (NOx), sulfur oxides (SOx), particle matter (PM) and unburnt hydrocarbons (UHC).

Internal combustion engines (ICEs) and gas turbines (GTs) are most commonly used to power ships. Efforts have been made to reduce the harmful emissions caused by ICEs and GTs. More strict regulations regarding the sulfur contents of marine fuels are expected to mitigate sulfur emissions. In addition, scrubbers and selective catalytic reduction (SCR) can be used to remove SOx, PM, and NOx from exhaust gas streams [3, 4]. Also, carbon capture and storage (CCS) can be used to reduce CO_2 emissions [5]. However, these scrubbers, SCR systems, and CCS systems require additional mass and volume onboard the vessel, consume energy, and lead to an increase in propulsion system costs. Moreover, not all harmful emissions can be eliminated using these systems [6].

In addition to these efforts, alternative fuels onboard ships have been researched. These studies have considered various fuels that can be produced renewably and that mitigate local emissions when these fuels are used onboard ships. Liquid hydrogen (LH_2), ammonia (NH_3), and methanol (CH_3OH) are seen as possibly viable options for use as alternative fuels onboard ships.

An alternative to the use of ICEs and GTs is the use of FCs onboard ships. FCs convert chemical energy to electrical energy via an electrochemical reaction instead of ICEs and GTs, which convert chemical energy to mechanical energy using combustion. Due to the difference in the energy conversion process, FCs produce little to no NOx, PM, and UHC emissions. FCs are currently not widely used in maritime applications, and many aspects regarding the installation of FC systems onboard ships remain to be researched [7]. Other research has considered the application of alternative fuels and fuel cells onboard ships, but the difference between using these various fuels in combination with fuel cells has not yet been researched in great detail. Therefore, it is currently unknown how FC systems operating on different alternative fuels compare to each other when the mass and volume requirements of the fuel processing systems and fuel storage systems are also considered at a ship integration detail level. Therefore, this thesis will analyze and compare the listed options on a baseline vessel in combination with proton exchange membrane fuel cells (PEMFCs):

- Liquid hydrogen storage
- Ammonia storage with cracker
- Methanol storage with reformer

To do so, the thesis will answer the following main question:

How can maritime fuel cell systems be applied effectively using liquid hydrogen, ammonia, and methanol and how do these compare to each other?

To solve this primary research question, the questions listed below will be answered:

1. What is the most suitable type of fuel cell for maritime applications?

2. What are the properties of ammonia crackers, methanol reformers, and other required fuel processing systems for proton exchange membrane fuel cells in maritime applications?
3. What are the properties of liquid hydrogen, ammonia, and methanol storage systems onboard ships?
4. Are there vessel designs or research projects that use liquid hydrogen, ammonia, or methanol as fuel in combination with fuel cells? If so, what are their specifications or findings?
5. From a technical viewpoint, how do maritime PEMFC-based power systems compare when fueled by liquid hydrogen, ammonia, or methanol?

To answer the main question, a case study where fuel cell and alternative fuel storage integration on an offshore vessel will be performed. The aim of the case study is to integrate the fuel cell and energy storage systems in an effective manner, meaning the ship can still execute its operations. To determine suitable technology for this case study and to determine design guidelines, the report will be structured as follows:

Question 1 will narrow down the research into one type of fuel cell that is suitable for application onboard ships. The selection of the fuel cell type and the reasoning behind it will be discussed in chapter 2.

After the fuel cell type is determined, question 2 will help to determine which fuel processing systems are required for the chosen fuel cell type in combination with liquid hydrogen, ammonia, or methanol. In this question, the term 'properties' relates to the physical properties of such systems. In addition, the dynamic operation of these systems is an important aspect, and it is also considered part of their properties. All these aspects will be listed in chapter 3.

Next, question 3 considers the storage conditions of alternative fuels. The term 'properties' covers the masses and volumes, safety aspects, and practical aspects regarding the storage and use of these fuels onboard ships. These properties will be discussed in chapter 4.

Once the fuel cell, fuel processing, and fuel storage technologies have been considered, relevant research projects and ship designs that integrate these technologies will be researched before starting the case study. This relates to question 4; Answering this question will obtain any relevant specifications or findings of relevant ship designs and research projects on alternative fuels. Chapter 5 will elaborate on ships in operation and under construction, vessel designs, and research projects that are relevant to this thesis.

Before starting the case study, the relevant assumptions and boundary conditions will be listed in chapter 6. Selecting the same boundary conditions for all systems on alternative fuels will help with making a fair comparison between these systems. Based on the choice of fuel cell type, required fuel processing steps, and fuel storage options, a selection of systems and technologies for implementation in the case study will be made. In addition, the vessel that is selected for the case study will be defined.

With the set boundary conditions, the case study is performed. This is done by first using the vessel's operational profile to calculate the required power and energy for the vessel to conduct its operations. Next, the required power for auxiliary components to support the power and energy storage systems is calculated. Using these power and energy requirements and the losses occurring in the systems, the components of the power and energy storage systems are sized. Further explanation of these steps and the results of the case study are given in chapter 7.

After these parts, a discussion about the results and methodology of the thesis will be made in chapter 8.

Lastly, a conclusion on the thesis will be drawn, and the main question will be answered in chapter 9. On the basis of this, recommendations for further research will be made.

2

Fuel Cells

In this chapter, the first research question will be answered:

What is the most suitable type of fuel cell for maritime applications?

To answer the first question, the working principles of fuel cells will first be introduced in section 2.1. After this, in section 2.2, the fuel cell types that are regarded as not suitable for maritime applications will be introduced, and it will be explained why these are not suitable. Next, suitable fuel cell types for maritime applications will be introduced in section 2.3, and their relevant properties will be addressed. Fourth, the balance of plant (BoP) components required to let fuel cell systems function correctly are touched upon in section 2.4. Next, complementary battery systems for fuel cells are reviewed in section 2.5. In addition, an overview of the fuel cells discussed in this chapter will be given in section 2.6. Lastly, the most important findings of this chapter will be listed in section 2.7.

2.1. Fuel Cell Principles

Fuel cells are used to convert chemical energy into electrical energy. Fuel cells are based on a redox reaction, with an oxidation reaction occurring at the anode and a reduction reaction occurring at the cathode. The general principle of a fuel cell relies on two electrodes (the anode and the cathode) in contact with an electrolyte. The electrolyte is chemically separated into two compartments by a membrane, this membrane enables ionic conductivity. While the ions travel from one electrode to the other through the electrolyte and membrane, the negatively charged electrons travel through the load, providing electrical power. A schematic drawing is shown in figure 2.1.

The core part of a fuel cell is called the Membrane Electrode Assembly (MEA), it consists of the anode, cathode, membrane, catalyst layers, and gas diffusion layer [8]. The MEA is usually stacked between the bipolar plates (BPs). These BPs consist of flow channels to guide fuel and air to the fuel cell and to remove reaction products from the fuel cell. In addition to the purpose of distributing fuel, air, and reaction products, BPs help to remove heat from the cell, prevent the leakage of gas and coolants, and provide mechanical support for the cell [9]. The gas diffusion layer (GDL) performs various tasks in the fuel cell. This includes water transportation, gas transportation and distribution, and thermal and electrical conduction [10]. The GDL is in contact with the bipolar plates and catalyst layers, and it may consist of several layers to improve performance [11]. The thickness of the electrodes in the MEA is determined by balancing between a large reactive surface area and reducing the distance that ions and electrons have to travel [12]. A thicker electrode allows for a larger electrode surface area, but it increases ohmic resistance. Individual fuel cells offer relatively low cell potentials, to supply electrical power at higher potentials, fuel cells are connected in series. Physically, these cells are stacked together and electrically connected to form a fuel cell stack. Fuel cell stacks provide electrical power at higher potentials and are used for commercial applications.

Fuel cells require cooling to maintain a suitable operating temperature because the electrochemical reactions within fuel cells are exothermic. The heat from cooling fuel cells is often used for other purposes. This process is called 'waste heat recovery' (WHR), and it increases the efficiency of a fuel

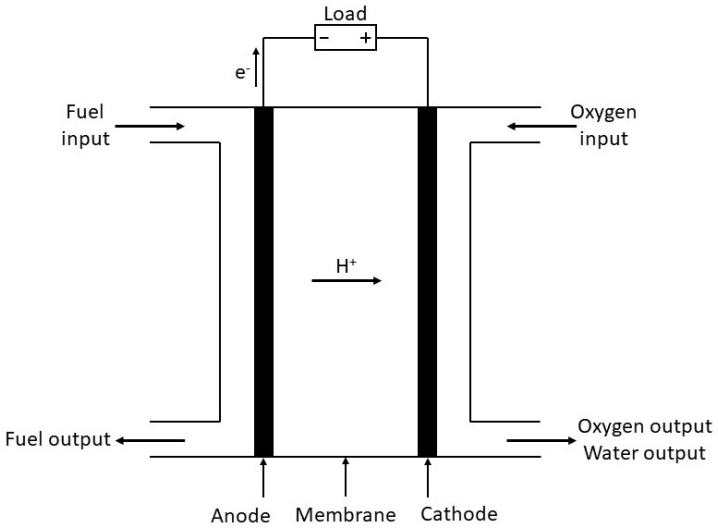

Figure 2.1: Schematic illustration of a fuel cell (example of PEMFC, PAFC & SOFC-H shown).

cell system. The waste heat from high-temperature fuel cells can be used directly for heat-demanding applications, or it can be used to generate steam to use in a steam turbine; this energy can then be used to generate electricity. For low-temperature fuel cells, the waste heat can either be used directly, or it can be converted into electrical energy using a thermoelectric generator (TEG) [13].

When fuel cells operate at high cell potentials and current densities, the fuel cells also operate at high power densities [14]. This is desirable when a high fuel cell power density is required. However, a tradeoff exists between maximizing a fuel cell's power density, efficiency, lifetime, and transient operation capabilities. For this reason, there is a limit to a fuel cell's desirable current density and voltage. Also, the theoretical maximum cell potential equals the equilibrium potential of water splitting, 1.23V. Fuel cells operate at lower cell potentials due to losses such as activation losses, internal current losses, resistive losses, and concentration losses [15]. An overview of the influence of FC losses of a polarization curve is shown in figure 2.2. Because high-temperature fuel cells produce water in vaporized form, their theoretical cell potentials are lower than those of fuel cells producing water in liquid form.

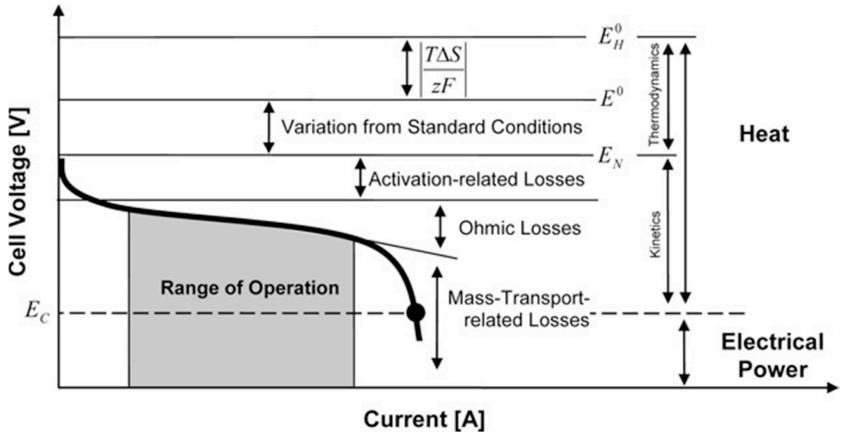

Figure 2.2: An overview of the effects of losses on a FC's polarization curve [16].

The fuel cells' electrodes are often made from porous materials. The porosity increases the surface area available for the chemical reactions in the fuel cell, thus increasing the fuel cell's current density. A disadvantage of these porous electrodes is that they can be blocked or flooded by fuel impurities or too large amounts of water, causing the current density of the cell to decrease. In chapter 3, more information about fuel purification processes to remove such impurities will be given.

At lower fuel cell temperatures, the electrochemical reactions within the cell occur at slower rates.

These slower reaction rates result in lower current densities. Therefore, highly effective catalysts are used to increase the reaction rates within the cell. At higher temperatures, the electrochemical reaction rates are larger. This reduces the need to use platinum catalysts [17].

As an individual fuel cell operates at small voltages, fuel cells for commercial use are combined into stacks. These stacks consist of series-connected fuel cells, which together provide a higher output voltage. These stacks are connected in parallel to form larger a larger FC system. The division of the FC system into separate stacks allows for a high level of redundancy since the performance of the individual stacks has limited influence on the others.

The composition of the fuel, the electrolyte, and the type of ions that travel through the membrane vary with each fuel cell type that exists. The most common fuel cell types are the alkaline fuel cell (AFC), direct methanol fuel cell (DMFC), phosphoric acid fuel cell (PAFC), molten carbonate fuel cell (MCFC), proton exchange membrane fuel cell (PEMFC) and the solid oxide fuel cell (SOFC). An overview of these fuel cell types with their oxidation- and reduction half-reactions and operating temperatures is shown in table 2.1.

Table 2.1: Different fuel cell types with their half-reactions and operating temperatures [17, 18].

FC type	Oxidation half reaction	Reduction half reaction	Operating temperature
DMFC	$CH_3OH + H_2O \rightarrow CO_2 + 6\,H^+ + 6\,e^-$	$\frac{3}{2}\,O_2 + 6\,H^+ + 6\,e^- \rightarrow 3\,H_2O$	+/- 75 °C
LT-PEMFC	$2\,H_2 \rightarrow 4\,H^+ + 4\,e^-$	$O_2 + 4\,H^+ + 4\,e^- \rightarrow 2\,H_2O$	+/- 75 °C
AFC	$2\,H_2 + 4\,OH^- \rightarrow 4\,H_2O + 4\,e^-$	$O_2 + 2\,H_2O + 4\,e^- \rightarrow 4\,OH^-$	+/- 90 °C
HT-PEMFC	$2\,H_2 \rightarrow 4\,H^+ + 4\,e^-$	$O_2 + 4\,H^+ + 4\,e^- \rightarrow 2\,H_2O$	+/- 160 °C
PAFC	$2\,H_2 \rightarrow 4\,H^+ + 4\,e^-$	$O_2 + 4\,H^+ + 4\,e^- \rightarrow 2\,H_2O$	+/- 180 °C
MCFC	$H_2 + {CO_3}^{2-} \rightarrow H_2O + CO_2 + 2\,e^-$	$\frac{1}{2}\,O_2 + CO_2 + 2\,e^- \rightarrow {CO_3}^{2-}$	+/- 650 °C
SOFC-O	$2\,H_2 + 2\,O^{2-} \rightarrow 2\,H_2O + 4\,e^-$	$O_2 + 4\,e^- \rightarrow 2\,O^{2-}$	500 - 1000 °C
SOFC-H	$2\,H_2 \rightarrow 4\,H^+ + 4\,e^-$	$O_2 + 4\,H^+ + 4\,e^- \rightarrow 2\,H_2O$	500 - 1000 °C

The suitability of fuel cell systems for maritime applications varies per fuel cell type. The following subsections will explain the main advantages and disadvantages per fuel cell type and mention if these fuel cell types are suitable for maritime applications.

2.2. Non-Maritime Fuel Cells

This section will provide an overview of the fuel cell types that are available which are not deemed suitable for maritime applications at this time. For each fuel cell type, the deemed lack of suitability for maritime applications will be explained.

2.2.1. Direct Methanol Fuel Cell

The DMFC uses methanol as fuel input, thus eliminating the need for an external fuel reformer. The methanol from the fuel is converted to hydrogen via reformation at the anode of the fuel cell. The typical operating temperatures of DMFCs lie in the range of 50-130 °C [19]. At these temperatures, the electrochemical reactions are relatively slow, causing a need for effective catalyst materials. The fuel cell requires water at the anode and produces water at the cathode. This makes water management relatively complex and reduces the fuel cell system's efficiency [19]. The main disadvantage of DMFCs is methanol crossover, where methanol can pass the membrane to the cathode side. At this side of the cell, the methanol can react with oxygen and form CO. This can poison the catalyst and limit the fuel cell's life [20], making the fuel cell less suitable for maritime applications. To mitigate this problem, the methanol concentration in the FC is lowered, reducing the FC's power output and furder reducing its efficiency. This lower efficiency is another drawback of DMFCs; Xing et al. [21] state this low efficiency currently limits the DMFC's applicability for maritime power systems.

2.2.2. Alkaline Fuel Cell

The application of AFCs originates from space applications. Temperatures in the fuel cell range from 90 °C for terrestrial applications to 260 °C for space applications [20]. The type of electrode and

the materials used in the catalyst layer vary with the operating temperature of the fuel cell [22]. An advantage of AFCs is that they can use non-noble catalyst materials, making them less expensive than fuel cells with noble catalyst materials [23]. Alkaline fuel cells offer good efficiencies. However, they suffer from drawbacks that limit their current application. For example, Tronstad et al. [24] stated that AFCs require pure oxygen to operate and that AFCs are prone to CO_2 poisoning. The requirement for air purification systems for AFCs makes AFCs less suitable for maritime applications.

2.2.3. Phosphoric Acid Fuel Cell

Phosphoric acid fuel cells are mainly used for stationary power applications. The phosphoric acid fuel cell inherited the name from the acid used in the electrolyte, which is stable up to temperatures of 200 °C. This makes the fuel cell less prone to CO poisoning than PEMFCs, and it facilitates water management within the cell [19]. The waste heat from the cell can be used in a WHR system to increase the system efficiency, and it may also be used to supply heat for fuel processing reactions such as reforming. According to Breeze, [19] efficiencies of the fuel cell itself range from 36% to 42 %, whilst this efficiency can reach 87% in combination with waste heat recovery. A drawback of PAFCs is their low volumetric and gravimetric power density; therefore, Elkafas et al. [25] stated that PAFCs are less suitable for maritime applications.

2.2.4. Molten Carbonate Fuel Cell

The molten carbonate fuel cell uses a mixture of alkali metal carbonates for the electrolyte. Because of the high operating temperature of the MCFC, WHR can be applied effectively. Another advantage of the fuel cell is that it is insensitive to CO poisoning. Instead, CO and water can be used inside the fuel cell to generate a shift reaction to produce more hydrogen [26]. The cell's theoretical efficiency is 60%, whilst this can increase to 80% in combination with WHR.

Not all sources agree on the potential of MCFCs for maritime applications, Fu et al. [27] mention MCFCs have potential in maritime applications because they can be used in combination with WHR and because the water management within the fuel cell is easier compared to low-temperature fuel cells. Xing et al. [21] state MCFCs state that MCFCs are commercially available but that they struggle with low power densities, high costs, and limited lifetime. Elkafas et al. [25] agree that MCFCs are less suitable for maritime applications because of their low power density. In addition, Joon [28] mentions the management of CO_2 in the fuel cell poses difficulties for the operation of MCFCs. For these reasons, MCFCs are considered as not suitable for maritime applications in this report.

2.3. Maritime Fuel Cells

This section will elaborate more extensively on the fuel cells considered suitable for maritime applications at this time. This will be done by first elaborating on PEMFCs in section 2.3.1. After this, SOFCs will be further explained in section 2.3.2.

2.3.1. Proton Exchange Membrane Fuel Cell

Proton exchange membrane fuel cells are the most common fuel cell type today. PEMFCs have theoretical cell potentials of up to 1.2 V but operate at practical cell voltages of approximately 0.7 V [29, 30]. They are available as low-temperature (LT) and high-temperature (HT) versions. LT-PEMFCs are currently the most mature but suffer from some drawbacks that HT-PEM developers are attempting to resolve. An example of a drawback occurring in LT-PEMFCs is the water management in the fuel cell. The fuel cell's membrane needs to be wetted at the anode side to prevent it from becoming dried out. At the cathode side, water is formed and needs to be removed from the cell to prevent it from flooding the porous layers and thus preventing gas transport. Water management within the cell can be mitigated by correctly designing the MEA and humidifying the incoming hydrogen gas stream [31]. The GDL also facilitates water management, as it is usually wet-proofed to prevent the pores in the GDL from becoming clogged with water [32].

Authayanun et al. [33] mention several advantages of HT-PEMFCs: Firstly, the higher operating temperature of HT-PEMFCs reduces CO poisoning of the Pt catalyst in the fuel cell. This is a benefit if the fuel cell is operated on reformed gas since that gas often contains small concentrations of CO. Also, the higher temperature facilitates better water management within the fuel cell because water generated at the cathode evaporates at higher temperatures and thus avoids flooding problems within the pores of

the electrode. Moreover, the electrochemical reactions within the fuel cell occur at higher rates, resulting in higher current densities. Lastly, the higher temperature of the fuel cell broadens the application of the waste heat recovered from the fuel cell. HT-PEMFCs also have several drawbacks [18]. First, HT-PEMFCs require a higher platinum loading than LT-PEMFCs to increase their lifetime. Despite this higher platinum loading, HT-PEMFCs have lower lifetimes than LT-PEMFCs. HT-PEMFCs could work for up to 20000 hours in laboratory conditions, but their practical lifetime is limited to approximately 5000 hours. Also, the heat management of HT-PEMFCs is more complicated than that of LT-PEMFCs. In addition, HT-PEMFCs have lower efficiencies than LT-PEMFCs.

Inal and Deniz [34] stated that the costs of automotive PEM fuel cells can decrease to $45/kW by 2025 if 500 000 units are produced annually. This allows for PEM fuel cells to potentially reach a cost level comparable to diesel engines in the future. The future cost of PEMFCs heavily depends on the number of fuel cells produced, Kampker et al. [35] modeled fuel cell cost and provided an estimation of the fuel cell cost dependent on the production quantities. This estimation is shown in figure 2.3.

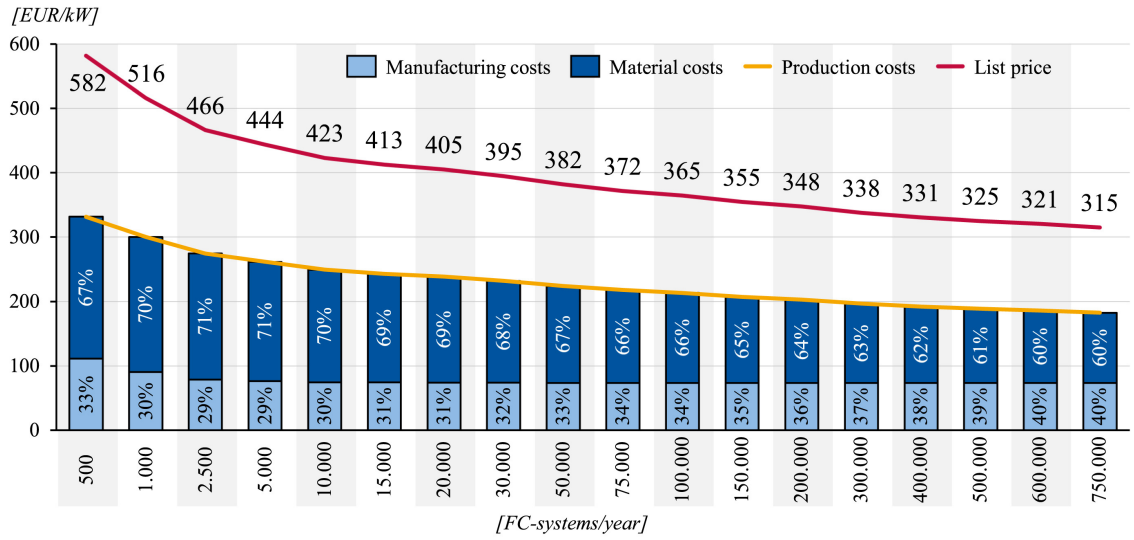

Figure 2.3: LT-PEMFC cost estimation depending on the annual production quantity [35].

HT-PEMFCs are more expensive than their LT counterparts. Wei et al. [36] state the production costs of HT-PEMFCs could lie within $1000-1700/kW (2013 prices) for production volumes between 50 000 and 100 units per year.

2.3.1.1. Fuel and Air Purity

PEM fuel cells are very prone to damage caused by impurities in the fuel and air inlets. CO, CO_2, S and NH_3 can be causes of poisoning of the catalyst layers within the fuel cell or blocking of the GDL or porous electrodes.

Patil et al. [37] stated that CO can form bonds with the Pt in the catalyst layers of the fuel cell; these bonds reduce the amount of active catalyst surface area, thus reducing the cell's current density. CO_2 particles at the anode side of the fuel cell can react with the Pt catalyst to produce CO particles, which can be harmful in the way mentioned earlier. Moradi Bilondi et al. [38] performed a numerical study on CO contamination effects on PEMFC performance. Their results were that even small traces of CO can lead to fuel cell degradation. A plot showing the effects of CO poisoning in a PEMFC is shown in figure 2.4. To mitigate this effect, Zamel and Lee [39] stated that the addition of oxygen in the fuel stream (oxygen bleeding) could significantly improve the performance of a PEMFC operating with CO impurities in the fuel.

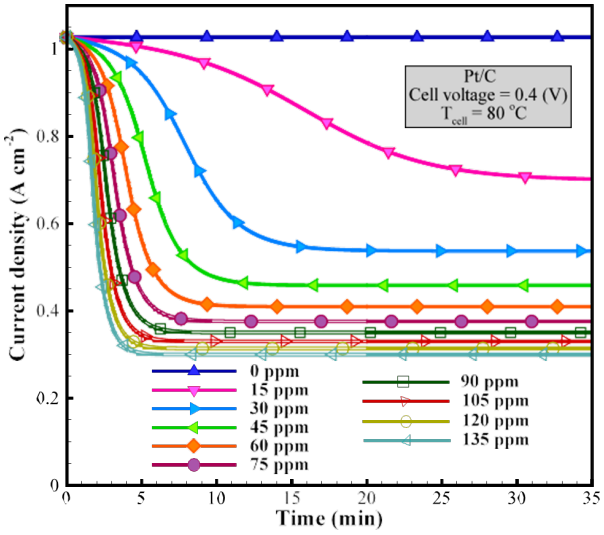

Figure 2.4: Effect of CO poisoning on PEMFC performance [38].

Another strong contaminant for PEMFCs is hydrogen sulfide (H_2S) [40]. H_2S can drastically reduce the fuel cell's performance when exposed to the anode or cathode. The effect is mainly caused by catalyst poisoning, which can occur at small ppm levels of H_2S. Because H_2S originates from fossil fuels, this contaminant does not pose a problem when the PEMFC is fuelled with renewable alternative fuels.

NH_3 impurities can also influence the fuel cell's performance. Isorna Llerena et al. [41] researched the effects of NH_3 impurities in HT- and LT-PEMFCs. They found NH_3 can either cause temporal performance decay of the fuel cell with long performance recovery times or damage it permanently. The former is the case for LT-PEMFCs, and the latter is for HT-PEMFCs. Figure 2.5 shows the effects of NH_3 impurities in the fuel supply of an LT-PEMFC and the fuel cell's recovery after the NH_3 supply is turned off.

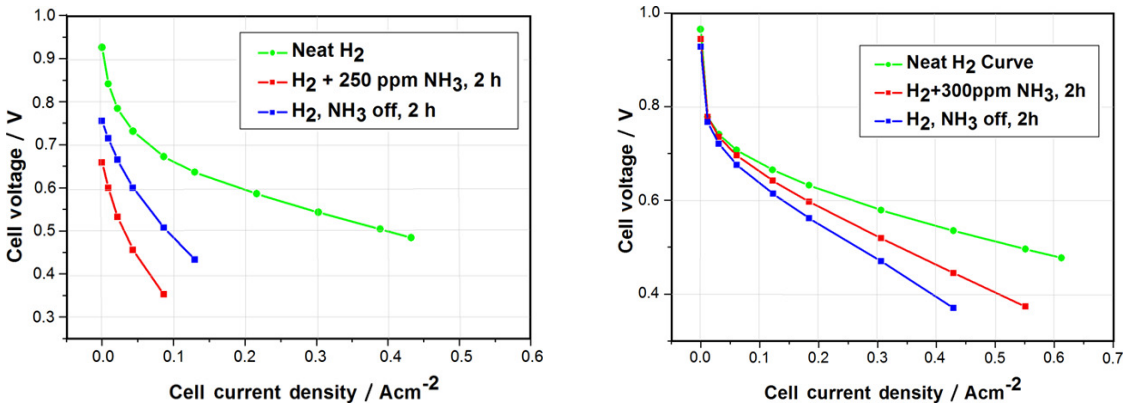

Figure 2.5: PEMFC performance example before, during and after exposure to NH_3 impurities in the fuel for LT-PEM (left) and HT-PEM (right) fuel cells [41].

2.3.1.2. Transients and Lifetime

PEMFC systems are not suitable for large load transients. Van Biert et al. [42] stated that PEMFCs can cope with large load transients within seconds but that their performance is often limited by the transient capabilities of external fuel processing systems if a different fuel than hydrogen is used. Also, they stated that PEMFCs might experience more degradation over time if they are exposed to load transients or peaks that the fuel cell is capable of handling. The dynamic response of PEMFCs is also studied by Huang et al. [43]. They showed that water management is critical for fuel cell performance under dynamic loading. The fuel cell can only cope with transients if the membrane is wetted sufficiently

at the anode side and if excess water is disposed of at the cathode side. The limited load transient capability also goes for HT-PEMFCs, Balsamo et al. [44] performed experiments on a 5 kW HT-PEMFC and showed the fuel cell could not respond adequately to load fluctuations. They therefore opted to use a battery pack to handle transients in the load power demand.

The dynamic operation of fuel cells has a significant influence on their lifetime. Zhang et al. [45] studied the influence of start-stop operating conditions on PEMFC degradation for automotive applications. The start-stop conditions caused damage in the catalyst layer of the fuel cell. Efforts to model the influence of transient operation of PEMFCs have been made. Vasilyev et al. [46] presented a modeling approach for the dynamic reliability assessment of PEMFC systems. They stated that dynamic models for PEMFC failure and degradation are still in the academic stage, and further research and development are required to produce models suitable for commercial applications. In addition, they state that failure of auxiliary components can lead to degradation or failure of PEMFCs themselves. It is thus required that the failure mechanisms of auxiliary components are also included when considering the degradation and failure of PEMFCs.

PEMFCs also experience degradation that is not primarily caused by transient operation or auxiliary components. Patil et al. [37] reviewed the degradation mechanisms in PEMFCs. They stated the fuel cell experiences chemical, mechanical, catalyst, and thermal degradation. First of all, chemical degradation is the effect where the polymer is chemically attacked by fluoride ions in the water produced by the fuel cell. Secondly, chemical degradation is caused by mechanical stresses caused by imperfections in the membranes, causing membrane fatigue. Examples of these imperfections include cracks, pinholes, tears, and punctures. These mechanical degradation effects are influenced by temperature and relative humidity. The degradation effects caused by humidity fluctuations are greater than those caused by temperature fluctuations. Next, the catalyst in a PEMFC degrades over time. This effect includes catalyst aging and the movement of particles in the catalyst. The result of this catalyst aging is a reduction of activity, slowing down the fuel cell's kinetics. Also, thermal degradation can occur if the fuel cell is operated at too high temperatures. These too-high temperatures can cause the membrane to collapse. Also, ice forming in cold start conditions can cause deterioration of the membrane and catalyst layers.

To mitigate the problem of fuel cell degradation, Xun et al. [47] stated fuel cell power could be downsized and stresses on fuel cells can be relieved if fuel cells are combined with a storage device such as a battery or a supercapacitor. Thounthong et al. [48] agree with the statement that fuel cell power can be downsized if batteries or supercapacitors are installed for coping with transients. In addition, they state the fuel cell can be operated at a more efficient power level if a battery or supercapacitor is used.

In conclusion, the lifetime of fuel cells is often considered poor (currently about 5000 hours for automotive applications [49]) compared to the current lifetime of internal combustion engines; this short lifetime needs to be considered when comparing the capital costs of a fuel cell system to a power system with a longer lifetime [50].

2.3.1.3. Commercially Available PEMFC Systems

Various manufacturers offer PEMFC systems, and some of their products are mentioned in this section.

First of all, Ballard [51] offers a fuel cell power pack for maritime applications. The fuel cell has an output power of 200 kW, a mass of 1000 kg, and a volume of 1.97 m^3. The fuel cell power pack includes the required BoP systems for the fuel cell to operate. The system needs hydrogen fuel according to ISO 14687:219 [52] type I (gaseous hydrogen) and grade D (quality sufficient for PEMFCs for road vehicles). The hydrogen purity must be 99.97% by mole fraction, and the maximum CO concentration is 0.2 ppm. The system produces unregulated direct current (DC) output. The peak fuel efficiency is 53.5%.

Next, PowerCell [53] offers a 200 kW LT-PEMFC system with a mass of 1070 kg and a volume of 1.45 m^3. The fuel efficiency is stated to be 54%. The fuel cell requires the same hydrogen input as Ballard's system according to ISO 14687:19. The required BoP components are included in the system. The system also produces unregulated DC electricity output. The fuel efficiency is similar to Ballard's system, at 54%.

Third, NedStack [54] offers a 600 kW containerized LT-PEMFC system, which includes the BoP components. The system has a mass of 15 t and is enclosed in a 20ft ISO-high cube container, giving it a volume of 42.88 m^3. This system uses its own air heating and purification system. It requires a pure hydrogen input of grade $\geq$ 2.5 (meaning a H_2 purity of 99.5% [55]) and a maximum CO concen-

tration of 0.2 ppm and it requires cooling water in- and output. The electrical power output is DC. The system's nominal hydrogen consumption is 59 kg/MWh of electrical energy, resulting in an efficiency of approximately 51%.

In addition, TECO [56] supplies a 325 kW PEMFC system, including BoP components. The unit has a volume of 2.33 m^3 and a mass of 1525 kg. Like the systems mentioned earlier, this system also operates on pure hydrogen. TECO also supplies the fuel cell systems in 10, 20, and 40 ft containerized form, supplying 1300 kW, 2600 kW, and 5200 kW of continuous power output, respectively. The fuel cell's efficiency, electric power output type, and required fuel specifications are not reported. The masses of the containerized solutions are also not reported.

Also, Corvus Energy [57] developed a 340 kW PEMFC for maritime applications. The system has a mass of 3100 kg and a volume of 2.33 m^3. All BoP components required for operation are included in the system, The system also requires hydrogen fuel input according to ISO 14687:2019, producing unregulated DC output. The system's efficiency is not reported.

Lastly, Zepp [58] produces a 150 kW fuel cell system with a 51% efficiency at maximum power and a 57.5% efficiency at 50% power. The system has a mass of 355 kg and a volume of 0.6 m^3. The system also includes BoP components.

The systems are thus generally available in smaller modules or larger containerized systems. From a ship stability perspective, it is desired that the fuel cell systems will be placed near the center of gravity. This is often below deck. At this location, it is difficult to install entire ISO containers. Therefore, the individual smaller-scale modules, are more likely to be installed than the NedStack and TECO containerized solutions.

All systems mentioned include BoP components required to let the fuel cells function correctly. Most fuel cell systems require hydrogen input according to ISO 14687:19 type I and grade D. As most systems produce unregulated DC output, additional power electronics are required to connect the system to a ship's alternating current (AC) or DC bus.

The average gravimetric and volumetric power densities of the fuel cell systems enclosed in modules are 192 w/kg and 136 W/l, respectively. An overview of the maritime PEMFC systems is given in table 2.2.

Table 2.2: Overview of commercially available PEMFC systems.

Brand	Model	Type	Power output kW	Volume m^3	Mass kg	Gravimetric power density W/kg	Volumetric power density W/l
Ballard	Fuel Cell System	Module	200	2.0	1000	200	102
Powercell	Marine System 200	Module	200	1.5	1070	187	138
TECO	FCM 400	Module	325	2.3	1500	213	139
Corvus Energy	Pelican FC System	Module	340	6.8	3100	110	50
Zepp	zepp.X150	Module	150	0.6	595	252	252
Nedstack	MT-FCPI-600	Container	600	42.9	15000	40	14
TECO	FCC 1600	Container	1300	19.0	n/a	n/a	68
TECO	FCC 3200	Container	2600	38.3	n/a	n/a	68
TECO	FCC 6400	Container	5200	77.0	n/a	n/a	68

2.3.2. Solid Oxide Fuel Cell

SOFCs operate at the highest temperatures of all fuel cell types considered in this report. SOFCs exist in types where oxygen anions are being conducted through the membrane (SOFC-O) and types where protons are being fed through the membrane (SOFC-H). Their membranes are made of ceramic materials, which become conductive to oxygen ions at higher temperatures [17]. These ceramic membranes are sensitive to temperature gradients in the time- and spatial domains. At large temperature gradi-

ents, cracks in the membrane can occur due to thermal stresses. These cracks lead to degradation or malfunctioning of the fuel cell and should thus be avoided.

As mentioned in section 2.1, fuel cells operating at higher temperatures offer lower theoretical cell potentials than LT fuel cells. However, the molecules in SOFCs have more kinetic energy than in LT fuel cells because of the higher temperature. This higher kinetic energy causes the molecules to split up more easily, thus reducing the activation energy barrier [59]. Therefore, the activation losses are smaller at higher temperatures. This results in a higher overall efficiency in SOFCs than in LT fuel cells. In addition, the waste heat from SOFCs can be used directly, or it can be converted into electrical energy. This results in a higher system efficiency. Van Veldhuizen et al. [60] researched cathode off-gas recirculation (COGR) and showed it increases the fuel cell's heat efficiency. For this method, the cathode off-gas is recirculated to the inlet side of the cathode to preheat the inlet air of the SOFC. Therefore, the amount of pre-heating required for air entering the fuel cell is reduced.

The technical maturity of SOFC systems is lower than that of PEMFC systems, especially in maritime applications. Van Veldhuizen et al. [61] studied the influence of ship motions on SOFCs and stated that ship motions have a considerable influence on the performance of an SOFC stack. Therefore, they recommend additional research on the influence of ship motions on maritime SOFC systems. However, they also state that ship motions and inclinations are not limiting factors for incorporating SOFCs in vessels because it is possible to adjust the location of the SOFC stacks in vessels to limit the accelerations on the stacks.

2.3.2.1. Fuel Acceptance

SOFCs can be operated on a wide range of fuels such as hydrogen, ammonia, and hydrocarbons [62]. An advantage of SOFCs is that they are not susceptible to CO and CO_2 poisoning, CO can even serve as a fuel for SOFCs [63]. As for other fuel cell types, SOFCs are susceptible to sulfur poisoning [62]. All fuels that could contain sulfur therefore need to be desulfurized before being used in SOFC systems. Vahc et al. [64] support this statement, adding that sulfur also influences the reforming reactions in SOFCs. They state sulfur in SOFCs influences the internal reforming reaction more than the electrochemical reaction.

Ammonia can be used in an SOFC without an external cracker. Jeerh et al. [65] reviewed direct ammonia SOFCs and stated the cracking process of ammonia can be executed inside SOFCs. In an SOFC-O, the ammonia is first cracked at the anode. After this, the hydrogen resulting from this cracking process is used to produce electricity. Because the nitrogen on the anode side of the SOFC-O can react with water resulting from the oxidation half-reaction, nitrous oxides (NOx) can be formed. Specific catalyst types can be used to limit the production of NOx. Another option to mitigate the formation of NOx is the use of SOFC-Hs instead of SOFC-Os. The formation of NOx in SOFC-Hs is prevented because water is formed at the cathode side instead of the anode side, preventing the nitrogen atoms from reacting with oxygen atoms resulting in NOx. Another difference between the SOFC-O and the SOFC-H is that the fuel is diluted with water in an SOFC-O at the anode side, whereas this does not occur in an SOFC-H. This results in higher power densities in SOFC-Hs compared to SOFC-Os.

Methanol can be directly reformed at the anode side of an SOFC. This is practical since it reduces the need to use an external reformer and because the operating temperature of SOFCs lies in the same range as the temperatures required for reforming reactions [66]. Reforming reactions are endothermic and therefore require heat input to occur. Peters et al. [66] state the endothermic reforming reaction can thus be used to cool the fuel cell. When such reactions occur within a SOFC, these reactions take place before the hydrogen oxidation reaction at the cathode. This means the reaction to cool the fuel cell (reforming) takes place before the reaction in which heat is produced (hydrogen oxidation). This can cause the temperatures at the locations where the reforming reactions take place to decrease locally. This is known as the formation of cold spots in the fuel cell. The formation of strong cold spots is undesirable because it creates temperature gradients in the fuel cell, causing a risk of thermal cracks in the porous membrane [67]. Some level of pre-reforming is therefore desirable for SOFC operation on hydrocarbons and alcohols, but most of the fuel can be reformed within the fuel cell [68]. In practice, a mixture of methanol and hydrogen is then used as fuel for the SOFC, where the hydrogen is directly oxidized at the anode, and the methanol is internally reformed before the resulting hydrogen is oxidized.

2.3.2.2. Transients and Lifetime

As mentioned earlier, SOFCs have a ceramic membrane for which large thermal gradients over time can cause thermal stresses and cracks in the membrane. Therefore, the fuel cell must be heated or

cooled down over a relatively long timeframe. This results in long start-up times for SOFCs, meaning that another storage device is required to cope with transients onboard a vessel's power grid that require start-up or shutdown of the fuel cell.

Multiple sources have evaluated the transient capabilities of SOFCs after start-up. Mueller et al. [69] state SOFCs can respond to load fluctuations quickly when they have reached operating conditions. These reactions can take place in the order of milliseconds. However, the transient capabilities of SOFCs are mainly influenced by the speed of the balance of plant components to keep the fuel cell within operating conditions. Azizi and Brouwer [70] support this statement by saying the transient capabilities of SOFCs are usually limited by the inflow of cathode input air and hydrogen. They also state control measures are required to prevent steep temperature gradients and electrical or mass transport fluctuations. In addition, Gemmen and Johnson [71] stated large load transients can cause the current in a fuel cell to reverse, which is unfavorable from a degradation perspective.

In conclusion, SOFCs can handle load transients once they are turned on. However, they can respond so fast that temperature gradients can occur and external components influence their transient capabilities. Therefore, mitigation measures to prevent damage to the fuel cell, which slow down the transient capabilities of the SOFC system, need to be taken. An external energy storage device (such as a battery) is required when an SOFC is operated on a fluctuating load.

2.3.2.3. Commercially Available SOFCs

SOFCs are currently in an earlier development stage, and fewer specifications about these systems for maritime applications can be found than with PEMFCs. Fuel cell energy [72] produces a 250 kW SOFC which can be operated on hydrogen and natural gas. The fuel cell is meant for stationary power applications and produces regulated AC power. The electrical efficiency based on the fuel is 62% for natural gas and 65% for hydrogen. The system has a volume of 78.7 m^3, giving it a volumetric energy density of 3 W/l. The system's mass is not reported.

Convion, [73] produces a 60 kW SOFC with a volume of 13.5 m^3. This yields a volumetric energy density of 4 W/l, while the system's mass is not reported. The SOFC system can run on natural gas or biogas and is designed for stationary purposes. The fuel cell produces regulated AC power output. The electrical efficiency is 60%, the total efficiency is 83% when WHR is used.

Next, Bloom Energy produces several SOFC systems for different applications. They produce a 75 kW natural gas-fuelled SOFC system for maritime applications called the 'Maritime Energy Server' [74]. The system produces regulated AC power output. It has a mass of 1837 kg, giving it a gravimetric energy density of 41 W/kg. The electrical efficiency is 55% to DC voltage, the total efficiency can be increased to 85% in combination with WHR. The dimensions and volume of the system are not reported. Bloom also produces a stationary SOFC system [75] with a power output of 330 kW, which can be fuelled bu natural gas, blended hydrogen, pure hydrogen, or biogas. This system has a volume of 29.8 m^3, giving it a volumetric energy density of 12 W/l. The mass is 17300 kg, yielding a gravimetric energy density of 19 W/kg. The system also produces regulated AC output power with an electrical efficiency of 65-53%.

SolydEra [76] produces several SOFCs, but they do not report specifications or applications. Alma [77] produces SOFCs for maritime applications. Their SOFCs are currently being installed on various vessels for testing and demonstration purposes. These fuel cells are operated on various fuels, such as liquid organic hydrogen carriers (LOHCs), ammonia, and LNG. System specifications are not yet reported.

An overview of the specifications of SOFC systems is listed in table 2.3.

Table 2.3: Overview of commercially available SOFC systems.

Brand	Model	Application	Power output kW	Volume m^3	Mass kg	Gravimetric power density W/kg	Volumetric power density W/l
Fuel Cell Energy	Solid Oxide Fuel Cell	Stationary	250	78.8	n.r.	n.r.	3
Convion	C60	Stationary	60	13.5	n.r.	n.r.	4
Bloom Energy	Maritime Server	Maritime	75	n.r.	1837	41	n.r.
Bloom Energy	Energy Server 5.5	Stationary	330	26.7	n.r.	n.r.	12

2.4. Balance of Plant Components

To allow for fuel cell operation under the desired conditions, a balance of plant (BoP) system is required. Examples of BoP components are [78, 79]:

- Air filters that filter the inlet air to remove salt and other undesired impurities that can result in the degradation of the fuel cell stack.
- Heaters that heat the inlet air to the desired operating temperature when ships are sailing in cold conditions. These heaters are also used to heat the fuel cell to operating temperatures during start-up.
- Humidifiers that humidify the process air to wet the membranes of the fuel cells.
- Heat exchangers to recover the waste heat from the fuel cell's cooling medium.
- Pumps to pump liquid fuels, cooling media and water.
- Blowers to direct air and gaseous fuel flows towards and away from the fuel cell.
- Compressors to supply gases at elevated pressures when desired.
- Pressure regulators to control the pressures of air, liquid and vapour flows and to prevent safety issues caused by large pressures.
- Control valves to control the air, liquid and vapour flows to and from the fuel cell to influence the fuel cell's operating parameters.

These BoP components all require power to function; this leads to a lower efficiency of the total fuel cell system compared to the efficiency of the individual fuel cell stacks. Also, these components require maintenance, and they are prone to performance degradation and malfunction. The output of these BoP components may be nonlinear over their operating range, and their ability to cope with transients may also vary. The BoP system thus influences the performance of the fuel cell system, and needs to be considered when designing a fuel cell system.

2.5. Battery Support Systems

Fuel cells have a longer lifetime, and fuel cell systems can respond better to transients when they are used in combination with batteries. Such battery support systems aid the fuel cell by discharging themselves when the load demand is high and charging themselves using fuel cell power when the load demand is low.

The size and power of the battery support system varies with the power system's specifications and the vessel's operating profile [80]. This thus needs to be calculated per vessel and autonomy. To extend the lifetime of the batteries, their depth of discharge (DoD) is often limited, decreasing the energy densities.

Several suppliers produce battery systems for maritime applications. As a guideline, C-Job [81] uses a gravimetric energy density of 0.13 MJ/kg (at 30% DoD) and a volumetric energy density of 0.09 GJ/m^3 (at 30%). The gravimetric- and volumetric power densities are 118.2 W/kg and 86.3 W/l, respectively. The investment costs of batteries are assumed to be around 600-700 €/kWh.

2.6. Comparison

A summary of the fuel cell systems mentioned in this chapter with their costs, efficiencies, and TRLs is shown in table 2.4. Regarding costs, LT-PEMFCs have the lowest costs, which are expected to decrease in the future. HT-PEMFCs and SOFCs are currently more expensive than LT-PEMFCs, but their costs are also expected to decrease in the future. The TRLs shown in the table are based on the suitability of each fuel cell type for maritime applications as discussed in section 2.2 and 2.3. The FC types labelled with a '-' are deemed not feasible for maritime applications. The FCs with a '+/-' are considered feasible for maritime applications, but suffer from drawbacks that result in those fuel cell types having a lower TRL than LT-PEMFCs. The LT-PEMFC is listed with a '+' and is considered as having the highest TRL for maritime applications. In this table, it can be seen that the LT-PEMFC has the highest TRL, followed by the HT-PEMFC and the SOFC. The other fuel cell types have the lowest TRL compared to the LT-PEMFC, HT-PEMFC, and SOFC.

Table 2.4: Overview of fuel cell costs, efficiencies, and technological readiness level (TRL) for installation onboard ships.

Fuel cell type	**Investment costs**	**Efficiency**	**TRL (maritime applications)**
DMFC	$1825/kW [82]	40-50% [83]	-
LT-PEMFC	$337-623/kW[1](future) [35]	40-60% [18]	+
AFC	$400-600/kW (2005) [84]	50-60% [85]	-
HT-PEMFC	$1000-1700/kW (2014) [36]	30-50% [18]	+/-
PAFC	$6300-7000/kW (2015) [86]	36-45% [19]	-
MCFC	$5300-6200/kW (2015) [86]	up to 60% [26]	-
SOFC	$3165-5411/kW (2014) [87]	50-65% [18]	+/-

DNV GL [24] performed a study on the use of fuel cells in shipping, which compared the same fuel cell types as this report and concluded that LT-PEMFCs, HT-PEMFCs, and SOFCs are the three most promising FC types for maritime applications.

2.7. Conclusion

This chapter reviewed the operational principles of fuel cells and their auxiliary systems to answer the question: What is the most suitable type of fuel cell for maritime applications?

First, the basic principles behind fuel cells were explained. After this, the chapter touched upon various fuel cell types that exist. The PEMFC and SOFC are currently considered viable options for installation onboard ships. The PEMFC has the highest power density and technical maturity, but it requires very pure hydrogen fuel input, and the possibilities for WHR with this FC type are limited. Despite its drawbacks, the LT-PEMFC is currently regarded as the most mature fuel cell type because of its highest TRL and power density and lowest cost.

Fuel cell stacks operate in combination with BoP systems, which allows them to operate within the desired operating conditions. These BoP components influence the efficiency and load response of the fuel cell system. Battery systems may aid fuel cells connected to fluctuating electrical loads. These battery systems can cope with transients in the load demand using peak shaving and gap filling. This allows the fuel cell to operate on a more constant power level.

[1] Converted from euro to US dollar with an exchange rate of 1.07$/€ [88].

3

Fuel Processing

Most fuel cells mentioned in chapter 2 require some form of fuel processing before the fuel can be used. Therefore, the following question will be answered in this chapter:

What are the properties of ammonia crackers, methanol reformers, and other required fuel processing systems for proton exchange membrane fuel cells in maritime applications?

In this question, the term 'properties' relates to the specifications of such systems, their TRL, and the influence these systems have on a vessel's power system. To answer this question, all fuel processing techniques discussed in this chapter will be divided into three categories:

- Fuel conversion
- CO removal
- Fuel purification

A conclusion on the question about fuel processing will be given at the end of the chapter, in section 3.5.

3.1. Fuel Conversion

Fuel conversion is the process of converting a hydrogen carrier such as methanol or ammonia to hydrogen. The processes to do this will be described in this section.

3.1.1. Methanol Reforming

The conversion process from methanol (or any other hydrocarbon) into hydrogen is called reforming. According to Li et al. [89], steam methanol reforming, partial oxidation reforming, and autothermal reforming are the three most common types of methanol reforming for hydrogen production. The latter two do not need heat input, but they yield low hydrogen output and hydrogen content in the exit gas. Steam methanol reforming is thus favorable over the other two options from an efficiency perspective. Welaya et al. [90] also favor steam reforming over other methods because it yields the highest fuel efficiency.

In a steam methanol reformer (SMR), the main reaction is given in equation 3.1 [91].

$$CH_3OH + H_2O \rightleftharpoons 3\,H_2 + CO_2 \qquad \Delta H^0_{298K} = 49\ kJ/mol_{CH_3OH} \tag{3.1}$$

Ranjekar and Yadav [92] researched the reactions occurring in methanol steam reformers. They stated that, besides the SMR reaction, two main side reactions occur in the reactor. These reactions are methanol decomposition (MD) and water gas shift (WGS); they are given in equations 3.2 and 3.3, respectively.

$$CH_3OH \rightleftharpoons 2\,H_2 + CO \qquad \Delta H^0_{298K} = 90\ kJ/mol_{CH_3OH} \tag{3.2}$$

$$H_2O + CO \rightleftharpoons H_2 + CO_2 \qquad \Delta H^0_{298K} = -41\ kJ/mol_{CO} \tag{3.3}$$

Gurau et al. [93] state that all three above reactions and their reverse reaction reeds must be considered when modeling methanol steam reformers. Reactions 3.1 (MSR) and 3.2 (MD) are endothermic when they happen from left to right, and reaction 3.3 (WGS) is exothermic when it happens from left to right. Considering that these reactions are equilibrium reactions, they can occur in both directions. This can be an issue when the H_2 and CO_2 percentages increase at the end of the reactor; this can cause the WGS reaction to occur backward and produce CO. The output of a steam methane reformer therefore consists of syngas. When using SMR to provide H_2 for a PEMFC, further CO removal is required to avoid poisoning of the fuel cell. This CO removal can be performed using another WGS reaction, preferential oxidation or selective methanation.

Pluijlaar and van Biert [94] researched the use of a reformer in combination with LT-PEMFCs and CCS running on methanol and found one data point that suggested the reformer operates on 80% efficiency.

3.1.2. Ammonia Decomposition

Ammonia cannot be directly used in PEMFCs. In subsection 2.3.1, the impact of ammonia particles on the performance of PEMFCs has been touched upon. The decomposition of ammonia into hydrogen and nitrogen is therefore required for use in PEMFCs, this process happens in so-called 'ammonia crackers'. The process of ammonia decomposition is given in equation 3.4 [95].

$$2\,NH_3 \rightarrow 3\,H_2 + N_2 \qquad \Delta H^0_{298K} = 46\ kJ/mol_{NH_3} \tag{3.4}$$

This reaction is endothermic. In addition, as pressure is increased, the backward reaction is favored. This means high temperatures and low pressures are desirable for full ammonia decomposition [96]. According to Yin et al. [97], the process of ammonia decomposition can occur at temperatures above 350 °C. However, temperatures above 600 °C are required to form pure hydrogen.

Okanishi et al. [98] studied the direct use of ammonia in SOFCs and showed a SOFC can operate on pure ammonia for longer periods of time without significant performance degradation over time. SOFCs therefore do not require external ammonia crackers. However, Andriani and Bicer [96] state commercially available SOFCs running on ammonia are still under development.

3.2. Carbon Monoxide Removal

After the previously mentioned methanol reforming process, CO is often still present in the fuel at a level that could damage LT-PEMFCs. Further CO removal is therefore required when an LT-PEMFC is operated on a fuel containing CO particles. This section will elaborate on the various processes specifically intended to remove CO particles from the hydrogen gas stream.

3.2.1. Water Gas Shift

Besides the WGS reaction occurring in a methane steam reactor, WGS reactions can also occur in separate WGS reactors. The reaction occurring in separate WGS reactors is the same as in equation 3.3. Forward WGS reactions are exothermic, meaning heat from the reaction needs to be extracted when the reaction is proceeding. Zhou et al. [99] researched the current status of WGS reactions and stated that WGS reactions can occur at a relatively wide range of temperatures. The reaction kinetics are faster at high temperatures and slower at low temperatures. However, high temperatures allow the backward WGS reaction to occur because that reaction is endothermic. Therefore, WGS reactors exist in high- and low-temperature versions.

3.2.2. Preferential Oxidation

After WGS, the CO content of the hydrogen is still too high for use in LT-PEMFCs [100]. Therefore, Preferential Oxidation (PrOx) can be used to remove further CO particles. The main reaction occurring in PrOx is given in equation 3.5 [101].

$$2\,CO + O_2 \rightarrow 2\,CO_2 \qquad \Delta H^0_{298K} = -566\ kJ/mol_{O_2} \tag{3.5}$$

According to van Biert and Visser [18], PrOx reactions take place at temperatures between 80 and 200 °C. Hydrogen will also be oxidized during the PrOx reaction, as shown in equation 3.6 [101]; this lowers the efficiency of this reactor.

$$2\,H_2 + O_2 \rightarrow 2\,H_2O \qquad \Delta H^0_{298K} = -484\ kJ/mol_{O_2} \tag{3.6}$$

Valdés-López et al. [101], state the advantages of PrOx are that the process can occur continuously, the process can let small amounts of CO react, resulting in a high hydrogen purity. Also, the process has a low energy requirement. Disadvantages include the requirement of the control of the O_2 over CO ratio, the risk of explosion, the large volume requirement of the system, the system complexity, and the lower efficiency due to the hydrogen oxidation reaction.

3.2.3. Selective Methanation

Another method to remove CO from a hydrogen gas stream is Selective Methanation (SMET). During the process, carbon monoxide is reacted with hydrogen to form methane gas and water. Panagiotopoulou et al. [102] researched SMET and stated the main advantage of SMET over PrOx is that there is no oxygen required in the gas stream, reducing issues with hydrogen yield, dilution, safety and restrictions in the operating parameters. The reaction is shown in equation 3.7.

$$CO + 3\,H_2 \rightleftharpoons CH_4 + H_2O \qquad \Delta H^0_{298K} = -206\ kJ/mol_{CO} \tag{3.7}$$

The methane gas produced in this reaction acts as an inert gas in an LT-PEMFC. Therefore, the fuel cell is not damaged by this gas. To mitigate the problem of methane slip [103], measures must be taken to capture or burn the methane before it is released into the atmosphere.

Selective methanation can produce two undesirable side reactions, which are given in equations 3.8 and 3.9 [104].

$$CO_2 + 4\,H_2 \rightleftharpoons CH_4 + 2\,H_2O \qquad \Delta H^0_{298K} = -165\ kJ/mol_{CO_2} \tag{3.8}$$

$$CO_2 + H_2 \rightleftharpoons CO + H_2O \qquad \Delta H^0_{298K} = 41\ kJ/mol_{CO_2} \tag{3.9}$$

These reactions are undesirable because they consume hydrogen, reducing the process' hydrogen yield. In addition, the reverse WGS reaction shown in equation 3.9 produces CO.

3.3. Purification

After the processes mentioned earlier, some impurities may still be present in the fuel. These impurities need to be removed up to an extent where they can no longer damage the fuel cell. This section will therefore highlight some fuel purification processes that may be used to purify hydrogen.

3.3.1. Pressure Swing Adsorption

Pressure swing adsorption (PSA) is a technique to remove CO, CO_2, CH_4, and NH_3 impurities from a gas stream. The technique is based on the difference in adsorption of the molecules in the gas stream [105]. The molecules are adsorbed on a solid adsorbent at high pressure. After this, the pressure is lowered, and the molecules are desorbed. According to Chen et al. [106], the main advantages of PSA are simple operation, short cycle time, and operation at room temperature. Disadvantages of PSA include the large size of the vessels and the energy consumption of the compressors [107]. As the pressure in a PSA vessel varies, the resulting hydrogen stream has no continuous output. Therefore, two PSA vessels are often placed in parallel [107]. One vessel is then at high pressure whilst the other is at low pressure. The large volume requirements of PSA limit the suitability of this method for maritime purposes.

3.3.2. Temperature Swing Adsorption

Temperature swing adsorption (TSA) is a similar process to PSA. The difference is that TSA relies on a variation of temperature to adsorb and desorb molecules, whereas PSA does so with a variation in pressure. If an external heat source such as waste heat is available, TSA requires less power than PSA. A drawback of TSA is the longer cycle time compared to PSA due to the heating and cooling of the reactor, this limits the transient response of a power system using TSA.

3.3.3. Membrane Separation
Membrane separation is a method that relies on the difference in permeability of the various molecules in a gas stream. The method uses a membrane with a certain selectivity for the permeation of molecules. This method is suitable for hydrogen purification applications because hydrogen is a very permeable molecule, allowing it to pass through membranes easily. The force that drives the molecules to permeate through the membrane is a partial pressure difference between the two sides of the membrane [108]. Various membrane materials can be applied for membrane separation, with each membrane having different properties and costs [109].

3.3.4. Electrochemical Membrane Separation
Electrochemical membrane separation (EMS) relies on a principle that is similar to the operation of fuel cells. This method uses an electrochemical cell, where hydrogen is split into protons and electrons at the anode and recombined at the cathode. The protons are conducted through a membrane, whilst the electrons are transported through an electronic surface. This method yields high-purity hydrogen at the cathode side, whilst other gases are fed away at the cathode side. The power required for EMS is relatively low [18, 110].

3.3.5. Desulfurization
As mentioned earlier, fuel cells are very prone to sulfur poisoning. Desulfurization is therefore required if sulfur is present in the fuel. If fuels are produced renewably using a combination of green electricity, water, air, and CO_2, desulfurization is usually not required.

Van Rheinberg et al. [111] favor the removal of sulfur via sulfur adsorption on various adsorbents. This method is similar to pressure swing adsorption for the removal of CO, CO_2, and CH_4 impurities. The desulfurization processes are performed before other fuel processing steps since these fuel processing steps may also be influenced or degraded by sulfur.

3.4. Fuel Processing Overview
Bang et al. [112] studied five different CO removal and fuel purification processes for supplying high-purity hydrogen for use in PEMFC after steam methane reforming. They studied WGS, PrOx, SMET, WGS + SMET, and WGS + PrOx. The researchers found the option of using WGS in combination with PrOx was the only option that resulted in a CO concentration of below 10 ppm (for use in PEMFCs) and that did not emit methane into the atmosphere via the exhaust gas. An overview of the processes discussed in this chapter is given in table 3.1.

Table 3.1: Overview of fuel processing methods listed in this chapter.

Process name	**Process type**	**Process temperature** [18]
Steam reforming	Fuel conversion	500 - 1000 °C (depending on fuel)
Ammonia decomposition	Fuel conversion	320 - 600 °C
Water gas shift	CO removal	175 - 500 °C
Preferential oxidation	CO removal	120 - 175 °C
Selective methanation	CO removal	250 - 375 °C
Pressure swing adsorption & temperature swing adsorption	Purification	35 - 225 °C
Membrane separation	Purification	250 - 725 °C
Electrochemical membrane separation	Purification	250 - 725 °C
Desulfurization	Purification	300 - 550 °C

All fuels that contain sulfur must be desulfurized before other fuel processing steps. For converting green methanol into hydrogen, it is first required that the fuel is reformed. After this, the CO impurities need to be removed using WGS, PrOx, or SMET. Next, other impurities need to be removed using PSA, TSA, MS, or EMS. Green ammonia first needs to be cracked using AD, after this, PSA, TSA, MS or EMS may be used to further purify the hydrogen gas stream. Liquid hydrogen does not need to be converted, but is does need to be converted into gaseous hydrogen for use in fuel cells. This is done

using a vaporizer, which is a heat exchanger that inputs heat into the liquid hydrogen to convert it to gaseous hydrogen.

The suppliers of commercially available maritime fuel processing systems often combine some of these processes into their systems. The advantage from a ship design perspective is that these systems are available off the shelf and require little to no further engineering. The ship designer does need to be aware of the limited transient capabilities of fuel processing systems when designing a ship's power system.

Methanol reforming systems are readily available for maritime applications. An example of such a system is the Rix M2H2-1800 System [113]. According to the manufacturer, the system can supply hydrogen with a purity of 99.97%, sufficient for use in PEMFC systems. The system can deliver a maximum output of 10 kg of hydrogen per hour, which is chemically approximately 330 kW of hydrogen. The system has a mass of 1455 kg and a volume of 3.2 m^3. The cold start-up time of the system is under 12 hours, making it significantly longer than the start-up time of PEMFCs. The system has an optimal efficiency of 80-82% when operating at steady state. Rix Industries is also developing a system that integrates a methanol reformer, hydrogen purification system, LT-PEMFC, and the required BoP equipment in one enclosure to install onboard ships. Another example is from Advent Technologies [114], they are developing a methanol-fuelled system based on a methanol reformer and HT-PEMFC. Several vessels are currently fitted with up to 90 kW of these systems to serve as test and demonstration projects. Furthermore, Blue World Technologies [115] is also developing an HT-PEMFC system that can operate on methanol. Further information about this system is not available at this time.

Commercially available ammonia decomposition is offered by Amogy [116]. They are working on constructing an LT-PEM fuel cell-based power pack that can be operated on pure ammonia. The power pack will contain all fuel processing equipment and the balance of plant components required to operate the fuel cell. The power pack will have a length of 2.75 m, a width of 1.2 m, and a height of 2.2 m, giving it a total volume of 7.26 m^3. The system has a mass of 4000 kg, and it produces 200 kW of gross power output. An advantage of the power pack is that all components are mounted in an air-tight enclosure that can be vented directly. This means the room where the power packs reside does not need as many additional safety measures as a room where the individual components are mounted separately and are connected with single-walled pipes. The power pack's power output can be customized to DC or AC. The powerpack is stated to supply 2.1 kWh of electricity per kg of consumed ammonia. Which, at an energy density of ammonia of 18.6 MJ/kg, corresponds to an efficiency of 40.6%.

3.5. Conclusion

This chapter gave an overview of the most common fuel processing steps onboard ships. By doing so, it answered the question: What are the properties of ammonia crackers, methanol reformers, and other required fuel processing systems for proton exchange membrane fuel cells in maritime applications?

Firstly, desulfurization is required when sulfur-containing fuels are used in fuel cells. After this, fuel conversion is required to convert methanol or ammonia to hydrogen for use in fuel cells. Next, CO removal is required for syngas streams for use in PEMFCs. Lastly, other fuel purification steps may be required to remove the remaining impurities from hydrogen gas streams. These fuel processing steps occur at various temperatures and can be endo- or exothermic.

Fuel processing systems influence the ship's power system efficiency and require mass and volume onboard. In addition, fuel processing systems have limited capabilities to respond to changes in output demand rapidly, they thus influence the transient response of a ship's power system. These aspects must be considered when designing a ship's power system with fuel processing systems.

Some manufacturers combine fuel conversion processes in commercially available modules for ship installation to supply pure hydrogen to fuel cells. Others combine these fuel processing systems with fuel cells in modules for ship installation to convert ammonia or methanol to electricity.

4

Fuel Storage

This chapter gives more information on the energy storage systems required to store the various alternative fuels onboard the vessel. Based on this information, the third research question is answered. This question is:

What are the properties of liquid hydrogen, ammonia, and methanol storage systems onboard ships?

In this question, the term 'properties' relates to the specifications of the fuel storage systems, their TRLs, and the influence these systems have on ship designs. To answer this question, the main properties of liquid hydrogen, ammonia, and methanol will be described in the following sections. After this, a comparison will be made between the fuel storage masses and volumes of these various alternative fuels.

4.1. Liquid Hydrogen

Hydrogen can be produced in various ways. Nikolaidis and Poullikkas [117] reviewed the various hydrogen production processes. They stated that the most common forms of hydrogen production are steam methane reforming and pyrolysis. These methods use fossil fuel sources to produce hydrogen and cause harmful emissions such as CO_2, CO, and CH_4. Hydrogen can also be produced using water splitting through electrolysis [118]. This process is the reverse process that occurs in fuel cells. It thus requires water, electricity, and heat input (the latter depends on the potential used for water splitting), yielding hydrogen. Electrolysis can be powered using green electricity from renewable power generation methods. The hydrogen produced using renewable power is called 'green hydrogen' [119]. Green hydrogen still has environmental and human health impacts due to several factors, such as the production and installation of the renewable power plant and the electrolyzers [120], but this will not be considered further in this report.

4.1.1. Hydrogen Storage

Hydrogen can be stored on ships in compressed or liquefied form. In compressed form, hydrogen is stored at a pressure of 350 or 700 bar onboard the vessel. In liquefied form, the hydrogen gas is first liquefied before it is stored onboard the vessel. This is advantageous over hydrogen storage in compressed form because it allows for a higher gravimetric and volumetric energy density, thus requiring less mass and volume onboard the vessel [121]. For this reason, liquid hydrogen is considered in this thesis instead of compressed hydrogen. In hydrogen liquefication, hydrogen gas is first compressed before it is fed through several heat exchangers, which remove heat from the gas. Consequently, the temperature is lowered, and the gas is liquefied. When the liquid hydrogen is stored in a tank, the temperature difference between the liquid hydrogen and the surroundings causes heat from the surroundings to enter the liquid hydrogen storage tank. Consequently, the gas is heated, and part of the hydrogen is converted to gas. This causes the pressure in the tank to rise. This hydrogen gas is then vented from the tank to prevent the pressure in the tank from becoming too high. The hydrogen gas that is vented from the tank is called boil-off gas. Onboard vessels, this boil-off gas is often used to

supply hydrogen to the energy conversion system. When the vessel requires less power than the boil-off gas supplies, the excess boil-off gas must be vented into the atmosphere. This is undesirable from an economic and environmental perspective since venting hydrogen into the atmosphere is a waste of fuel and thus increases fuel costs. Simultaneously, hydrogen is an indirect greenhouse has [122], and hydrogen emission into the atmosphere should thus be minimized.

Hydrogen has a lower specific energy than diesel and is stored in insulated cylindrical or bi-lobe type C tanks or prismatic type B tanks. These tanks must be designed according to the IGC code [123]. The shape and insulation of the liquid hydrogen tanks lower the amount of hydrogen that can be stored per unit of volume of cuboid-shaped compartments reserved for fuel storage. In addition, these tanks and the insulation have more mass than tanks integrated into the ship's structure.

4.1.2. Hydrogen Safety and Regulations

Hydrogen is a highly flammable and odorless gas, and it burns with a colorless flame [124]. In addition, the risk of frostbite due to the low storage temperature of liquid hydrogen poses a health risk. Therefore, safety measures are required for the storage of hydrogen onboard ships. These safety measures mostly relate to preventing hydrogen and air mixtures from being ignited easily. These measures include:

- The use of double-walled pipes for hydrogen lines. This reduces the amount of hazardous zones onboard the vessel because of the flammability of hydrogen [125].
- A nitrogen purging system to purge all pipes and other hydrogen systems with nitrogen when the system is not in use or for maintenance.
- Ventilation and hydrogen detection systems for all hazardous zones.
- Requirements for the positioning of the liquid hydrogen tanks within the ship. There are several ways to comply with these requirements, one way of doing so is to place the fuel tanks within B/5 of the sides of the vessel [126].

4.2. Ammonia

Ammonia is also being considered as an alternative fuel. Ammonia is already being used in other industrial applications. The ammonia production methods are thus mature, and some ammonia infrastructure already exists. To produce ammonia, nitrogen and hydrogen are reacted in a Haber-Bosch process [127]. The reaction in this process is the opposite as given in equation 3.4. The Haber-Bosch process takes place under high temperatures (between 400 and 500 °C) and at elevated pressures (between 15 and 20 MPa) [127]. To produce green ammonia using this process, nitrogen from outside air, green hydrogen, and electricity are required [128]. The nitrogen from the outside air can be captured with relative ease, this is a benefit of using ammonia as an energy carrier over other energy carriers.

4.2.1. Ammonia Storage

Like hydrogen, ammonia can be stored in liquid form. This is desirable since it results in a higher volumetric and gravimetric energy density compared to ammonia in gaseous form. The storage temperature of liquid ammonia is higher than that of hydrogen, ammonia can be stored at -33.3 °C [129]. Ammonia can be stored in insulated cylindrical or bi-lobe type C tanks or prismatic type B tanks, resulting in additional mass and reduced fuel storage volume compared to cuboid-shaped tanks integrated into the ship's structure.

4.2.2. Ammonia Safety and Regulations

While the flammability of ammonia is low, ammonia is a very toxic substance [130]. Therefore, safety measures must be taken to prevent the ammonia from coming into contact with people or the environment. In addition, there is a risk of frostbite because of the low storage temperatures of liquid ammonia. For ship and power system design, relevant safety measures include:

- Using double-walled piping for all ammonia fuel pipes outside the tank connection space and fuel treatment room. Doing this leads to a decrease in the amount of hazardous zones subjected to regulations because of the toxicity of ammonia.
- Ammonia systems should be purged with nitrogen when required (e.g. for maintenance or when the systems are not used for longer periods of time).

- All hazardous zones should be ventilated and fitted with ammonia detection systems.
- Positioning the ammonia tanks within the ship according to regulations. An example of this is to place the tanks within B/5 of the sides of the vessel [126]

4.3. Methanol

Methanol is the third alternative fuel being considered in this report. It is liquid at ambient temperature and has the highest volumetric energy density of all alternative fuels considered in this report. This fuel can be produced renewably by a process called methanol synthesis. The reaction equations for this process are the backward reactions from in equations 3.3 and 3.2.

To form green methanol, green electricity and green hydrogen are required. In addition, CO_2 is required to produce methanol. As mentioned in chapter 3, methanol reforming onboard ships will result in CO_2 emissions. The origin of the CO_2 for the production of methanol and the destination of the emissions resulting from methanol reforming thus determine if the methanol is a renewable fuel and if it is used in a renewable manner. Methanol can be produced renewably if it is produced with CO_2 obtained from CCS onboard ships or from direct air capture of CO_2. The implementation of CCS onboard ships and the use of direct air capture and their financial and environmental impacts are not considered in this thesis. Another carbon-neutral way to produce methanol is by using biomass [131].

4.3.1. Methanol Storage

Because methanol can be stored in liquid form under ambient conditions, no pressure-resistant or independent tanks are required. Like diesel tanks, methanol tanks can be part of the ship's structure. This results in the energy density and specific energy of the methanol itself being almost equal to that of the methanol fuel in combination with the tank. The only volumetric limitation is a tank filling limit of 98% of the tank's volume.

4.3.2. Methanol Safety and Regulations

Because Methanol is liquid at room temperature, it can be stored at ambient conditions in cuboid-shaped tanks. Several safety measures need to be taken because of the low flashpoint and toxicity of methanol. These measures include:

- The use of double-walled piping to reduce the amount of hazardous zones onboard the ship [125]. These hazardous zones are classified as so because of the toxicity and flammability of methanol.
- The usage of nitrogen to inert the methanol tanks and to purge methanol piping and other systems to prevent flammable oxygen and methanol mixtures.
- The application of ventilation and methanol detection systems for all hazardous zones onboard the vessel.
- Installation of cofferdams between methanol tanks and other compartments within the vessel. The application of cofferdams between methanol tanks and the outside air is currently mandatory, but it is under review. All methanol storage tanks installed under the lowest waterline do not require cofferdams between the tank and the vessel's outer hull. An illustration of these cofferdam requirements is shown in figure A.4.

4.4. Fuel Storage Mass and Volume

The gravimetric and volumetric energy storage densities per fuel depend on various factors. These factors include the geometry of the tanks, the type and thickness of the insulation of the tank, and the minimum and maximum filling limits. In addition, the best placement of the fuel tanks and the influence they have on the vessel depend per vessel. The actual energy densities per fuel thus need to be calculated per case.

C-Job made an approximation of the the energy storage densities for liquid hydrogen, ammonia and methanol [81]. This approximation can be used to gain insight into the energy densities per fuel. The results from this approximation are shown in table 4.1.

Table 4.1: Overview of alternative fuel storage properties.

Process name	LH2	NH3	CH3OH	Unit
Fuel energy density	120	18.6	19.9	MJ/kg
Storage mass ratio	0.17	2.12	1.00	kg_{fuel}/kg_{tank}
Storage energy density	17.7	12.6	19.9	MJ/kg
Fuel volumetric energy density	8.5	12.7	15.8	GJ/m^3_{fuel}
Storage volume ratio	0.40	0.50	0.98	m^3_{fuel}/m^3_{tank}
Storage volumetric energy density	3.40	6.40	15.5	GJ/m^3_{tank}

From this table, it can be concluded that liquid hydrogen has the lowest energy densities compared to ammonia and methanol. The actual storage volume and mass ratios considered in this thesis will be calculated when the designs have been made.

4.5. Conclusion

This chapter reviewed the fuel storage methods for liquid hydrogen, ammonia, and methanol to answer the question: What are the properties of liquid hydrogen, ammonia, and methanol storage systems onboard ships?

Methanol has the highest energy densities, but the fuel contains carbon, and the fuel is toxic and flammable. Therefore, mitigation measures are required to ensure the carbon emissions are used in a renewable way, the risk of fire and explosion is minimized, and the fuel will not come into contact with people and animals. Ammonia has intermediate energy densities compared to the other two alternative fuels. Ammonia is very toxic, and mitigation measures are required to prevent it from coming into contact with people, animals, or the environment. Liquid hydrogen has the lowest energy densities compared to the other two alternative fuels. It is also a very flammable substance, and fire and explosion avoidance measures must thus be taken.

General guidelines for the storage masses and volumes of these alternative fuels can be found, but the actual storage masses and volumes of these alternative fuels are to be calculated for each design individually.

5

Current Designs and Research

Some vessels are currently in operation, being built or developed using fuel cell systems and alternative fuels onboard ships. In addition, current research projects aim to gain more knowledge on fuel cell systems and alternative fuels. The findings of these designs and research projects are relevant for designing new vessels. Therefore, these findings will be summarized in this chapter. By doing so, the following question will be answered:

Are there vessel designs or research projects that use liquid hydrogen, ammonia, or methanol as fuel in combination with fuel cells? If so, what are their specifications or findings?

To answer this question, hydrogen-, ammonia- and methanol-fuelled vessels will be discussed in the following sections. When this report states a vessel is fuelled with a certain fuel, it means that this fuel is bunkered to the vessel. This can mean that the bunkered fuel is a hydrogen carrier that is processed onboard the vessel. After the relevant vessels, relevant scientific research projects will be mentioned. Next, some observations regarding current vessels and research projects will be mentioned. Lastly, a conclusion will be drawn.

5.1. Hydrogen-Fuelled Vessels

Some fuel cell-powered vessels sailing on hydrogen are currently in operation, being built, and being designed. Norled [132] operates a liquid hydrogen-fuelled ferry called the 'MF Hydra'. This ferry is 82 m long and can carry up to 80 cars and 299 passengers. Its liquid hydrogen tank has a capacity of 4 tons, with a length of 10 m and a diameter of 3.5 m. The tank is vacuum-insulated and operates at pressures between 2 and 3 bar. Two 200 kW Ballard PEMFCs power the vessel, and the vessel uses a battery support system with a storage capacity of 1.5 MWh.

Another two hydrogen fuel cell-powered ferries are currently under construction for the Vestfjorden ferries [133]. Current news articles do not state if this vessel uses compressed or liquefied hydrogen as fuel. These ferries will have a capacity of 12 trucks, 120 cars, and 599 passengers. The fuel cells will be delivered by PowerCell, with each vessel having an installed power of 13 MW. The vessel's autonomy will be up to four hours.

A smaller vessel is currently in operation in the Port of Rotterdam, and it has been designed and commissioned by the SWIM consortium [134]. The vessel is a hydrogen-fuelled water taxi powered by a 45 kW Zepp.solutions fuel cell and a 50 kW and 33 kWh battery. The ship has a length of 8.8 m, a capacity of 12 passengers, and an autonomy of 9 hours at a cruising speed of 16 km/h. The water taxi was launched at the beginning of 2023, and results about the performance of the vessel have not been published at the time of writing this report.

Future Proof Shipping [135] exploits refitted inland vessels that sail on compressed hydrogen using PEMFCs. They currently have one 110 m inland container vessel in operation powered by three 275 kW PEMFCs. The hydrogen is stored in two containerized tanks with a capacity of 500 kg each. Three other inland vessels are set to enter service in 2024 and 2025.

5.2. Ammonia-Fuelled Vessels

Regarding ammonia-fuelled ships running on fuel cells, the ShipFC project [136] aims to install a 2 MW ammonia fuel cell system onboard the 'Viking Energy', an offshore vessel. The fuel cell system will be based on SOFCs supplied by Alma Clean Power. The installment of the SOFC system is planned for the end of 2023, results are not available at the time of writing of this report.

Other SOFC systems have been installed on vessels and research has been performed on installing SOFCs on ships, but these installations mainly focus on LNG-fuelled SOFCs. For example, Russo et al. [137] investigated the installment of an LNG-fuelled 12 MW SOFC system on a cruise ship. Their finding was that the SOFC plant required more volume than an ICE system of the same power output but that the SOFC plant had a larger efficiency and would reduce the vessel's emissions. Another example of LNG-fuelled SOFC systems onboard ships is the study performed by Micoli et al. [138]. The authors performed a case study of a 16.94 MW SOFC system installed onboard a cruise ship. The SOFC plant provided hotel loads to the vessel and assisted the ICE generator sets. The system was fuelled by LNG and produced lower emissions than the ICE generator sets. The SOFC system was 839 t heavier and consumed 4892 m^3 more volume than an ICE generator set with the same power output (286 t and 834 m^3). This required modifying the vessel's design but did not significantly influence its stability.

5.3. Methanol-Fuelled Vessels

When using methanol as fuel, many shipping companies use ICEs to power the vessel [139]. The maritime installations of methanol reformers or fuel cells that can run on methanol are currently very limited and not in a commercial phase.

Maritime Partners is developing a methanol fuel cell system-powered towboat called the Hydrogen One [140], which uses a Rix Industries methanol reformer system and PowerCell fuel cells. The system also includes a battery storage system and a power control system. As this vessel is still under development, there are no results from the real-life performance of it yet.

Several commercial projects aim to develop fuel cell-powered ships using Methanol as the energy carrier. In a past demonstration project, the RiverCell consortium demonstrated the implementation of a HT-PEMFC system installed in a ship section [141]. The system was fuelled by methanol, and results from this demonstration project are used for future projects from the consortium partners. Freudenberg and Lürssen Werft have partnered to develop methanol-fuelled fuel cell systems for mega yachts [142]. The first yacht from this partnership, project COSMOS, is under development. These two companies are also involved in the Pa-X-ell 2 project, which is led by Meyer Werft [143]. The aim of this project is to develop a maritime HT-PEMFC system that can operate on methanol or LNG.

5.4. Scientific Research

Next to these commercial applications, scientific research is also being conducted on several different topics. SH2IPDRIVE [144] is a Dutch hydrogen research project that focuses on applying fuel cells onboard ships in combination with hydrogen or hydrogen carriers. The project is divided into work packages with their own purposes and targets. The work packages include theoretical knowledge gathering, system modeling, ship design, integration, practical aspects, and real-life testing of several vessels equipped with the technologies from earlier stages.

The HELENUS consortium [145] aims to integrate a SOFC system in a cruise ship. Several fuels are considered since SOFCs can operate on several fuels. This research project is also divided into several work packages, which include conceptualization & development, testing & validation, and analysis of the broader impact of the considered topics. The project started in 2022, and a conclusion is expected in 2027. Another SOFC research project, the METHAPU project [146], took place between 2006 and 2010. The project researched SOFC technology onboard ships. Under this project, a 20 kW SOFC module was placed in a vessel. Results showed no CO and SO_2 emissions, low NOx emissions and a 40% CO_2 emission reduction compared to a diesel-fuelled ICE [147].

Other research projects such as NAUTILUS [148], AmmoniaDrive [149], and MENENS [150] study the implementation of alternative fuels onboard ships. However, they either consider ICEs as a power generation system instead of FCs, or they use LNG as a fuel instead of the alternative fuels considered in this report.

5.5. Overview

From researching current vessels in operation and under development and considering research projects, several observations can be made:

- Fuel cell systems are often used as auxiliary power supply instead of as main power source.
- It will take several years before the practical experiences resulting from the current usage of fuel cells in ships will be available to the public.
- Ammonia and methanol are often considered for use in combination with ICEs or GTs instead of fuel cells. This is because ICEs and GTs currently have a higher TRL than FC systems. In addition, the refit of ICEs or GTs to be operated on hydrogen, ammonia, or methanol is often cheaper than purchasing and installing a new FC-based power system.
- SOFC projects in maritime applications predominantly use LNG as fuel. This is mainly because LNG is widely available worldwide and cheap compared to alternative fuels, and LNG storage onboard ships has a higher TRL than alternative fuels.
- No research projects have been found that compared fuel cell systems running on liquid hydrogen, ammonia, or methanol for a specific vessel with potential power system designs.

When considering all of the above items, it is concluded that there is a literature gap around a comparison of maritime fuel cell systems using liquid hydrogen, ammonia, or methanol as fuels.

5.6. Conclusion

This section listed the most relevant vessel designs and research projects for this thesis to answer the question: Are there vessel designs or research projects that use liquid hydrogen, ammonia, or methanol as fuel? If so, what are their specifications or findings?

Based on vessel designs and research projects, it was seen that PEMFC-powered vessels fuelled by hydrogen are currently in operation in small quantities. These vessels are often smaller in size and have limited autonomy. More hydrogen-fuelled vessels are currently being developed. Methanol and ammonia-fuelled vessels using PEMFCs as primary power source are currently not in commercial operation. Some projects use ammonia or methanol-fuelled fuel cell systems to demonstrate their technological feasibility. When connecting these findings to the research question in this chapter, it can be concluded that fuel cell-powered vessels are still in development, and experience from operating these vessels is yet to be gained. Some specifications about these systems were mentioned in this chapter, but no in-depth information about these ships is available to the public.

The limited amount of vessels in operation using the technologies discussed in this report and the lack of studies that compared the use of liquid hydrogen, ammonia, and methanol for use in fuel cells as primary power source result in a literature gap.

6

Design Boundary Conditions

Before designing the power generation and energy storage systems, the boundary conditions for these systems will be determined. This will ensure that all designs use the same systems where possible, allowing for a fair comparison of the systems after they have been designed. This chapter will list which systems will be used as guidelines for power and energy storage system designs and the primary assumptions for the power and energy storage system designs. In addition, it will describe the vessel used for the case study.

First, the power modules to be used are listed in section 6.1. Next, the fuel storage options will be described in section 6.2. After this, the assumptions for auxiliary components are stated in section 6.3. Lastly, the vessel's relevant properties will be listed in section 6.4.

The choice for particular systems or components is primarily based on choosing systems representative of the current technology status and whose specifications are publicly available. All specifications and values that are not publicly known will be estimated.

6.1. Power Modules

Power modules that integrate fuel cells and fuel processing systems will be used to convert fuel to electrical energy. The term 'power module' (PM) will be used from this moment onwards for all systems that integrate a fuel cell, BoP components, fuel processing equipment, or a combination of these. This section lists which power modules are used as design guidelines and will explain why they are chosen.

6.1.1. Hydrogen Power Modules

As mentioned in section 2.3.1.3, multiple manufacturers offer PEMFC systems for maritime applications. The PowerCell Marine System 200 [53] shall be used as a design guideline. This fuel cell is representative of the current TRL in maritime fuel cell systems. In addition, this fuel cell is designed to be placed in a non-hazardous zone, which facilitates the design of the engine room. Also, the manufacturer makes most of the required information about the fuel cell publicly available, allowing for the results of this research to be verified. A more detailed description of the fuel cell's specifications is given in appendix A.1.1.

6.1.2. Ammonia Power Modules

To convert ammonia to electrical power, Amogy [116] produces a 200 kW (170 kW net) power pack incorporating an ammonia cracker, hydrogen purification equipment, and a 200 kW fuel cell. This power pack will be used as a guideline for an ammonia-based fuel cell system. No other maritime PEMFC-based systems fuelled by ammonia are known to the author at the time of writing of this report. The specifications of this power pack are given in appendix A.1.2.

6.1.3. Methanol Power Module

At the time of writing of this report, the only manufacturer known to the author that produces maritime methanol reforming systems for use with LT-PEMFCs is Rix Industries. This manufacturer produces a power module integrating a 250 kW PEMFC with a methanol reformer and a membrane-based fuel purification system. This module will be used as a design guideline for a methanol-based maritime fuel cell system. The specifications of this system are given in appendix A.1.3.

6.2. Fuel Storage

Fuel storage may be done in independent tanks (for LH2 and NH3) or integrated tanks (for CH3OH). Integrated tanks are part of the ship's structure, but independent tanks are not. This section lists the design starting points and assumptions used for designing fuel storage systems.

6.2.1. Type C Tanks

Independent tanks are available in types A, B, or C. The tank type indicates the standards to which the tank has been designed [126]. Type A tanks are designed according to classical ship structural design methods. Type B tanks are designed to determine the actual stress levels, fatigue life, and crack propagation characteristics using model tests, simulation methods, and analysis methods. Type C tanks are designed to include fracture mechanics and crack propagation criteria in pressure vessel criteria. Due to the brittleness of steels at low temperatures, the design basis for type C tanks is best suited for cryogenic tanks.

Type C tanks are available in cylindrical, spherical, or bi-lobed forms, whereas a bi-lobed tank combines two merged spherical or cylindrical-shaped tanks. The advantage of spherical tanks is that they have the lowest surface area to volume ratio, meaning less surface area is available for heat transfer between the tank and the environment, thus minimizing boil-off losses. However, spherical-shaped tanks offer lower volumetric energy densities when positioned in rectangular-shaped spaces than cylindrical or bi-lobe tanks. Therefore, cylindrical or bi-lobed tanks may be used. Bi-lobe tanks can be advantageous over cylindrical tanks since they can achieve a higher volumetric energy density than cylindrical tanks. For this reason, bi-lobe tanks will be used in the energy storage system. A render of a bi-lobe tank is shown in figure 6.1.

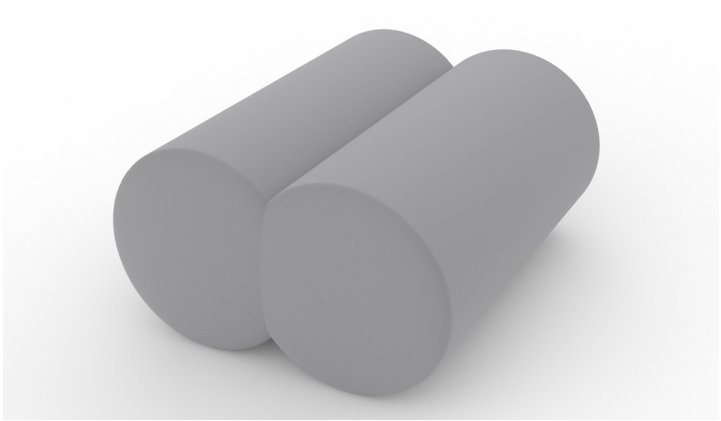

Figure 6.1: Example of a bi-lobe tank.

The best way to insulate type C tanks is to use a vacuum between the inner and outer shell of the tank. The insulation thickness of LH2 tanks must be 0.5 m or greater, while the insulation thickness of NH3 tanks should be greater than 0.18 m. In addition, these tanks have minimum and maximum filling limits and should be placed outside certain distances from the fuel hold's top, bottom, and sides. The relevant information for dimensioning and calculating the net storage volumes of independent type C tanks is given in appendix A.2.1.

6.2.2. Integrated Tanks

Integrated methanol tanks can be shaped in the same way as current diesel tanks. The inside plating of methanol tanks must be treated with a special coating to prevent methanol from damaging the steel. Cofferdams need to be applied between methanol tanks and the outside air or between methanol tanks and other holds onboard the ship. These cofferdams must have a thickness of 0.9 m and should be equipped with methanol detection and ventilation systems. Methanol tanks placed against the ship's outer hull below the lowest waterline do not require cofferdams between the tank and the outer hull.

The parts of the methanol tanks that are not filled with methanol, i.e., the gaps at the tops of the tanks, must be filled with nitrogen to prevent the formation of flammable methanol-oxygen mixtures. The relevant information for dimensioning and calculating the net storage volumes of integrated methanol tanks is given in appendix A.2.2.

6.3. Other Equipment

The power and energy storage systems considered in this thesis will vary in electrical, cooling, ventilation air, nitrogen purging, process air, and fuel pump demand. Because of these variations in requirements, the differences between these systems should be calculated. This section lists how the power and energy requirements for the auxiliary systems will be calculated.

To provide a visual illustration of the various components of the power and energy storage systems and the connections between them, an overview is shown in appendix F.

6.3.1. Batteries

Several suppliers offer battery systems for maritime applications. These systems are often enclosed in racks that allow for series connection of the batteries to achieve higher voltages than the individual batteries. As a design guideline, the Praxis GreenBattery-Power system is used. This system is used because it has approval from several classification societies and because it can achieve relatively high charge and discharge rates of 3C, which is convenient for coping with load transients in maritime fuel-cell-based power systems. The main specifications of the reference battery system are listed in appendix A.3.1.

6.3.2. Power Electronics

The majority of the power systems listed above produce unregulated DC power output. The delivered electrical power by the power modules and batteries must be converted to suit the ship's power grid voltage. This is done using DC-DC converters. An example of a DC-DC converter is the Siemens Sinamics DCP [151]. The dimensions, losses, and cooling requirements of this unit will be used in designing the maritime power systems. The main specifications of this system are given in A.3.2.

6.3.3. Cooling Equipment

The cooling demand of the power modules is assumed to equal the energy lost from the fuel input. It is assumed the power modules, batteries, and power electronics must be cooled. All power systems will have two cooling loops separated by a heat exchanger. The cooling loop on the equipment side of the heat exchanger is a closed loop with a hot water temperature of 65 °C and a cold water temperature of 45 °C. The seawater cooling loop is an open loop with a seawater inlet temperature of 30 °C and an outlet temperature of 40 °C. This results in a heat exchanger effectiveness of 57%. The total heat demand for cooling will be calculated using equation 6.1. The total power required per cooling loop will be calculated using equation 6.2. The derivation of both formulas and the explanations of the terms used are given in section B.1.1.

$$\dot{Q}_{cooling} = \frac{P_{PM}}{\eta_{PM}} \cdot (1 - \eta_{PM}) + \dot{Q}_{batteries} + \dot{Q}_{DC-DC} \tag{6.1}$$

$$P_{e,cooling} = \frac{\dot{Q}_{cooling} \cdot \sum \zeta \cdot \frac{1}{2} \cdot v^2}{c_p \cdot |\Delta T| \cdot \eta_{pump}} \tag{6.2}$$

6.3.4. Ventilation Air Supply

Air supply to equipment (process air) and spaces within the ship (ventilation air) is provided by blowers for low-pressure air supply and compressors for high-pressure air supply. The required air volume flow for ventilation air depends on the volume of each respective space and the number of air changes per hour required according to regulations. An overview of the required air changes per hour for different compartments and other spaces onboard the vessel is given in table A.9. The required power for the ventilation air supply will be calculated using equation 6.3. The derivation of this formula and the explanations of the terms used is given in section B.1.2.

$$P_{e,ventilation} = \frac{\dot{V}_{ventilationair} \cdot \sum \zeta \cdot \frac{1}{2} \cdot \rho_{air} \cdot v_{air}^2}{\eta_{blower}} \tag{6.3}$$

6.3.5. Fuel Preparation

Liquid hydrogen and liquid ammonia must be vaporized before they enter the fuel cell or cracker. This vaporization will take place in the TCS (tank connection space). The expansion of this gas is performed by the input of heat by means of a heat exchanger. Waste heat from the fuel cells or power packs is used for this purpose. The methanol power modules should be fuelled by a mixture of methanol (62.5% by mass) and deionized water (37.5% by mass). The mixturization of these substances is performed by a water mixing system. The power requirements of the fuel and deionized water pumps will be calculated using equation 6.4. The derivation of this formula and the explanations of the terms used is given in section B.1.3.

$$P_{e,fuelpump} = \frac{\dot{V}_{fuel} \cdot \sum \zeta \cdot \frac{1}{2} \cdot \rho_{fuel} \cdot v_{fuel}^2}{\eta_{pump}} \tag{6.4}$$

6.3.6. Process Air Supply

The PEMFCs require 1 mol of oxygen per 2 moles of hydrogen. Using this relation, the required amount of power for process air supply is calculated using equation 6.5.

$$P_{e,processair} = \frac{a \cdot P_{PM} \cdot M_{O2} \cdot \sum \zeta \cdot \frac{1}{2} \cdot v_{air}^2}{\eta_{FC} \cdot LHV_{H2} \cdot 2M_{H2} \cdot x_{O2} \cdot \eta_{blower}} \tag{6.5}$$

Fuel cells require more process air to be supplied than is consumed based on the stoichiometric ratio. To account for this, the amount of process air flow is assumed to be two times the amount of air required according to the stoichiometric ratio. For power packs operating on NH3 and CH3OH, it is assumed that the fuel processing steps require the same amount of process air as the fuel cell. Considering these aspects, the factor a in formula 6.5 is 2 for power modules operating on H2 and 4 for power modules operating on NH3 and CH3OH. The derivation of this formula and the explanations of the terms used is given in section B.1.4.

6.3.7. Nitrogen Supply

Nitrogen is used onboard the ship to inert the vent mast, purge power modules, piping, and inert methanol fuel tanks. It is assumed the nitrogen for this purpose is produced onboard the vessel using membrane separation. In this process, oxygen is compressed before it is passed through a membrane. After this, two compressors bring the resulting nitrogen to the correct pressure for storing it in a buffer tank. Each compressor is assumed to have a pressure ratio between 3 and 3.5, an isentropic efficiency of 75%, and a mechanical and electrical efficiency of 10%. The power from each compressor is calculated using equation 6.6. The derivation of this formula and the explanations of the terms used is given in section B.2.

$$P_{e,comp} = \frac{c_p \cdot T_0 \cdot \dot{m}}{\eta_{isentropic} \cdot \eta_{comp}} \cdot \left(PR^{\left(\frac{\gamma - 1}{\gamma}\right)} - 1 \right) \tag{6.6}$$

6.4. Vessel Definition

The vessel considered for the case study is an offshore ship. The vessel has a large deck for transport and crane application purposes. The vessel has space below deck to accommodate machinery spaces, fuel tanks, and cargo holds. The vessel can operate globally and is capable of operating in DP3 (dynamic positioning class 3). The main consequence of DP3 for power system design is that one compartment's flooding or fire should not lead to a loss of dynamic positioning capabilities. More concretely, the power system should be capable of delivering the total power required for propulsion while one compartment is not in operation.

6.4.1. Main Specifications

The main dimensions of the vessel shall be as given in table 6.1.

Table 6.1: Main specifications of the offshore ship used for the case study.

Item	Quantity
Length over all	217 m
Length between perpendiculars	204 m
Moulded breadth	49 m
Depth	17 m
Draught	8.5 m
Installed Power	55 MW

The base case for the power system of the vessel is that it has four ICE gensets installed which are fuelled by MDO. The ICEs are the Wärtsilä 12V46DF [152], having a power output of 13.74 MW per engine. The engines are positioned in two engine rooms, allowing for a power output of 27.48 MW with redundancy for DP3 operation. The four gensets generate AC electric power which is fed to the ship's AC grid.

The layout of the lower decks is shown in figure C.1. The sides of the vessel are used for ballast water tanks, which are wider than B/5. As a result, the parts of the vessel between the PS and SB water tanks automatically comply with the B/5 requirement for the positioning of fuel tanks.

The voids on the lower decks serve as a space reservation for equipment for other purposes than heavy lifting such as pipelaying equipment, cablelaying equipment, moonpools or motion compensated platforms. When changing the vessels power system to fuel cell-based systems operating on alternative fuels, this space will be used for the power generation and energy storage systems. The consequence of using these voids is a loss of capabilities of the vessel.

Similar vessels to the one used in the case study have been designed to use LNG as a fuel. These vessels have considered the blast radius from the LNG vent pipes, and it has been shown that a vent mast can be installed on the vessel.

6.4.2. Required Power and Operational Profile

For the vessel's power requirement, it is assumed the vessel operates in one of four states for a certain period. The vessel has peak load cases defined for four different states, these peak load cases are given in table 6.2.

Table 6.2: Electric peak load cases for the offshore vessel.

Load case	Total peak load (ekW)	Fraction of time
Free sailing	21000	6%
Manouvering	13000	6%
Harbour	900	12%
Dynamic positioning	22500	76%

The power and energy systems will be designed for autonomies of 7, 14, 21, 28, and 35 days. For each autonomy, the fraction of time per load case will be used to size the power and energy storage systems.

6.5. Conclusion

This chapter covered the components to be used in the case study and design assumptions for the power and energy storage systems to be designed. A selection of power modules to convert LH2, NH3, or CH3OH to electricity has been made, and the storage methods for each fuel have been selected. In addition, the methods and assumptions to estimate the power consumption of auxiliary systems have been described. Lastly, the vessel to be considered in the case study is described. Using these boundary conditions, all power and energy storage systems can be designed according to the same assumptions.

7

Power and Energy Storage System Design

This chapter will elaborate on the results of the design process of the offshore vessel's power and energy storage system. By elaborating on these systems, the fifth research question will be answered:

From a technical viewpoint, how do maritime PEMFC-based power systems compare when fueled by liquid hydrogen, ammonia, or methanol?

First, in section 7.1 the required power and energy will be calculated based on the vessel's operational profile. After this, the design of the power systems will be shown in section 7.2. Next, the energy storage system designs are listed in section 7.3. Lastly, the properties of the two systems combined will be discussed in section 7.4.

7.1. Required Power and Energy

This section lists the vessel's power and energy requirements resulting from its operations and auxiliary power demand. The sum of the operational and auxiliary power demands will be given so that the power generation and energy storage systems can be sized to meet these requirements.

7.1.1. Operations

Based on the load cases given in table 6.2, the operational profile will consist as follows:

- The vessel will first lay in port for 12% of the total trip time.
- After this, the vessel will maneuver out of port to open sea.
- Next, the vessel will sail to the installation site for 3% of the total trip time.
- After arriving at the installation site, the vessel will maneuver to it's correct position.
- At the vessel's correct position, it will lay in DP.
- Upon completing the crane operation on DP, the vessel will maneuver to the next location. There the vessel will operate in DP again. This process will repeat itself till 6% of the total trip time is spent on maneuvering and 76% of the time is spent in DP condition.
- After completion of the operations, the ship will sail back to port for 3% of the total trip time.

This single operational profile is assumed to be used to compare the various power generation and energy storage systems. The operational profile can change per assignment that the vessel is performing. The assumed operational profile leads to the required energy for operations as given in table 7.1.

Table 7.1: Energy required for operations per autonomy.

Autonomy	Required energy
7 days	3219 MWh
14 days	6495 MWh
21 days	9765 MWh
28 days	13028 MWh
35 days	16380 MWh

The values listed in table 7.1 will be used to size the energy storage system. The power requirement for DP will be used to size the power system since this is the operational condition with the largest power requirement. As listed in chapters 2 and 3, the components in the power system cannot cope with large load transients. Therefore, batteries will be used for peak shaving and gap filling during load transients. The largest load fluctuation will be used to size the battery system. This is the fluctuation between harbor condition and manoeuvering, giving a total load fluctuation of 12.1 MW within one hour.

7.1.2. Auxiliary

In addition to the power that the ship consumes for operations, auxiliary systems also require power input. The required power for these auxiliary systems includes:

- Power consumption from the batteries and DC-DC converters.
- Blowers to provide ventilation air to the power system and energy storage system compartments.
- Cooling pumps to cool power modules, batteries, DC-DC converters and engines.
- Compressors to compress air and nitrogen for purging with nitrogen.
- Blowers to provide process air to power modules.
- Pumps for fuel and deionized water.

The power requirements for the auxiliary systems are calculated using the approach given in section 6.3. listed in table 7.3. There is a relative difference in auxiliary power consumption between the various autonomies for the methanol-based power systems. This results from the requirement to purge methanol fuel tanks with nitrogen once the fuel in the tank is consumed. As the fuel tanks increase in size for larger autonomies, more nitrogen is required over the voyage. This difference is two MW between the power system with an autonomy of 7 days and 35 days. As this difference is too small to influence the results, the auxiliary power requirement similar to the autonomy of 35 days is assumed for all autonomies.

To obtain the required energy for the voyage, the auxiliary power is multiplied by the autonomy. Table 7.2 shows the resulting energy requirements.

Table 7.2: Energy required for auxiliary systems per autonomy and fuel.

Autonomy	LH2 MWh	NH3 MWh	CH3OH MWh	MDO MWh
7 days	115	157	138	69
14 days	230	314	277	138
21 days	345	471	415	207
28 days	460	627	554	277
35 days	575	784	694	346

7.1.3. Total Power & Energy Requirements

When power is delivered from the power modules, this power is first converted to regulated DC power using a DC-DC converter. This DC-DC converter is connected to the ship's DC bus. From the DC bus, consumers are provided with power. The power drawn from the DC bus for operations is converted to AC using an inverter. The auxiliary power consumers are assumed to be supplied with electrical power

from the DC bus. The losses of the control electronics for the auxiliary system components are assumed to be a part of the pump, compressor, or blower losses. The converter, inverter, and bus efficiencies must also be considered when calculating the vessel's total power and energy requirements. For the internal combustion engine case, it is assumed the generator sets provide unregulated AC electrical power. This power is converted to regulated AC and is fed to an AC bus. The consumers can be fed with AC power directly from this AC bus. To illustrate which components are considered in each case, the single-line diagrams are shown in figures 7.1 and 7.2.

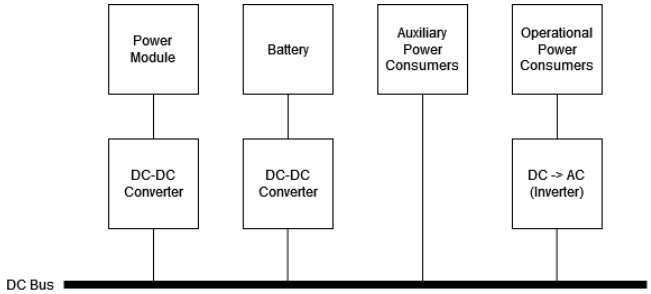

Figure 7.1: Single-line diagram showing the main electrical connections onboard the ship for the LH2, NH3, and CH3OH power systems.

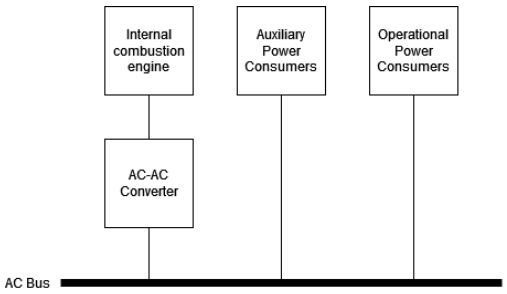

Figure 7.2: Single-line diagram showing the main electrical connections onboard the MDO power system.

Using the efficiencies of the components shown in the single-line diagram, the amount of power that the power modules must deliver is calculated. The results are shown in table 7.3.

Table 7.3: Power requirements per fuel type. The power module efficiency in the last column is the efficiency at maximum power.

Fuel	**Mission power** MW	**Auxiliary power** MW	**Total power** MW	**Power module efficiency**
LH2	24.8	0.7	25.5	48%
NH3	24.8	0.9	25.7	41%
CH3OH	24.8	0.8	25.6	40%
Diesel	24.8	0.4	25.2	40%

The energy required onboard the vessel for fuel storage is calculated similarly to the power: the energy supplied to consumers is divided by the inverter, bus, DC-DC converter, and power module efficiency. The efficiencies in table 7.3 are used for the power module efficiencies. The vessel is not constantly operating at its maximum power. Maximum power is only provided during short instances when the vessel operates in DP conditions with a strong current and an unfavorable heading. To account for the vessel not constantly operating at maximum power, the total energy required is multiplied by a factor of 0.4. The required amount of energy for the fuel is shown in table 7.4.

Table 7.4: Energy required in fuel per autonomy and fuel.

Autonomy	**LH2** MWh	**NH3** MWh	**CH3OH** MWh	**Diesel** MWh
7 days	7439	8886	8984	8552
14 days	15004	17923	18123	17253
21 days	22556	26942	27243	25936
28 days	30094	35946	36348	34604
35 days	37830	45185	45693	43504

The energy flows from fuel input to electrical power output to consumers are shown in figure 7.3. The largest energy loss is the loss from LHV fuel input to electrical power module output. Following this loss, the power modules themselves consume some of the power they generate for BoP components.

The energy flow to other auxiliary consumers, as described in subsection 7.1.2, are also visualized in figure 7.3.

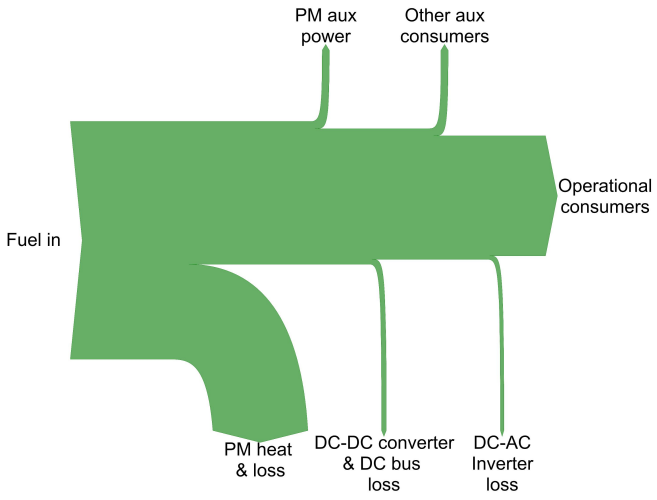

Figure 7.3: Sankey diagram showing the energy flow from fuel input to operational consumer output.

7.2. Power System Design

The power system is sized based on the required power and load transients. Based on the required installed power found in section 7.1.3 and the DP3 redundancy requirements, the number of power modules and the division into compartments as shown in appendix D were designed. An overview of the various power systems is shown in figure 7.4.

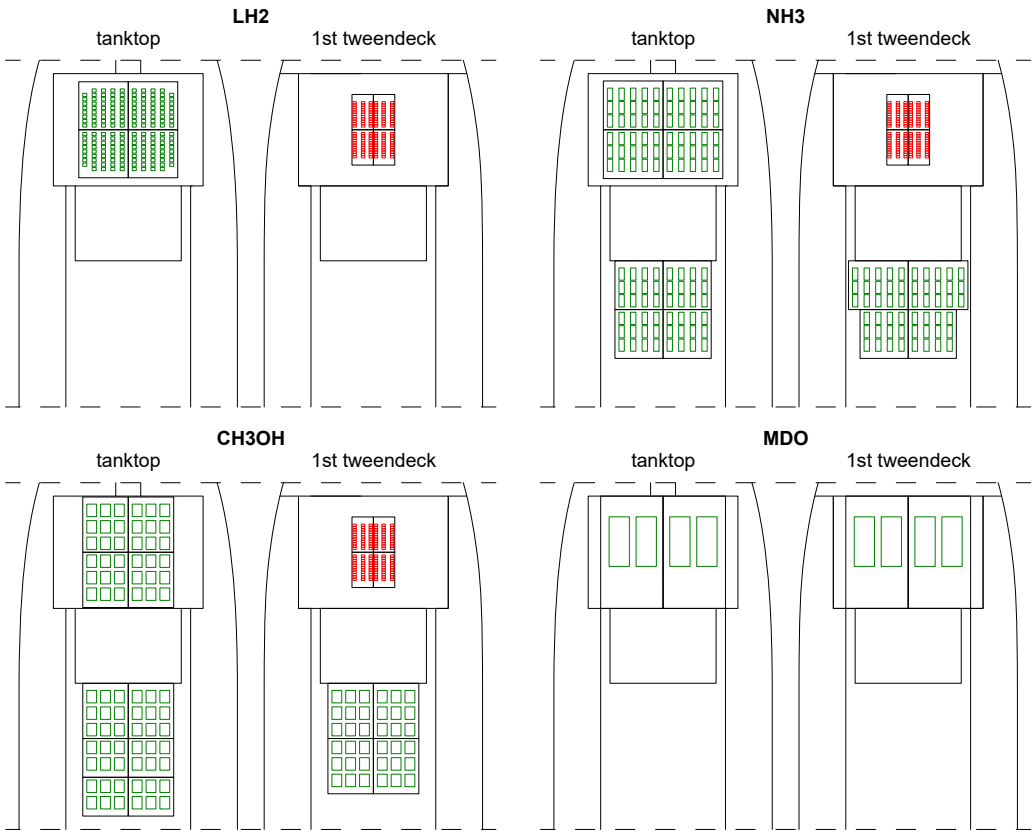

Figure 7.4: Overwiew of the power systems installed for each fuel. The power modules or internal combustion engines are indicated in green, the batteries are indicated in red.

When dividing the power system into compartments for DP3 redundancy, each compartment was sized to have approximately the same amount of surface area. Because he volumetric power densities of the power modules and internal combustion engines vary per fuel, the amount of compartments that is required also varies. Table 7.5 shows the total installed power, the amount of compartments in which the power system is installed and total power remaining with the loss of the largest compartment.

Table 7.5: Installed power and power with the loss of the largest compartment (DP3) per fuel.

Fuel	**Installed power** MW	**Number of compartments**	**DP3 Power** MW
LH2 (FC)	34.32	4	25.74
NH3 (FC)	28.56	12	26.01
CH3OH (FC)	28.04	14	25.83
MDO (ICE)	54.96	2	27.48

Given the power modules' load transient capabilities, they can deliver the largest load fluctuation in approximately 30 minutes. During this period, 6130 kWh of energy is consumed, requiring 99 batteries to be operational. When installing the battery packs in four compartments for DP3 redundancy, the amount of installed batteries is 132. During the periods where the vessel is consuming less power, the batteries are charged again; the batteries do not require recharging using shore power. Using the mass of the installed components and the volume of the compartments with the components installed in them, the total masses and volumes of the various systems were calculated. The total masses and volumes are shown in figures 7.5 and 7.6.

The masses of the LH2 and CH3OH power systems are significantly lower than that of the MDO base case and NH3 power system. The volume of the LH2 power system is significantly lower than the other systems. When dividing the installed power of each of the four systems as listed in table 7.5 by

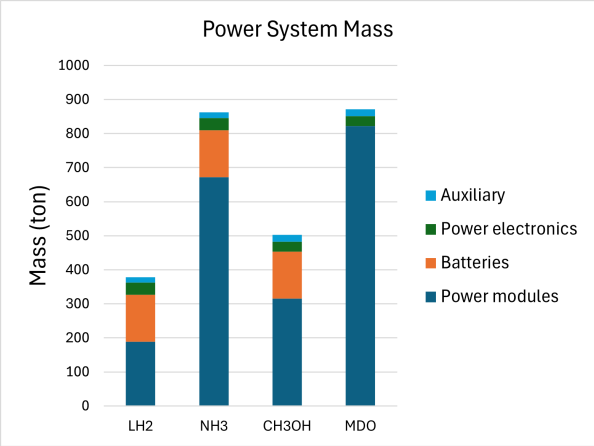

Figure 7.5: Power system mass per fuel.

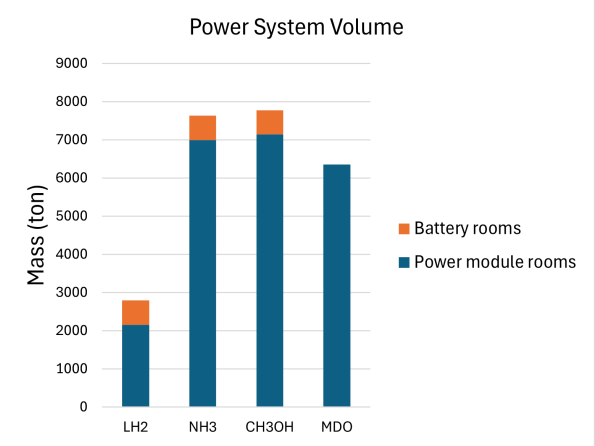

Figure 7.6: Power system volume per fuel.

their own mass and volume, the gravimetric and volumetric power densities in figure 7.7 and 7.8 are found.

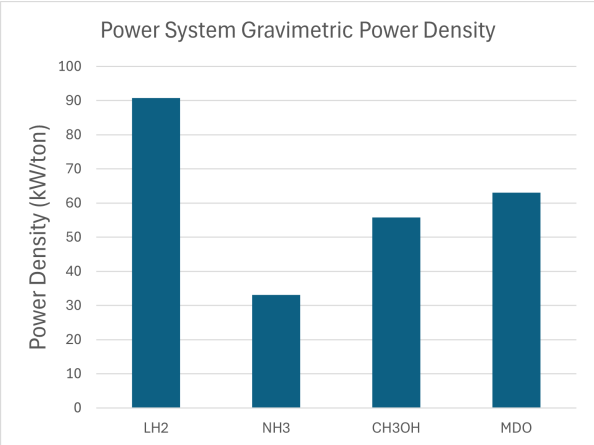

Figure 7.7: Power system gravimetric energy density per fuel.

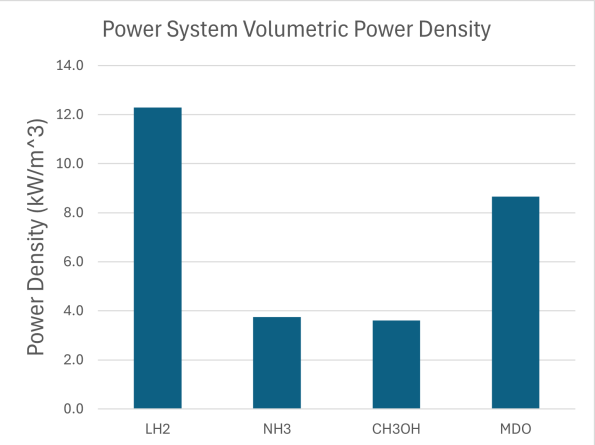

Figure 7.8: Power system volumetric energy density per fuel.

The resulting power densities show that LH2 based power systems offer the highest power output per unit of mass and per unit of volume. MDO based power systems have an intermediate power density compared to LH2.

7.3. Energy Storage System Design

Using the required amount of energy given in section 7.1.1, the fuel storage tanks were sized and positioned onboard the vessels. The arrangements of the energy storage systems are shown in appendix E. An overview of the size of the energy storage systems for an autonomy of 35 days is shown in figure 7.9. The routing of piping and ducting between the components of the energy storage and power generation systems is show in appendix F.

When varying the autonomy of the ship, the energy storage masses and volumes as given in figures 7.10 and 7.11 were calculated.

The mass of the MDO case is the lowest in all cases. This is caused by the intermediate LHV of MDO, reducing the weight of the fuel. In addition, MDO does not require independent tanks, which eliminates the need for large amounts of additional steel weight to construct the MDO tanks. After MDO, LH2 offers the lowest energy storage system mass. LH2 has a very high LHV, higher than that of MDO. This causes LH2 to require very little mass to store a certain amount of energy. LH2 requires independent tanks, causing additional mass compared to MDO. CH3OH is advantageous in terms of mass because the fuel does not require independent tanks; the tanks can thus be integrated into the

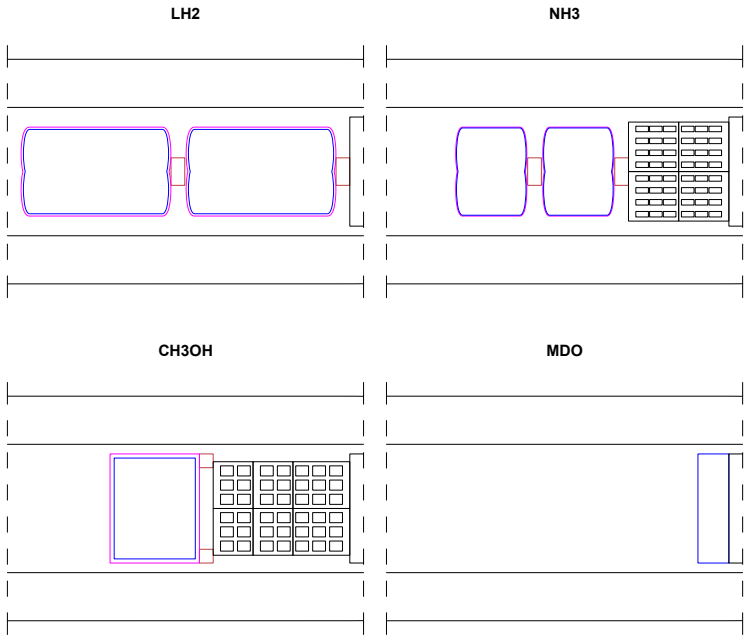

Figure 7.9: Overview of the energy storage systems for an autonomy of 35 days. The top view of the tanktop is shown in each figure. The inner tanks are indicated in blue, the outer tanks or cofferdams are indicated in magenta, the TCS is indicated in brown.

ship's structure. The low LHV of CH3OH causes the mass of the energy storage system to be higher than that of MDO and LH2 but lower than that of NH3. NH3 has a relatively low LHV, and it requires independent tanks. These two factors cause the mass of the NH3 storage system to be higher than the storage systems of other fuels.

The difference in energy storage system volumes is always linked to the LHV and fuel density. For LH2 and NH3, the tanks' double walls and filling limits contribute to their large volume requirements. As CH3OH tanks require cofferdams, this increases the volume requirements of CH3OH storage systems.

The gravimetric and volumetric energy densities of the energy storage systems are calculated per autonomy and shown in figures G.1 and G.2. The energy density increases with autonomy, because the TCS and bunker stations are assumed to have the same size for all autonomies. The gravimetric and volumetric energy densities of the various fuels for an autonomy of 35 days are shown in figures 7.12 and 7.13.

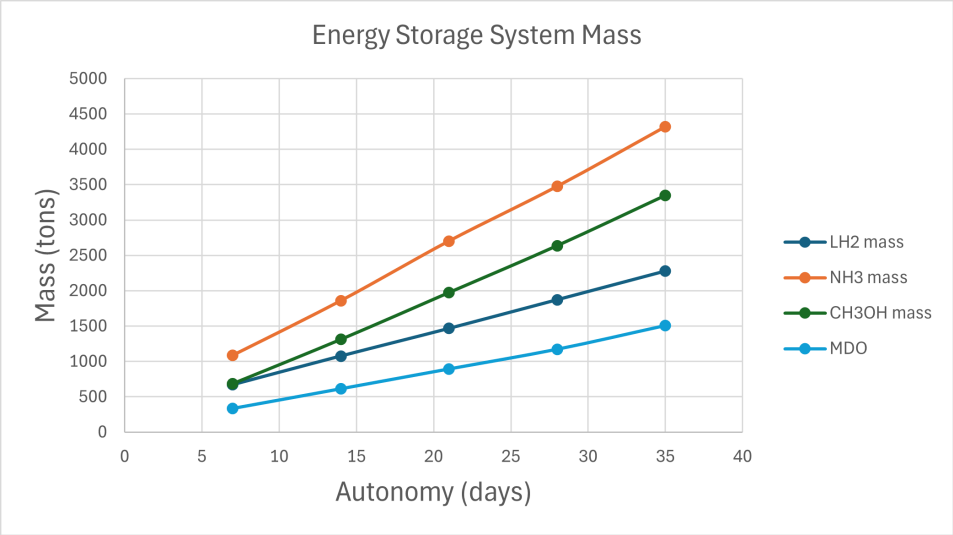

Figure 7.10: Energy storage system mass per fuel and autonomy.

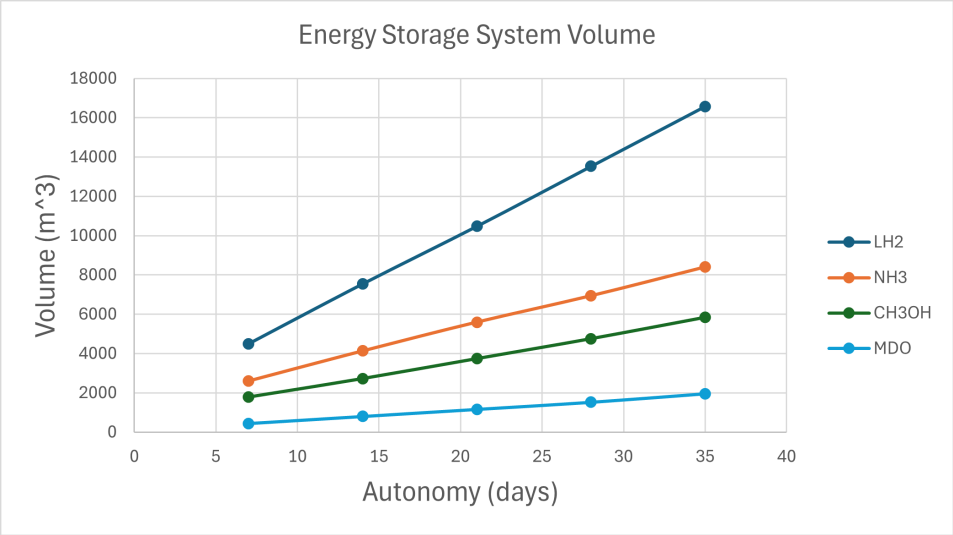

Figure 7.11: Energy storage system volume per fuel and autonomy.

Figures 7.12 and 7.13 show MDO has the highest energy density in mass and volume. NH3 and CH3OH have intermediate volumetric and gravimetric energy densities. LH2 has a higher gravimetric energy density than NH3 and CH3OH but has the lowest volumetric energy density of all fuels.

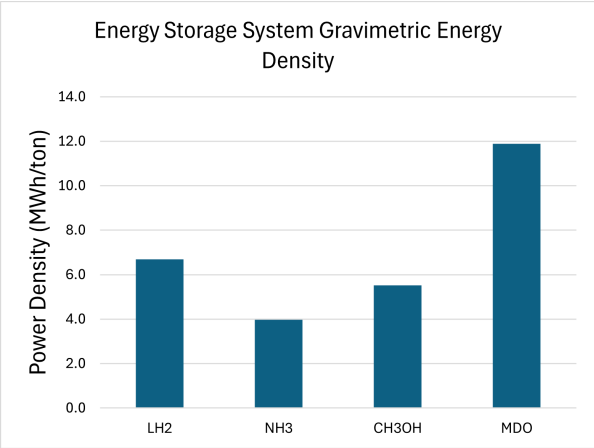

Figure 7.12: Energy storage system gravimetric energy density per fuel.

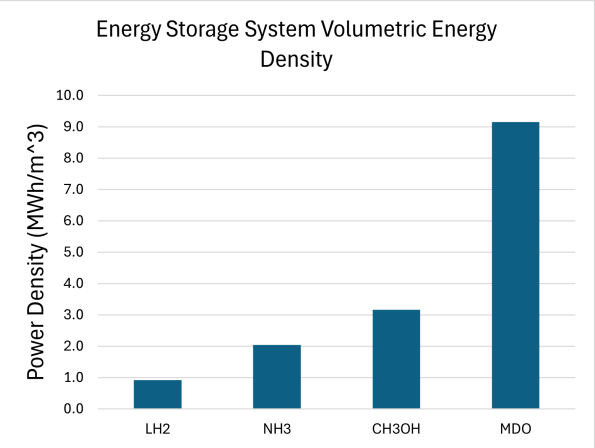

Figure 7.13: Energy storage system volumetric energy density per fuel.

7.4. Combined Systems

When the masses and volumes of the power and energy storage systems are combined, the total masses and volumes per fuel type are found. The results are shown in figures 7.14 and 7.15.

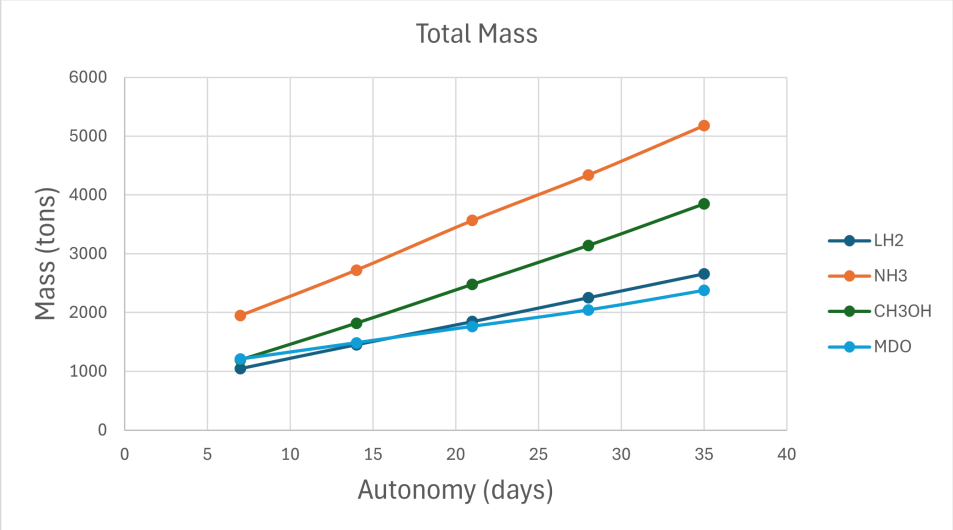

Figure 7.14: Total mass for power and energy storage systems per fuel and autonomy.

The MDO-ICE and LH2-PM systems are comparable in terms of mass. For lower autonomies, CH3OH-PM systems are comparable to LH2-PM and MDO-ICE systems. For higher autonomies, CH3OH-PM systems are heavier than LH2-PM and MDO-ICE. NH3-PM systems are heavier than all other systems for all autonomies.

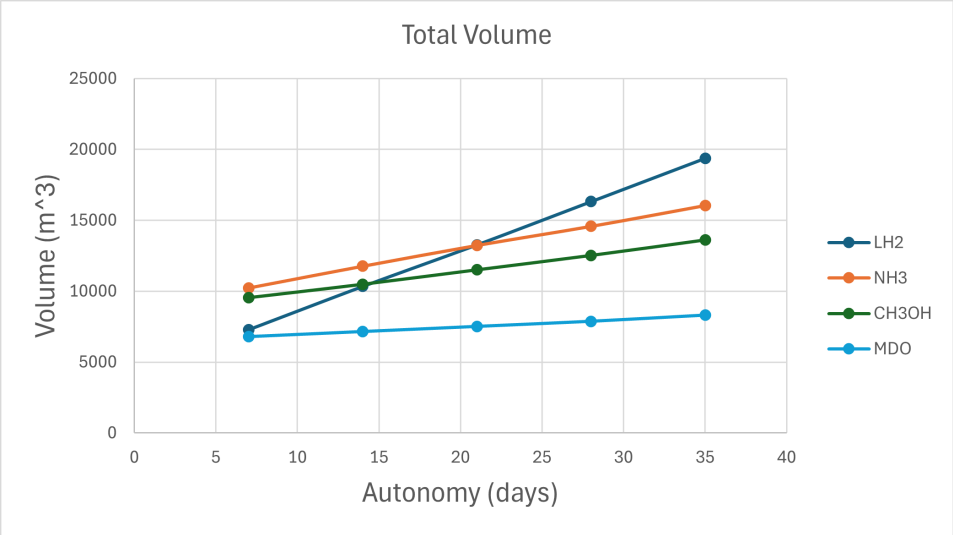

Figure 7.15: Total volume for power and energy storage systems per fuel and autonomy.

MDO-ICE systems offer the lowest volume for all autonomies. When considering alternative fuels, LH2-PM systems consume less volume than NH3-PM and CH3OH-PM systems for lower autonomies. This changes for higher autonomies because the LH2 storage system's volumetric energy density is lower than that of NH3 and CH3OH storage systems. The power system fuelled by NH3 is smaller than the one fuelled by CH3OH. However, the difference between the sizes of these systems is so small that the larger volumetric energy density of the CH3OH storage system compensates for it.

The alternative fuel-based systems require more volume onboard the vessel than the conventional MDO-ICE base case. This volume cannot be used for other purposes onboard the vessel. In the case of the offshore vessel, this volume could have been used to install other systems such as pipelaying equipment, cable laying equipment, moonpools, or motion-compensated platforms. To illustrate how much of this usable volume is lost when installing LH2-PM, NH3-PM, or CH3OH-M instead of MDO-ICE systems, the lost volume is expressed as a percentage compared to the MDO-ICE base case. The results of this calculation are shown in figure 7.16.

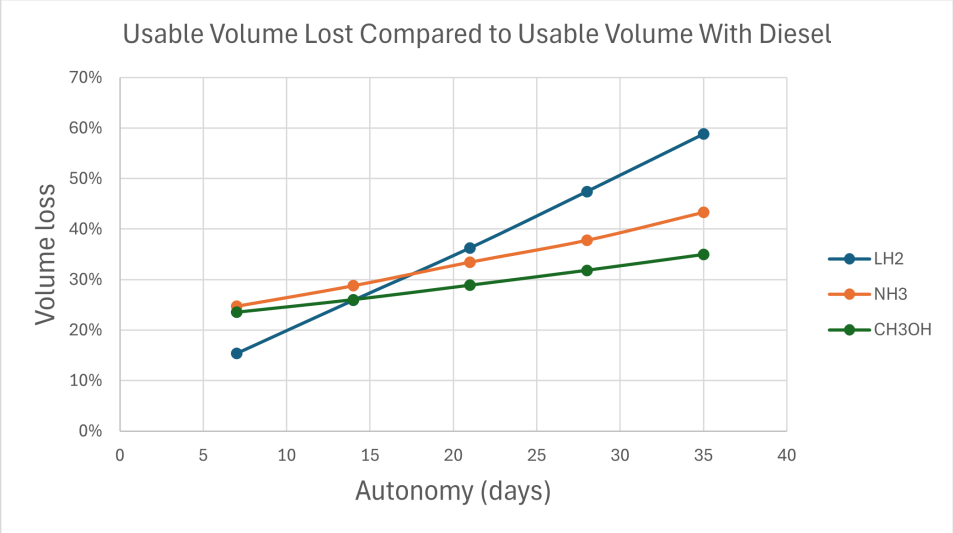

Figure 7.16: Loss of volume compared to an ICE power system with a diesel storage system per fuel and autonomy.

The trends seen in figure 7.16 are similar to those of the total volume plot in figure 7.15. The volume that can no longer be used leads to a reduction in the vessel's capabilities. Regarding the case study, several remarks can be made:

- The power and energy storage system designs strongly depend on the vessel selected for the case study and its operating profile. The offshore ship considered in the case study has relatively much space available for the installation of PEMFC-based power systems and storage systems for alternative fuels. Other vessels might be more volume-critical, causing greater difficulty in implementing such systems. This vessel has been designed with a vent mast for LNG, facilitating the installation of vent masts for LH2, NH3, and CH3OH. Vent mast positioning requirements with a hazardous zone radius of 25m might lead to problems when designing smaller vessels. In addition, the DP3 redundancy requires more power modules and batteries to be installed onboard than required for the mission. This causes the costs, mass, and volume of the power system to increase; this problem does not occur for vessels where no redundancy is required. Also, this vessel has large load fluctuations between the various operational profiles. This leads to a requirement for a larger battery support system to handle load transients. Vessels with smaller load fluctuations over time require fewer batteries to handle these transients.
- The designs were made based on estimations and assumptions of the performance of the system's components. Designs with higher accuracy can be achieved by modeling the total system, including the behavior of the power modules, batteries, load, electrical power busses, auxiliary equipment, ducting, and piping. In addition, more elaborate specifications of the components are required to obtain designs with high detail levels.
- The trends in volume and mass requirements for the power and energy storage systems are expected to be similar for different vessels, because the dimensions of the power modules, the margins between components, and the volumetric and gravimetric energy densities are assumed to be equal for other vessels.
- The choice for the most favorable alternative fuel might not always be dependent on mass and volume, but also on other factors. For instance, flammability, toxicity and fuel availability might also influence a ship owner's decision to use a certain fuel.

The case study shows that designing a maritime PEMFC system operating on alternative fuels is possible. Due to the modularity of the components used, the systems could have been designed for a range of output powers. These powers range from a few hundred kilowatts to the megawatt scale.

The vessel considered in the case study has abundant volume on the lower decks that can be used for power and energy storage systems. In smaller vessels, the volume requirements of such systems might limit the potential for the application of maritime PEMFC systems in combination with alternative fuel storage.

7.5. Conclusion

This chapter elaborated on the power and energy storage system designs to answer the research question: "From a technical viewpoint, how do maritime PEMFC-based power systems compare when fueled by liquid hydrogen, ammonia, or methanol?".

The most favorable power and energy storage system designs were made for all alternative fuels and the base case on MDO. All systems using fuel cells are combined with battery systems to handle load transients. Liquid hydrogen-PEMFC power systems offer the highest power density of all considered systems. MDO energy storage systems offer the highest gravimetric and volumetric energy density of all considered systems. For the PEMFC systems operating on alternative fuels, methanol energy storage systems offer the highest volumetric energy density and liquid hydrogen energy storage systems offer the highest gravimetric energy density. The power requirement of auxiliary systems and electrical losses in the ship's power system have been considered. The use of alternative fuels in combination with fuel cells reduces the usable volume onboard the vessel.

The most favorable power and energy storage systems use power modules that integrate the PEMFC, fuel processing equipment, and BoP equipment in one enclosure to reduce the number of hazardous zones. Batteries are used to handle load transients on the system.

As this case study is based on a specific vessel, its results are mainly valid for this particular vessel. The trends for mass and volume requirements by the power and energy storage systems are expected

to remain similar for other vessels. If a higher level of detail is required, more detailed component specifications and modeling of the entire system are required. In addition, total mass and volume are not the only performance indicators for selecting a ship's power system and fuel.

8

Discussion

This report discusses the main findings of this thesis and the limitations of the results. It will do so by first discussing the economics of FC systems in section 8.1. Next, WTW emissions and externalities will be discussed will be discussed in section 8.2. Lastly, the technological maturity of the components will be mentioned in section 8.3.

8.1. Economics

After designing the various power and energy storage systems, the costs of these systems have not been calculated. It is assumed the costs of a maritime PEMFC system lie in the order of 1500-2000 $/kW, and those of maritime NH3 and CH3OH cracking/reforming systems lie in the order of 2000-2500 $/kW. The costs of ICEs are assumed to be approximately 550 $/kW; batteries are assumed to cost approximately 700 $/kWh. This brings the total CAPEX of PEMFC-based power systems several orders of magnitude higher than the costs of ICE-MDO systems.

8.2. WTW Emissions and Externalities

This thesis considers the local emissions from using liquid hydrogen, ammonia, and methanol onboard ships. To assess the total environmental impact of using alternative fuels, one should calculate the total WTW (well-to-wake) emissions, which include the emissions resulting from fuel production and transportation. In addition, the environmental impact of producing, disposing of, and recycling fuel cells, fuel processing systems, batteries, and other equipment should be considered when comparing fuels and power systems.

In addition to the environmental impacts resulting from the use of maritime power systems and alternative fuels, this use can also affect societal aspects. An example of where these aspects occur is the mining of rare earth elements to produce fuel cells, fuel processing systems, and batteries. This is often done in low-wage countries with poor labor conditions [153]. Massive consumption of rare earth elements could have undesired externalities and should be considered when researching the use of maritime PEMFC systems operating on alternative fuels.

Conversely, using sustainable alternative fuels that result in low WTW emissions can offer lower external environmental costs. For all external costs, it holds that the ship owner will not directly pay for or benefit from these costs. Legislators try to let ship owners pay for these externalities by means of taxes, or they let ship owners benefit from externalities by means of subsidies. However, this may not compensate for the large cost difference between renewable and fossil fuels.

8.3. Technological Maturity

As stated earlier in this thesis, the current TRL of maritime fuel cell system and fuel processing systems is limited. This can be seen by the limited amount of commercially available systems. When fuel cell and fuel processing technology progresses, it is likely that this changes the feasibility for implementation of this technology onboard ships.

9 Conclusion

This report was written to describe the findings of the thesis with the following main research question:

How can maritime fuel cell systems be applied effectively using liquid hydrogen, ammonia, and methanol and how do these compare to each other?

The following five sub-questions were formulated and answered to answer this main research question. The conclusions on each research question are listed below:

1. What is the most suitable type of fuel cell for maritime applications?

The PEMFC and SOFC are currently considered viable options for installation onboard ships. The PEMFC has the highest power density and technical maturity, but it requires very pure hydrogen fuel input and the possibilities for WHR with this FC type are limited. Despite its drawbacks, the LT-PEMFC is currently regarded as the most mature fuel cell type because of its highest TRL and power density, and lowest cost.

Fuel cell stacks operate with BoP systems, allowing them to operate within the desired operating conditions. These BoP components influence the efficiency and load response of the fuel cell system. Battery systems may aid fuel cells connected to fluctuating electrical loads. These battery systems can cope with transients in the load demand using peak shaving and gap filling. This allows the fuel cell to operate on a more constant power level.

2. What are the properties of ammonia crackers, methanol reformers, and other required fuel processing systems for proton exchange membrane fuel cells in maritime applications?

Firstly, desulfurization is required when sulfur-containing fuels are used in fuel cells. After this, fuel conversion is required to convert methanol or ammonia to hydrogen for use in fuel cells. Next, CO removal is required for syngas streams for use in PEMFCs. Lastly, other fuel purification steps may be required to remove the remaining impurities from hydrogen gas streams. These fuel processing steps occur at various temperatures and can be endo- or exothermic.

Fuel processing systems influence the ship's power system efficiency and require mass and volume onboard. In addition, fuel processing systems have limited capabilities to respond to changes in output demand rapidly; they thus influence the transient response of a ship's power system. These aspects must be considered when designing a ship's power system with fuel processing systems.

Some manufacturers combine fuel conversion processes in commercially available modules for ship installation to supply pure hydrogen to fuel cells. Others combine these fuel processing systems with fuel cells in modules for ship installation to convert ammonia or methanol to electricity.

3. What are the properties of liquid hydrogen, ammonia, and methanol storage systems onboard ships?

Liquid hydrogen has the lowest energy density compared to the other two alternative fuels. It is also a very flammable substance, more flammable than methanol and ammonia. Fire and explosion prevention measures must thus be taken. Ammonia has an intermediate gravimetric and volumetric

energy density compared to the other two alternative fuels. Ammonia is very toxic, and mitigation measures are required to prevent it from coming into contact with people, animals, or the environment. The flammability limits of ammonia should also be considered when designing ammonia storage systems. Methanol has the highest gravimetric and volumetric energy density, but the fuel contains carbon, and the fuel is toxic and flammable. Therefore, mitigation measures are required to ensure the carbon emissions are used in a renewable way, the risk of fire and explosion is minimized, and the fuel will not come into contact with people and animals.

General guidelines for the storage masses and volumes of these alternative fuels can be found, but the actual storage masses and volumes of these alternative fuels are to be calculated for each design individually.

4. Are there vessel designs or research projects that use liquid hydrogen, ammonia, or methanol as fuel in combination with fuel cells? If so, what are their specifications or findings?

Based on vessel designs and research projects, it was seen that PEMFC-powered vessels fuelled by hydrogen are currently in operation in small quantities. These vessels are often smaller in size and have limited autonomy. More hydrogen-fuelled vessels are currently being developed. Methanol and ammonia-fuelled vessels using PEMFCs as primary power source are currently not in commercial operation. Some projects use ammonia or methanol-fuelled fuel cell systems to demonstrate their technological feasibility. When connecting these findings to the main research question, it can be concluded that fuel cell-powered vessels are still in development, and experience from operating these vessels is yet to be gained. Some specifications about these systems were mentioned in this chapter, but no in-depth information about these ships is available to the public.

The limited amount of vessels in operation using the technologies discussed in this report and the lack of studies that compared the use of liquid hydrogen, ammonia, and methanol for use in fuel cells as primary power sources further confirm there is a literature gap around the topic of this thesis.

5. From a technical viewpoint, how do maritime PEMFC-based power systems compare when fueled by liquid hydrogen, ammonia, or methanol?

A case study on an offshore heavy lift vessel was performed to compare different PEMFC-based power system and energy storage system configurations. The power and energy storage system designs were made for all alternative fuels and a base case on MDO. All systems using fuel cells are combined with battery systems to handle load transients.

Liquid hydrogen-PEMFC systems offer the highest power density of all considered systems, and MDO-ICE systems offer the highest energy density. For the PEMFC systems operating on alternative fuels, methanol-PEMFC systems offer the highest volumetric energy density, and liquid hydrogen-PEMFC systems offer the highest gravimetric energy density. The power requirement of auxiliary systems and electrical losses in the ship's power system have been considered. The use of alternative fuels in combination with fuel cells reduces the usable volume onboard the vessel.

The most favorable power and energy storage systems use power modules that integrate the PEMFC, fuel processing equipment, and BoP equipment in one enclosure to reduce the number of hazardous zones. Batteries are used to handle load transients on the system.

As this case study is based on a specific vessel, the results of the case study are mainly valid for this particular vessel. The trends for mass and volume requirements by the power and energy storage systems are expected to remain similar for other vessels. If a higher level of detail is required, more detailed component specifications and modeling of the entire system are required. In addition, total mass and volume are not the only performance indicators for selecting a ship's power system and fuel.

How can maritime fuel cell systems be applied effectively using liquid hydrogen, ammonia, and methanol and how do these compare to each other?

Maritime fuel cell systems can be integrated into power modules that can be installed onboard ships. These modules are pre-designed and offer power outputs in the order of several hundred kilowatts. The power modules can be installed in larger quantities onboard vessels to produce larger power outputs. This allows for multiple types of vessels with a broad range of power requirements to be fitted with power modules.

The comparison of various alternative fuels for use with fuel cells onboard ships contributes to choosing an alternative fuel for a specific vessel type. For smaller autonomies, liquid hydrogen-fueled PEMFC

systems are more compact than liquid ammonia and methanol-fueled systems. At larger autonomies, liquid ammonia or methanol-fueled systems will consume less volume than their liquid hydrogen-fuelled counterparts. The alternative fuel type that is most suitable for the vessel strongly depends on the vessel's operational profile, autonomy, and available volume for power and energy storage systems.

When considering suitable power and energy storage systems, the energy loss of auxiliary power consumers should also be considered, as their energy consumption cannot be neglected.

Current literature shows maritime fuel cell systems are not currently installed in many vessels. Therefore, how they will perform onboard ships for longer periods is uncertain. The limited development state of fuel cell technology is thus an important aspect that complicates the installation of fuel cells onboard ships.

This thesis compared maritime fuel cell systems operating on alternative fuels from a technical perspective. For purposes where costs are also an important indicator when comparing various fuels, it is recommended that further research into the economic feasibility of installing and operating fuel cell systems and alternative fuels onboard ships is performed.

9.1. Recommendations

To further assess the feasibility of maritime fuel cell systems onboard ships, the following research topics are recommended:

- Modelling of the various systems under dynamic operating conditions. Modeling PEMFC systems in combination with fuel processing systems, batteries, load, electrical systems, and auxiliary systems can gain more detailed insight into the sizing of the system's components and the performance of the system in real-life dynamic conditions. These dynamic models can be validated and improved with systems that are in service, increasing the models' accuracy.
- A detailed study of the economics of maritime PEMFC systems operating on alternative fuels can give possible operators of such systems and legislators further insight into the economic feasibility of maritime PEMFC systems operating on alternative fuels. These studies should include OPEX and CAPEX of the systems themselves, fuel prices, emission taxes, subsidies, and future prospects of all costs and gains.
- Liquid hydrogen, ammonia, and methanol are considered as energy carriers for this thesis. Future research may also be conducted on other energy carriers that may be beneficial over the ones considered in this thesis.
- This thesis mainly regarded LT-PEMFCs. Future research may also consider other FC types, such as HT-PEMFCs and SOFCs.
- The power systems considered in this thesis are primarily based on FCs. Future research may also consider the combination of FCs with (gas) turbines, combustion engines, and other energy converters to improve the power system's efficiency.
- Carbon capture and storage is not considered in this thesis. As methanol contains carbon, CCS can be used to mitigate the ship's carbon emissions. On the other hand, CCS systems consume power, require mass and volume allocation onboard the vessel, and do not capture all carbon emissions. The influence of maritime CCS systems should thus be researched.

References

[1] L. Al-Ghussain, "Global warming: Review on driving forces and mitigation," *Environmental Progress & Sustainable Energy*, vol. 38, no. 1, pp. 13–21, 2019. DOI: https://doi.org/10.1002/ep.13041. eprint: https://aiche.onlinelibrary.wiley.com/doi/pdf/10.1002/ep.13041. [Online]. Available: https://aiche.onlinelibrary.wiley.com/doi/abs/10.1002/ep.13041.

[2] M. Kampa and E. Castanas, "Human health effects of air pollution," *Environmental Pollution*, vol. 151, no. 2, pp. 362–367, 2008, Proceedings of the 4th International Workshop on Biomonitoring of Atmospheric Pollution (With Emphasis on Trace Elements), ISSN: 0269-7491. DOI: https://doi.org/10.1016/j.envpol.2007.06.012. [Online]. Available: https://www.sciencedirect.com/science/article/pii/S0269749107002849.

[3] J. Yang *et al.*, "Controlling emissions from an ocean-going container vessel with a wet scrubber system," *Fuel*, vol. 304, p. 121 323, 2021, ISSN: 0016-2361. DOI: https://doi.org/10.1016/j.fuel.2021.121323. [Online]. Available: https://www.sciencedirect.com/science/article/pii/S0016236121012023.

[4] R. Vignesh and B. Ashok, "Critical interpretative review on current outlook and prospects of selective catalytic reduction system for de-nox strategy in compression ignition engine," *Fuel*, vol. 276, p. 117 996, 2020, ISSN: 0016-2361. DOI: https://doi.org/10.1016/j.fuel.2020.117996. [Online]. Available: https://www.sciencedirect.com/science/article/pii/S0016236120309923.

[5] P. Zhou and H. Wang, "Carbon capture and storage—solidification and storage of carbon dioxide captured on ships," *Ocean Engineering*, vol. 91, pp. 172–180, 2014, ISSN: 0029-8018. DOI: https://doi.org/10.1016/j.oceaneng.2014.09.006. [Online]. Available: https://www.sciencedirect.com/science/article/pii/S0029801814003229.

[6] J. C. Summers, S. Van Houtte, and D. Psaras, "Simultaneous control of particulate and nox emissions from diesel engines," *Applied Catalysis B: Environmental*, vol. 10, no. 1, pp. 139–156, 1996, ISSN: 0926-3373. DOI: https://doi.org/10.1016/0926-3373(96)00028-8. [Online]. Available: https://www.sciencedirect.com/science/article/pii/0926337396000288.

[7] Á. Benet, A. Villalba-Herreros, R. d'Amore-Domenech, and T. J. Leo, "Knowledge gaps in fuel cell-based maritime hybrid power plants and alternative fuels," *Journal of Power Sources*, vol. 548, p. 232 066, Nov. 2022, ISSN: 0378-7753. DOI: 10.1016/J.JPOWSOUR.2022.232066.

[8] K. Scott, "Membrane electrode assemblies for polymer electrolyte membrane fuel cells," *Functional Materials for Sustainable Energy Applications*, pp. 279–311, Jan. 2012. DOI: 10.1533/9780857096371.3.279.

[9] A. Hermann, T. Chaudhuri, and P. Spagnol, "Bipolar plates for pem fuel cells: A review," *International Journal of Hydrogen Energy*, vol. 30, no. 12, pp. 1297–1302, 2005, Cancun 2003, ISSN: 0360-3199. DOI: https://doi.org/10.1016/j.ijhydene.2005.04.016. [Online]. Available: https://www.sciencedirect.com/science/article/pii/S0360319905000935.

[10] G. Athanasaki, A. Jayakumar, and A. M. Kannan, "Gas diffusion layers for pem fuel cells: Materials, properties and manufacturing – a review," *International Journal of Hydrogen Energy*, vol. 48, pp. 2294–2313, 6 Jan. 2023, ISSN: 0360-3199. DOI: 10.1016/J.IJHYDENE.2022.10.058.

[11] P. C. Okonkwo and C. Otor, "A review of gas diffusion layer properties and water management in proton exchange membrane fuel cell system," *International Journal of Energy Research*, vol. 45, pp. 3780–3800, 3 2021. DOI: https://doi.org/10.1002/er.6227. [Online]. Available: https://onlinelibrary.wiley.com/doi/abs/10.1002/er.6227.

[12] J. W. Haverkort, "A theoretical analysis of the optimal electrode thickness and porosity," *Electrochimica Acta*, vol. 295, pp. 846–860, Feb. 2019, ISSN: 0013-4686. DOI: 10.1016/J.ELECTACTA.2018.10.065.

[13] M. Saufi Sulaiman, B. Singh, and W. Mohamed, “Experimental and theoretical study of thermoelectric generator waste heat recovery model for an ultra-low temperature pem fuel cell powered vehicle,” *Energy*, vol. 179, pp. 628–646, 2019, ISSN: 0360-5442. DOI: https://doi.org/10.1016/j.energy.2019.05.022. [Online]. Available: https://www.sciencedirect.com/science/article/pii/S0360544219308850.

[14] O. Z. Sharaf and M. F. Orhan, “An overview of fuel cell technology: Fundamentals and applications,” *Renewable and Sustainable Energy Reviews*, vol. 32, pp. 810–853, Apr. 2014, ISSN: 13640321. DOI: 10.1016/j.rser.2014.01.012.

[15] B. Gou, W. Na, and B. Diong, *Fuel Cells: Dynamic Modeling and Control with Power Electronics Applications*, 2nd ed. CRC Press, Taylor & Francis Group, 2020.

[16] T. Wilberforce *et al.*, “Modelling and simulation of proton exchange membrane fuel cell with serpentine bipolar plate using matlab,” *International Journal of Hydrogen Energy*, vol. 42, pp. 25 639–25 662, 40 2017, ISSN: 0360-3199. DOI: https://doi.org/10.1016/j.ijhydene.2017.06.091. [Online]. Available: https://www.sciencedirect.com/science/article/pii/S0360319917324035.

[17] V. S. Bagotsky, A. M. Skundin, and Y. M. Volfkovich, *Electrochemical Power Sources: Batteries, Fuel Cells and Supercapacitors*. John Wiley & Sons, Inc, 2015.

[18] L. van Biert and K. Visser, *Fuel cells systems for sustainable ships*. 2022. DOI: 10.1016/B978-0-12-824471-5.00010-4.

[19] P. Breeze, *Fuel Cells*, 1st ed. Joe Hayton, Elsevier, 2017.

[20] M. S. Alias, S. K. Kamarudin, A. M. Zainoodin, and M. S. Masdar, “Active direct methanol fuel cell: An overview,” *International Journal of Hydrogen Energy*, vol. 45, pp. 19 620–19 641, 38 Jul. 2020, ISSN: 03603199. DOI: 10.1016/j.ijhydene.2020.04.202.

[21] H. Xing, C. Stuart, S. Spence, and H. Chen, “Fuel cell power systems for maritime applications: Progress and perspectives,” *Sustainability (Switzerland)*, vol. 13, pp. 1–34, 3 Feb. 2021, ISSN: 20711050. DOI: 10.3390/su13031213.

[22] T. B. Ferriday and P. H. Middleton, *Alkaline fuel cell technology - a review*, May 2021. DOI: 10.1016/j.ijhydene.2021.02.203.

[23] A. T. Hamada, M. F. Orhan, and A. M. Kannan, “Alkaline fuel cells: Status and prospects,” *Energy Reports*, vol. 9, pp. 6396–6418, Dec. 2023, ISSN: 23524847. DOI: 10.1016/j.egyr.2023.05.276.

[24] T. Tronstad, H. H. Åstrand, G. P. Haugom, and L. Langfeldt. “Emsa study on the use of fuel cells in shipping.” (2017), [Online]. Available: https://www.emsa.europa.eu/publications/download/4545/2921/23.html. accessed Nov. 28, 2023.

[25] A. G. Elkafas, M. Rivarolo, E. Gadducci, L. Magistri, and A. F. Massardo, *Fuel cell systems for maritime: A review of research development, commercial products, applications, and perspectives*, Jan. 2023. DOI: 10.3390/pr11010097.

[26] R. R. Contreras, J. Almarza, and L. Rincón, “Molten carbonate fuel cells: A technological perspective and review,” *Energy Sources, Part A: Recovery, Utilization and Environmental Effects*, 2021, ISSN: 15567230. DOI: 10.1080/15567036.2021.2013346.

[27] Z. Fu *et al.*, “Fuel cell and hydrogen in maritime application: A review on aspects of technology, cost and regulations,” *Sustainable Energy Technologies and Assessments*, vol. 57, Jun. 2023, ISSN: 22131388. DOI: 10.1016/j.seta.2023.103181.

[28] K. Joon, “Critical issues and future prospects for molten carbonate fuel cells,” *Journal of Power Sources*, vol. 61, no. 1, pp. 129–133, 1996, ISSN: 0378-7753. DOI: https://doi.org/10.1016/S0378-7753(96)02349-X. [Online]. Available: https://www.sciencedirect.com/science/article/pii/S037877539602349X.

[29] G. Kaur, *PEM Fuel Cells: Fundamentals, Advanced Technologies, and Practical Application*. Candice Janco, Elsevier, 2022. DOI: https://doi.org./10.1016/C2020-0-00143-X.

[30] K. Benmouiza and A. Cheknane, "Analysis of proton exchange membrane fuel cells voltage drops for different operating parameters," *International Journal of Hydrogen Energy*, vol. 43, no. 6, pp. 3512–3519, 2018, ISSN: 0360-3199. DOI: https://doi.org/10.1016/j.ijhydene.2017.06.082. [Online]. Available: https://www.sciencedirect.com/science/article/pii/S0360319917323583.

[31] Q. Liu, F. Lan, J. Chen, C. Zeng, and J. Wang, "A review of proton exchange membrane fuel cell water management: Membrane electrode assembly," *Journal of Power Sources*, vol. 517, p. 230 723, Jan. 2022, ISSN: 0378-7753. DOI: 10.1016/J.JPOWSOUR.2021.230723.

[32] S. Park, J. W. Lee, and B. N. Popov, "A review of gas diffusion layer in pem fuel cells: Materials and designs," *International Journal of Hydrogen Energy*, vol. 37, pp. 5850–5865, 7 Apr. 2012, ISSN: 0360-3199. DOI: 10.1016/J.IJHYDENE.2011.12.148.

[33] S. Authayanun, K. Im-Orb, and A. Arpornwichanop, *A review of the development of high temperature proton exchange membrane fuel cells*, 2015. DOI: 10.1016/S1872-2067(14)60272-2.

[34] O. B. Inal and C. Deniz, "Assessment of fuel cell types for ships: Based on multi-criteria decision analysis," *Journal of Cleaner Production*, vol. 265, Aug. 2020, ISSN: 09596526. DOI: 10.1016/j.jclepro.2020.121734.

[35] A. Kampker, H. Heimes, M. Kehrer, S. Hagedorn, P. Reims, and O. Kaul, "Fuel cell system production cost modeling and analysis," *Energy Reports*, vol. 9, pp. 248–255, 2023, 2022 9th International Conference on Power and Energy Systems Engineering, ISSN: 2352-4847. DOI: https://doi.org/10.1016/j.egyr.2022.10.364. [Online]. Available: https://www.sciencedirect.com/science/article/pii/S2352484722022995.

[36] M. Wei *et al.*, *A total cost of ownership model for high temperature pem fuel cells in combined heat and power applications*, 2014.

[37] V. Patil *et al.*, "Degradation mechanisms in pem fuel cells: A brief review," *Materials Today: Proceedings*, Apr. 2023, ISSN: 2214-7853. DOI: 10.1016/J.MATPR.2023.03.603.

[38] A. Moradi Bilondi, M. Abdollahzadeh, M. Kermani, H. Heidary, and P. Havaej, "Numerical study of anode side co contamination effects on pem fuel cell performance; and mitigation methods," *Energy Conversion and Management*, vol. 177, pp. 519–534, 2018, ISSN: 0196-8904. DOI: https://doi.org/10.1016/j.enconman.2018.09.076. [Online]. Available: https://www.sciencedirect.com/science/article/pii/S0196890418310781.

[39] N. Zamel and X. Li, "Transient analysis of carbon monoxide poisoning and oxygen bleeding in a pem fuel cell anode catalyst layer," *International Journal of Hydrogen Energy*, vol. 33, pp. 1335–1344, 4 Feb. 2008, ISSN: 0360-3199. DOI: 10.1016/J.IJHYDENE.2007.12.060.

[40] V. A. Sethuraman and J. W. Weidner, "Analysis of sulfur poisoning on a pem fuel cell electrode," *Electrochimica Acta*, vol. 55, pp. 5683–5694, 20 Aug. 2010, ISSN: 0013-4686. DOI: 10.1016/J.ELECTACTA.2010.05.004.

[41] F. I. Llerena, A. de las Heras Jiménez, E. L. González, F. S. Manzano, and J. M. A. Márquez, "Effects of ammonia impurities on the hydrogen flow in high and low temperature polymer electrolyte fuel cells," *Fuel Cells*, vol. 19, pp. 651–662, 6 Dec. 2019, ISSN: 16156854. DOI: 10.1002/fuce.201900031.

[42] L. van Biert, M. Godjevac, K. Visser, and P. V. Aravind, "A review of fuel cell systems for maritime applications," *Journal of Power Sources*, vol. 327, 2016, ISSN: 03787753. DOI: 10.1016/j.jpowsour.2016.07.007.

[43] Z. Huang, J. Shen, S. H. Chan, and Z. Tu, "Transient response of performance in a proton exchange membrane fuel cell under dynamic loading," *Energy Conversion and Management*, vol. 226, Dec. 2020, ISSN: 01968904. DOI: 10.1016/j.enconman.2020.113492.

[44] F. Balsamo, C. Capasso, T. Coppola, L. Micoli, R. Russo, and O. Veneri, "A case study on high-temperature fuel cells for hybrid electric ship propulsion," Institute of Electrical and Electronics Engineers Inc., 2023. DOI: 10.1109/ESARS-ITEC57127.2023.10114817.

[45] T. Zhang, P. Wang, H. Chen, and P. Pei, *A review of automotive proton exchange membrane fuel cell degradation under start-stop operating condition*, 2018. DOI: 10.1016/j.apenergy.2018.04.049.

[46] A. Vasilyev, J. Andrews, S. J. Dunnett, and L. M. Jackson, “Dynamic reliability assessment of pem fuel cell systems,” *Reliability Engineering & System Safety*, vol. 210, p. 107 539, Jun. 2021, ISSN: 0951-8320. DOI: 10.1016/J.RESS.2021.107539.

[47] Q. Xun, Y. Liu, and E. Holmberg, “A comparative study of fuel cell electric vehicles hybridization with battery or supercapacitor,” in *2018 International Symposium on Power Electronics, Electrical Drives, Automation and Motion (SPEEDAM)*, 2018, pp. 389–394. DOI: 10.1109/SPEEDAM.2018.8445386.

[48] P. Thounthong, V. Chunkag, P. Sethakul, B. Davat, and M. Hinaje, “Comparative study of fuel-cell vehicle hybridization with battery or supercapacitor storage device,” *IEEE Transactions on Vehicular Technology*, vol. 58, pp. 3892–3904, 8 2009, ISSN: 00189545. DOI: 10.1109/TVT.2009.2028571.

[49] H. L. Nguyen, J. Han, X. L. Nguyen, S. Yu, Y.-M. Goo, and D. D. Le, “Review of the durability of polymer electrolyte membrane fuel cell in long-term operation: Main influencing parameters and testing protocols,” *Energies*, vol. 14, no. 13, 2021, ISSN: 1996-1073. DOI: 10.3390/en14134048. [Online]. Available: https://www.mdpi.com/1996-1073/14/13/4048.

[50] Z. Hua, Z. Zheng, E. Pahon, M. C. Péra, and F. Gao, *A review on lifetime prediction of proton exchange membrane fuel cells system*, May 2022. DOI: 10.1016/j.jpowsour.2022.231256.

[51] Ballard Power Systems. “Fuel cell power for marine applications.” (2023), [Online]. Available: https://www.ballard.com/docs/default-source/spec-sheets/fcwavetm-specification-sheet.pdf?sfvrsn=6e44dd80_16. accessed Sep. 29, 2023.

[52] International Organization for Standardization, “Hydrogen fuel quality — Product specification,” ISO, Tech. Rep. ISO 14687:2019(E), 2019.

[53] PowerCell Group. “Marine system 200.” (2023), [Online]. Available: https://powercellgroup.com/segments/marine/. accessed Sep. 29, 2023.

[54] Nedstack Fuel Cell Technology BV. “Pemgen mt-fcpi-600.” (2023), [Online]. Available: https://nedstack.com/en/pemgen-solutions/maritime-power-installations/pemgen-mt-fcpi-600. accessed Sep. 29, 2023.

[55] T. Aarhaug. “Hydrogen purity introduction.” (2019), [Online]. Available: https://www.sintef.no/globalassets/projectweb/metrohyve-2/2-1-metrohydraite-aarhaug_hp_v1.pdf. accessed Nov. 8, 2023.

[56] TECO. “Teco marine fuel cell.” (2023), [Online]. Available: https://teco2030.no/solutions/teco-marine-fuel-cell/. accessed Oct. 10, 2023.

[57] Corvus Energy. “Corvus energy pelican fuel cell system.” (2023), [Online]. Available: https://corvusenergy.com/products/fuel-cell-systems/corvus-pelican-fuel-cell-system/. accessed Nov. 7, 2023.

[58] Zepp.solutions. “Zepp.x150.” (2023), [Online]. Available: https://zepp.solutions/en/x150/. accessed Nov. 7, 2023.

[59] J. E. McMurry, R. C. Fay, and J. K. Robinson, *Chemistry*, 7th ed. Pearson Education Limited, 2016.

[60] B. N. van Veldhuizen, L. van Biert, A. Amladi, T. Woudstra, K. Visser, and P. V. Aravind, “The effects of fuel type and cathode off-gas recirculation on combined heat and power generation of marine sofc systems,” *Energy Conversion and Management*, vol. 276, Jan. 2023, ISSN: 01968904. DOI: 10.1016/j.enconman.2022.116498.

[61] B. van Veldhuizen, E. Zera, L. van Biert, S. Modena, K. Visser, and P. Aravind, “Experimental evaluation of a solid oxide fuel cell system exposed to inclinations and accelerations by ship motions,” *Journal of Power Sources*, vol. 585, p. 233 634, Nov. 2023, ISSN: 0378-7753. DOI: 10.1016/J.JPOWSOUR.2023.233634. [Online]. Available: https://linkinghub.elsevier.com/retrieve/pii/S0378775323010108.

[62] P. K. Das, K. Jiao, Y. Wang, B. Frano, and X. Li, *Fuel Cells for Transportation: Fundamental Principles and Applications*. 2023. DOI: 10.1016/C2021-0-01629-1.

[63] F. Baldi, S. Moret, K. Tammi, and F. Maréchal, "The role of solid oxide fuel cells in future ship energy systems," *Energy*, vol. 194, Mar. 2020, ISSN: 03605442. DOI: 10.1016/j.energy.2019.116811.

[64] Z. Y. Vahc, C. Y. Jung, and S. C. Yi, "Performance degradation of solid oxide fuel cells due to sulfur poisoning of the electrochemical reaction and internal reforming reaction," *International Journal of Hydrogen Energy*, vol. 39, pp. 17 275–17 283, 30 Oct. 2014, ISSN: 0360-3199. DOI: 10.1016/J.IJHYDENE.2014.08.064.

[65] G. Jeerh, M. Zhang, and S. Tao, "Recent progress in ammonia fuel cells and their potential applications," *Journal of Materials Chemistry A*, vol. 9, pp. 727–752, 2 Jan. 2021, ISSN: 20507496. DOI: 10.1039/d0ta08810b.

[66] R. Peters, R. Dahl, U. Klüttgen, C. Palm, and D. Stolten, "Internal reforming of methane in solid oxide fuel cell systems," *Journal of Power Sources*, vol. 106, no. 1, pp. 238–244, 2002, Proceedings of the Seventh Grove Fuel Cell Symposium, ISSN: 0378-7753. DOI: https://doi.org/10.1016/S0378-7753(01)01039-4. [Online]. Available: https://www.sciencedirect.com/science/article/pii/S0378775301010394.

[67] R. Peters, E. Riensche, and P. Cremer, "Pre-reforming of natural gas in solid oxide fuel-cell systems," *Journal of Power Sources*, vol. 86, no. 1, pp. 432–441, 2000, ISSN: 0378-7753. DOI: https://doi.org/10.1016/S0378-7753(99)00440-1. [Online]. Available: https://www.sciencedirect.com/science/article/pii/S0378775399004401.

[68] L. van Biert, K. Visser, and P. V. Aravind, "A comparison of steam reforming concepts in solid oxide fuel cell systems," *Applied Energy*, vol. 264, p. 114 748, Apr. 2020, ISSN: 0306-2619. DOI: 10.1016/J.APENERGY.2020.114748.

[69] F. Mueller, F. Jabbari, and J. Brouwer, "On the intrinsic transient capability and limitations of solid oxide fuel cell systems," *Journal of Power Sources*, vol. 187, pp. 452–460, 2 Feb. 2009, ISSN: 0378-7753. DOI: 10.1016/J.JPOWSOUR.2008.11.057.

[70] M. A. Azizi and J. Brouwer, "Progress in solid oxide fuel cell-gas turbine hybrid power systems: System design and analysis, transient operation, controls and optimization," *Applied Energy*, vol. 215, pp. 237–289, Apr. 2018, ISSN: 0306-2619. DOI: 10.1016/J.APENERGY.2018.01.098.

[71] R. S. Gemmen and C. D. Johnson, "Effect of load transients on sofc operation—current reversal on loss of load," *Journal of Power Sources*, vol. 144, pp. 152–164, 1 Jun. 2005, ISSN: 0378-7753. DOI: 10.1016/J.JPOWSOUR.2004.12.027.

[72] Fuel Cell Energy. "Solid oxide fuel cells." (2023), [Online]. Available: https://www.fuelcellenergy.com/platform/solid-oxide-fuel-cell-platforms. accessed Oct. 10, 2023.

[73] Convion. "Convion products." (2023), [Online]. Available: https://convion.fi/products/. accessed Oct. 10, 2023.

[74] Bloom Energy. "Maritime server." (2023), [Online]. Available: https://www.bloomenergy.com/wp-content/uploads/bloom-energy-marine-energy-server.pdf. accessed Nov. 13, 2023.

[75] Bloom Energy. "The bloom energy server 5.5." (2023), [Online]. Available: https://www.bloomenergy.com/wp-content/uploads/bloom-energy-server-datasheet-2023.pdf. accessed Nov. 13, 2023.

[76] SolydERA. "Products." (2023), [Online]. Available: https://solydera.com/en/business-areas-solutions/. accessed Nov. 13, 2023.

[77] Alma Clean Power. "Our product." (2023), [Online]. Available: https://almacleanpower.com/what-we-do. accessed Nov. 13, 2023.

[78] T. Vidović, I. Tolj, G. Radica, and N. B. Ćoko, "Proton-exchange membrane fuel cell balance of plant and performance simulation for vehicle applications," *Energies*, vol. 15, 21 2022, ISSN: 1996-1073. DOI: 10.3390/en15218110. [Online]. Available: https://www.mdpi.com/1996-1073/15/21/8110.

[79] F. Segura and J. M. Andújar, "Step by step development of a real fuel cell system. design, implementation, control and monitoring," *International Journal of Hydrogen Energy*, vol. 40, pp. 5496–5508, 15 Apr. 2015, ISSN: 0360-3199. DOI: 10.1016/J.IJHYDENE.2015.01.178.

[80] W. Jung, M. Choi, J. Jeong, J. Lee, and D. Chang, "Design and analysis of liquid hydrogen-fueled hybrid ship propulsion system with dynamic simulation," *International Journal of Hydrogen Energy*, 2023, ISSN: 0360-3199. DOI: https://doi.org/10.1016/j.ijhydene.2023.09.205. [Online]. Available: https://www.sciencedirect.com/science/article/pii/S0360319923048243.

[81] C-Job Naval Architects, *Sustainability crash course*, Personal communication, 2023.

[82] M. F. Sgroi *et al.*, "Cost analysis of direct methanol fuel cell stacks for mass production," *Energies*, vol. 9, no. 12, 2016, ISSN: 1996-1073. DOI: 10.3390/en9121008. [Online]. Available: https://www.mdpi.com/1996-1073/9/12/1008.

[83] T. Chan. "Methanol fuel cells: Powering the future." (2020), [Online]. Available: https://www.methanol.org/wp-content/uploads/2020/04/Methanol-Fuel-Cell-Powering-the-Future-webinar-presentation.pdf. accessed Nov. 8, 2023.

[84] M. Ni, "Current status of fuel cell technologies," *Energy Exploration & Exploitation*, vol. 23, no. 3, pp. 207–214, 2005. DOI: 10.1260/014459805774852083.

[85] G. Mulder, P. Coenen, A. Martens, and J. Spaepen, "Market-ready stationary 6 kw generator with alkaline fuel cells," *ECS Transactions*, vol. 12, no. 1, p. 743, 2008. DOI: 10.1149/1.2921601. [Online]. Available: https://dx.doi.org/10.1149/1.2921601.

[86] L. Chick, M. Weimar, G. Whyatt, and M. Powell, "The case for natural gas fueled solid oxide fuel cell power systems for distributed generation," *Fuel Cells*, vol. 15, no. 1, pp. 49–60, 2015. DOI: https://doi.org/10.1002/fuce.201400103. eprint: https://onlinelibrary.wiley.com/doi/pdf/10.1002/fuce.201400103. [Online]. Available: https://onlinelibrary.wiley.com/doi/abs/10.1002/fuce.201400103.

[87] "Manufacturing cost analysis of 1 kw and 5 kw solid oxide fuel cell (sofc) for auxilliary power applications." (2014), [Online]. Available: https://www.energy.gov/eere/fuelcells/articles/manufacturing-cost-analysis-1-kw-and-5-kw-solid-oxide-fuel-cell-sofc. accessed Nov. 12, 2023.

[88] Wisselkoers.nl. "Wisselkoers usd." (2023), [Online]. Available: https://www.wisselkoers.nl/dollar-euro. accessed Nov. 13, 2023.

[89] C. Li *et al.*, "4e analysis of a novel proton exchange membrane fuel cell/engine based cogeneration system with methanol fuel for ship application," *Energy*, vol. 282, p. 128 741, 2023, ISSN: 0360-5442. DOI: https://doi.org/10.1016/j.energy.2023.128741. [Online]. Available: https://www.sciencedirect.com/science/article/pii/S0360544223021357.

[90] Y. M. Welaya, M. M. E. Gohary, and N. R. Ammar, "Steam and partial oxidation reforming options for hydrogen production from fossil fuels for pem fuel cells," *Alexandria Engineering Journal*, vol. 51, pp. 69–75, 2 2012, ISSN: 11100168. DOI: 10.1016/j.aej.2012.03.001.

[91] D. R. Palo, R. A. Dagle, and J. D. Holladay, "Methanol steam reforming for hydrogen production," *Chemical Reviews*, vol. 107, pp. 3992–4021, 10 Oct. 2007, ISSN: 00092665. DOI: 10.1021/cr050198b.

[92] A. M. Ranjekar and G. D. Yadav, "Steam reforming of methanol for hydrogen production: A critical analysis of catalysis, processes, and scope," *Industrial and Engineering Chemistry Research*, vol. 60, pp. 89–113, 1 Jan. 2021, ISSN: 15205045. DOI: 10.1021/acs.iecr.0c05041.

[93] V. Gurau, A. Ogunleke, and F. Strickland, "Design of a methanol reformer for on-board production of hydrogen as fuel for a 3 kw high-temperature proton exchange membrane fuel cell power system," *International Journal of Hydrogen Energy*, vol. 45, 56 2020, ISSN: 03603199. DOI: 10.1016/j.ijhydene.2020.08.179.

[94] D. Pluijlaar and L. V. Biert, "Using renewable methanol, pem fuel cells and on-board carbon capture to reduce well-to-propeller ship emissions," *Proceedings of the International Naval Engineering Conference*, 2022. DOI: 10.24868/10671. [Online]. Available: https://doi.org/10.24868/10671.

[95] E. Spatolisano, L. A. Pellegrini, A. R. de Angelis, S. Cattaneo, and E. Roccaro, *Ammonia as a carbon-free energy carrier: Nh3 cracking to h2*, Jul. 2023. DOI: 10.1021/acs.iecr.3c01419.

[96] D. Andriani and Y. Bicer, "A review of hydrogen production from onboard ammonia decomposition: Maritime applications of concentrated solar energy and boil-off gas recovery," *Fuel*, vol. 352, p. 128 900, Nov. 2023, ISSN: 0016-2361. DOI: 10.1016/J.FUEL.2023.128900.

[97] S. Yin, B. Xu, X. Zhou, and C. Au, "A mini-review on ammonia decomposition catalysts for on-site generation of hydrogen for fuel cell applications," *Applied Catalysis A: General*, vol. 277, no. 1, pp. 1–9, 2004, ISSN: 0926-860X. DOI: https://doi.org/10.1016/j.apcata.2004.09.020. [Online]. Available: https://www.sciencedirect.com/science/article/pii/S0926860X04007975.

[98] T. Okanishi *et al.*, "Comparative study of ammonia-fueled solid oxide fuel cell systems," *Fuel Cells*, vol. 17, no. 3, pp. 383–390, 2017. DOI: https://doi.org/10.1002/fuce.201600165. eprint: https://onlinelibrary.wiley.com/doi/pdf/10.1002/fuce.201600165. [Online]. Available: https://onlinelibrary.wiley.com/doi/abs/10.1002/fuce.201600165.

[99] L. Zhou *et al.*, "For more and purer hydrogen-the progress and challenges in water gas shift reaction," *Journal of Energy Chemistry*, vol. 83, pp. 363–396, 2023, ISSN: 2095-4956. DOI: https://doi.org/10.1016/j.jechem.2023.03.055. [Online]. Available: https://www.sciencedirect.com/science/article/pii/S2095495623002206.

[100] S. Xiao, J. Xu, Y. Wang, J. Wang, and X. Xu, "Investigation of a methanol processing system comprising of a steam reformer and two preferential oxidation reactors for fuel cells," *International Journal of Hydrogen Energy*, vol. 47, no. 68, pp. 29 242–29 254, 2022, ISSN: 0360-3199. DOI: https://doi.org/10.1016/j.ijhydene.2022.06.245. [Online]. Available: https://www.sciencedirect.com/science/article/pii/S0360319922028804.

[101] V. F. Valdés-López, T. Mason, P. R. Shearing, and D. J. Brett, "Carbon monoxide poisoning and mitigation strategies for polymer electrolyte membrane fuel cells – a review," *Progress in Energy and Combustion Science*, vol. 79, p. 100 842, Jul. 2020, ISSN: 0360-1285. DOI: 10.1016/J.PECS.2020.100842.

[102] P. Panagiotopoulou, D. I. Kondarides, and X. E. Verykios, "Selective methanation of co over supported ru catalysts," *Applied Catalysis B: Environmental*, vol. 88, no. 3, pp. 470–478, 2009, ISSN: 0926-3373. DOI: https://doi.org/10.1016/j.apcatb.2008.10.012. [Online]. Available: https://www.sciencedirect.com/science/article/pii/S0926337308003986.

[103] P. Balcombe *et al.*, "How to decarbonise international shipping: Options for fuels, technologies and policies," *Energy Conversion and Management*, vol. 182, pp. 72–88, Feb. 2019, ISSN: 0196-8904. DOI: 10.1016/J.ENCONMAN.2018.12.080.

[104] S. Sahebdelfar and M. T. Ravanchi, "Carbon monoxide clean-up of the reformate gas for pem fuel cell applications: A conceptual review," *International Journal of Hydrogen Energy*, vol. 48, pp. 24 709–24 729, 64 Jul. 2023, ISSN: 0360-3199. DOI: 10.1016/J.IJHYDENE.2022.08.258.

[105] S.-I. Yang, D.-Y. Choi, S.-C. Jang, S.-H. Kim, and D.-K. Choi, "Hydrogen separation by multi-bed pressure swing adsorption of synthesis gas," *Adsorption*, vol. 14, pp. 583–590, 4 2008, ISSN: 1572-8757. DOI: 10.1007/s10450-008-9133-x. [Online]. Available: https://doi.org/10.1007/s10450-008-9133-x.

[106] W.-H. Chen, W.-H. Chen, R.-Y. Chein, A. T. Hoang, K. Manatura, and S. R. Naqvi, "Optimization of hydrogen purification via vacuum pressure swing adsorption," *Energy Conversion and Management: X*, p. 100 459, Sep. 2023, ISSN: 2590-1745. DOI: 10.1016/J.ECMX.2023.100459. [Online]. Available: https://linkinghub.elsevier.com/retrieve/pii/S2590174523001150.

[107] L. van Biert, "Solid oxide fuel cells for ships system integration concepts with reforming and thermal cycles," 2020. DOI: 10.4233/uuid:dd1f7899-38ee-4c78-a5b0-a6fa92c90f56. [Online]. Available: https://doi.org/10.4233/uuid:dd1f7899-38ee-4c78-a5b0-a6fa92c90f56.

[108] G. Bernardo, T. Araújo, T. da Silva Lopes, J. Sousa, and A. Mendes, "Recent advances in membrane technologies for hydrogen purification," *International Journal of Hydrogen Energy*, vol. 45, pp. 7313–7338, 12 Mar. 2020, ISSN: 0360-3199. DOI: 10.1016/J.IJHYDENE.2019.06.162.

[109] S. Dube, J. Gorimbo, M. Moyo, C. G. Okoye-Chine, and X. Liu, "Synthesis and application of ni-based membranes in hydrogen separation and purification systems: A review," *Journal of Environmental Chemical Engineering*, vol. 11, p. 109 194, 1 Feb. 2023, ISSN: 2213-3437. DOI: 10.1016/J.JECE.2022.109194.

[110] G. N. B. Durmuş, E. O. Eren, Y. Devrim, C. O. Colpan, and N. Özkan, "High-temperature electrochemical hydrogen separation from reformate gases using pbi/mof composite membrane," *International Journal of Hydrogen Energy*, vol. 48, pp. 23 044–23 054, 60 Jul. 2023, ISSN: 0360-3199. DOI: 10.1016/J.IJHYDENE.2023.03.192.

[111] O. van Rheinberg, K. Lucka, H. Köhne, T. Schade, and J. T. Andersson, "Selective removal of sulphur in liquid fuels for fuel cell applications," *Fuel*, vol. 87, no. 13, pp. 2988–2996, 2008, ISSN: 0016-2361. DOI: https://doi.org/10.1016/j.fuel.2008.03.020. [Online]. Available: https://www.sciencedirect.com/science/article/pii/S0016236108001233.

[112] E. S. Bang, M. H. Kim, and S. K. Park, "Options for methane fuel processing in pemfc system with potential maritime applications," *Energies*, vol. 15, 22 Nov. 2022, Says something about the best option for fuel processing when used with PEMFC., ISSN: 19961073. DOI: 10.3390/en15228604.

[113] Rix Industries. "M2h2 series mobile hydrogen generator." (2023), [Online]. Available: https://www.rixindustries.com/hydrogen-generation-systems. accessed Sep. 26, 2023.

[114] Advent Technologies. "Marine." (2024), [Online]. Available: https://serene.advent.energy/marine/. accessed Apr. 18, 2024.

[115] Blue World Technologies ApS. "Ht pem fuel cell system." (2024), [Online]. Available: https://www.blue.world/products/high-power-methanol-fuel-cell-platform/. accessed Apr. 18, 2024.

[116] Amogy. "Our products: A clean energy solution to accelerate the transition to a sustainable future." (2023), [Online]. Available: https://amogy.co/products/. accessed Sep. 27, 2023.

[117] P. Nikolaidis and A. Poullikkas, "A comparative overview of hydrogen production processes," *Renewable and Sustainable Energy Reviews*, vol. 67, pp. 597–611, Jan. 2017, ISSN: 1364-0321. DOI: 10.1016/J.RSER.2016.09.044.

[118] R. G. Bodkhe, R. L. Shrivastava, V. K. Soni, and R. B. Chadge, "A review of renewable hydrogen generation and proton exchange membrane fuel cell technology for sustainable energy development," *International Journal of Electrochemical Science*, vol. 18, 5 2023, ISSN: 14523981. DOI: 10.1016/j.ijoes.2023.100108.

[119] J. Incer-Valverde, Y. Lyu, G. Tsatsaronis, and T. Morosuk, "Economic evaluation of a large-scale liquid hydrogen regasification system," *Gas Science and Engineering*, p. 205 150, Oct. 2023, ISSN: 2949-9089. DOI: 10.1016/J.JGSCE.2023.205150. [Online]. Available: https://linkinghub.elsevier.com/retrieve/pii/S2949908923002789.

[120] T. Weidner, V. Tulus, and G. Guillén-Gosálbez, "Environmental sustainability assessment of large-scale hydrogen production using prospective life cycle analysis," *International Journal of Hydrogen Energy*, vol. 48, no. 22, pp. 8310–8327, 2023, ISSN: 0360-3199. DOI: https://doi.org/10.1016/j.ijhydene.2022.11.044. [Online]. Available: https://www.sciencedirect.com/science/article/pii/S0360319922052570.

[121] Y. Liu, P. Zhou, B. Jeong, and H. Wang, "Design and optimization of a type-c tank for liquid hydrogen marine transport," *International Journal of Hydrogen Energy*, 2023, ISSN: 0360-3199. DOI: https://doi.org/10.1016/j.ijhydene.2023.05.102. [Online]. Available: https://www.sciencedirect.com/science/article/pii/S0360319923023753.

[122] T. K. Tromp, R.-L. Shia, M. Allen, J. M. Eiler, and Y. L. Yung, "Potential environmental impact of a hydrogen economy on the stratosphere," *Science*, vol. 300, pp. 1740–1742, 5626 2003. DOI: 10.1126/science.1085169. [Online]. Available: https://www.science.org/doi/abs/10.1126/science.1085169.

[123] International Maritime Organization, "The International Code for the Construction and Equipment of Ships Carrying Liquefied Gases in Bulk (IGC CODE)," IMO, Tech. Rep. MSC.370(93), 2014.

[124] Y. S. H. Najjar, "Hydrogen safety: The road toward green technology," *International Journal of Hydrogen Energy*, vol. 38, pp. 10 716–10 728, 25 2013, ISSN: 0360-3199. DOI: https://doi.org/10.1016/j.ijhydene.2013.05.126. [Online]. Available: https://www.sciencedirect.com/science/article/pii/S036031991301358X.

[125] International Electrotechnical Commission, "Explosive atmospheres - Part 10-1: Classification of areas - Explosive gas atmospheres," IEC, Tech. Rep. IEC 60079-10-1:2020,IDT, 2021.

[126] International Maritime Organization, "International Code of Safety for Ship Using Gases or Other Low-flashpoint Fuels (IGF Code)," IMO, Tech. Rep. MSC.391(95), 2015.

[127] F. Y. Al-Aboosi, M. M. El-Halwagi, M. Moore, and R. B. Nielsen, "Renewable ammonia as an alternative fuel for the shipping industry," *Current Opinion in Chemical Engineering*, vol. 31, p. 100 670, Mar. 2021, ISSN: 2211-3398. DOI: 10.1016/J.COCHE.2021.100670.

[128] K. Machaj *et al.*, "Ammonia as a potential marine fuel: A review," *Energy Strategy Reviews*, vol. 44, p. 100 926, 2022, ISSN: 2211-467X. DOI: https://doi.org/10.1016/j.esr.2022.100926. [Online]. Available: https://www.sciencedirect.com/science/article/pii/S2211467X22001201.

[129] K. Machaj *et al.*, "Ammonia as a potential marine fuel: A review," *Energy Strategy Reviews*, vol. 44, p. 100 926, Nov. 2022, ISSN: 2211-467X. DOI: 10.1016/J.ESR.2022.100926.

[130] Y. Kojima, "Safety of ammonia as a hydrogen energy carrier," *International Journal of Hydrogen Energy*, 2023, ISSN: 0360-3199. DOI: https://doi.org/10.1016/j.ijhydene.2023.06.213. [Online]. Available: https://www.sciencedirect.com/science/article/pii/S03603199233166X.

[131] Methanol Institute. "Marine." (2023), [Online]. Available: https://www.methanol.org/renewable/. accessed Dec. 1, 2023.

[132] Norled. "The mf hydra." (2023), [Online]. Available: https://www.norled.no/en/news/the-mf-hydra-first-in-the-world/. accessed Nov. 21, 2023.

[133] SEAM. "Torghatten nord chooses norwegian technology for the world's first large-scale hydrogen-ferry project." (2023), [Online]. Available: https://www.seam.no/insights/torghatten-nord-chooses-norwegian-technology-for-large-scale-hydrogen-ferry-project. accessed Nov. 21, 2023.

[134] Swim H2. "Products: Hydrogen-electric drive trains." (2023), [Online]. Available: https://swimh2.com/our-product/. accessed Nov. 24, 2023.

[135] Future Proof Shipping. "Our fleet." (2023), [Online]. Available: https://futureproofshipping.com/about/fleet/. accessed Nov. 27, 2023.

[136] ShipFC. "About - shipfc." (2020), [Online]. Available: https://shipfc.eu/about/. accessed Nov. 21, 2023.

[137] R. Russo, T. Coppola, L. Micoli, and A. Pietra, "Preliminary investigation of a multi-mw solid oxide fuel cell power plant to be installed on board a cruise ship," *Chemical Engineering Transactions*, vol. 99, pp. 577–582, 2023, ISSN: 22839216. DOI: 10.3303/CET2399097.

[138] L. Micoli, T. Coppola, and M. Turco, "A case study of a solid oxide fuel cell plant on board a cruise ship," *Journal of Marine Science and Application*, vol. 20, pp. 524–533, 3 Sep. 2021, ISSN: 19935048. DOI: 10.1007/s11804-021-00217-y.

[139] Methanol Institute. "Marine." (2023), [Online]. Available: https://www.methanol.org/marine/. accessed Nov. 27, 2023.

[140] E. Haun. "Hydrogen one: Innovative towboat set to shake things up in the us." (2022), [Online]. Available: https://www.marinelink.com/news/hydrogen-one-innovative-towboat-set-shake-499381. accessed Nov. 24, 2023.

[141] e4ships. "Rivercell2." (2019), [Online]. Available: https://www.e4ships.de/english/inland-shipping/rivercell2/. accessed Dec. 4, 2023.

[142] Freudenberg. "For sustainable yachting." (2021), [Online]. Available: https://www.fst.com/news-stories/press-releases/2021/for-sustainable-yachting/. accessed Dec. 4, 2023.

[143] e4ships. “Pa-x-ell 2.” (2023), [Online]. Available: https://www.e4ships.de/english/maritime-shipping/pa-x-ell-2/. accessed Dec. 4, 2023.

[144] SH2IPDRIVE. “Home - sh2ipdrive.” (2023), [Online]. Available: https://sh2ipdrive.com/. accessed Nov. 21, 2023.

[145] HELENUS. “Consortium.” (2023), [Online]. Available: https://www.helenus.eu/consortium/. accessed Dec. 4, 2023.

[146] European Commission CORDIS. “Validation of renewable methanol based auxiliary power system for commercial vessels.” (2010), [Online]. Available: https://cordis.europa.eu/project/id/31414. accessed Dec. 4, 2023.

[147] M. C. Díaz-de-Baldasano, F. J. Mateos, L. R. Núñez-Rivas, and T. J. Leo, “Conceptual design of offshore platform supply vessel based on hybrid diesel generator-fuel cell power plant,” *Applied Energy*, vol. 116, pp. 91–100, 2014, ISSN: 0306-2619. DOI: https://doi.org/10.1016/j.apenergy.2013.11.049. [Online]. Available: https://www.sciencedirect.com/science/article/pii/S0306261913009550.

[148] NAUTILUS. “About the nautilus project.” (2023), [Online]. Available: https://nautilus-project.eu/test2/project-nautilus. accessed Dec. 4, 2023.

[149] AmmoniaDrive. “About.” (2022), [Online]. Available: https://ammoniadrive.tudelft.nl/. accessed Dec. 4, 2023.

[150] MENENS. “About us.” (2023), [Online]. Available: https://menens.nl/about/. accessed Dec. 4, 2023.

[151] Siemens. “Dc-dc converters for industrial applications.” (2024), [Online]. Available: https://www.siemens.com/global/en/products/drives/dc-dc-converter.html#CompactDCDCConverter. accessed Mar. 27, 2024.

[152] Wärtsilä. “Wärtsilä 46df dual fuel marine engine.” (2024), [Online]. Available: https://www.wartsila.com/marine/products/engines-and-generating-sets/dual-fuel-engines/wartsila-46df. accessed Mar. 27, 2024.

[153] J. Nayar. “Not so “green” technology: The complicated legacy of rare earth mining.” (2021), [Online]. Available: https://hir.harvard.edu/not-so-green-technology-the-complicated-legacy-of-rare-earth-mining/. accessed May 12, 2024.

[154] International Maritime Organization, “Interim Guidelines for the Safety of Ships Using Methyl/-Ethyl Alcohol as Fuel,” IMO, Tech. Rep. MSC.1/Circ.1621, 2020.

[155] M. J. Moran, H. N. Shapiro, D. D. Boettner, and M. B. Bailey, *Moran’s Principles of Engineering: Thermodynamics*, Global 9th edition. Wiley, 2017.

[156] J. Klein Woud and D. Stapersma, *Selected chapters of Marine Engineering: Design of Auxiliary Systems, Shafting and Flexible Mounting*. 2011, Lecture Notes Delft University of Technology (to be published as book).

[157] J. Klein Woud and D. Stapersma, *Design of Propulsion and Electric Power Generation Systems*. IMarEST, 2018.

A

Component Specifications

This appendix gives information on the components used for designing the various systems onboard the vessel.

A.1. Power Module Specifications

A.1.1. Marine System 200

In table A.1, the main specifications of the reference fuel cell type used in thesis are listed.

Table A.1: Specifications of the PowerCell Marine System 200.

Item	Specification
Total power output	200 kW, 550-1000 VDC & 45-405A
Dimensions	0.73m W x 0.9m D x 2.2m H
Volume	1.45 m^3
Mass	1070 kg
Space margins	See figure A.1
Efficiency	54% fuel efficiency
Hydrogen fuel input	ISO 14687:2019 pure hydrogen 0.5-3 bar/3-8 bar/8-12 bar
Ambient	5-45 °C, IP44, Non-hazardous zone (zone 2 NE), IEC 62282-3-200, IEC-60079-10-1
Cooling	<320 kW heat output

When installing these fuel cells onboard ships, minimum distances for positioning fuel cells side by side or next to a bulkhead should be considered. For the fuel cells, the margins are shown in figure A.1.

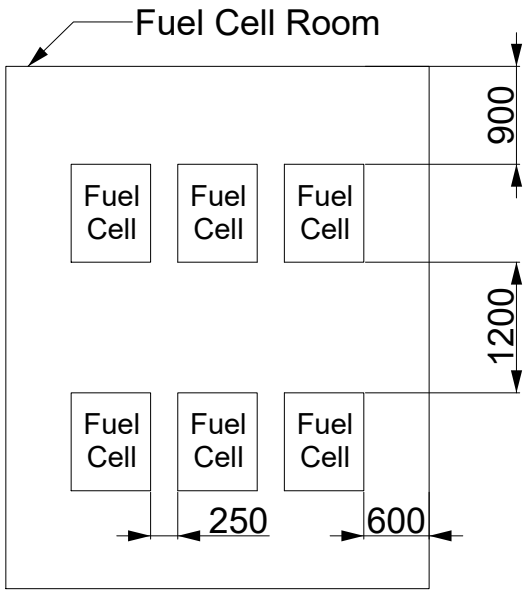

Figure A.1: Assumed space margins for positioning fuel cells in ships. Dimensions are given in mm.

A.1.2. Ammonia Power Packs

In table A.2, the main specifications of the reference ammonia power pack used in this thesis are listed.

Table A.2: Specifications of the Amogy Powerpack.

Item	**Specification**
Total power output	200 kW electrical, AC or DC
Dimensions	2.75m L x 1.2m W x 2.2m H
Volume	7.26 m^3
Mass	4000 kg
Space margins	See figure A.2
Efficiency	2.1 kWe/kg_{fuel} = 40.65%
Start-up time	2 hours from cold start-up
Power requirements	5 kW @ 24VDC + 35 kW @ 400VDC max, 25 kW @ 400VDC normal
Cooling	Exhaust water 180 L/h at 20-70 °C

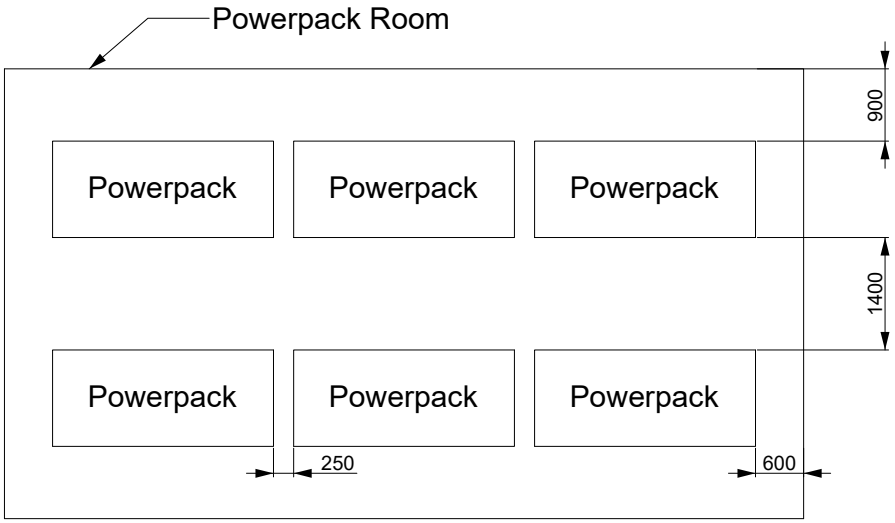

Figure A.2: Assumed space margins for positioning ammonia powerpacks in ships. Dimensions are given in mm.

A.1.3. Methanol Power Module

In table A.3, the main specifications of the reference methanol power system used in this thesis are listed.

Table A.3: Specifications of the Rix Industries M2 Power 250 system.

Item	Specification
Total power output	250 kW electrical, 500-1000VDC
Dimensions	2.8m L x 2.2m W x 2.3m H
Volume	14.17 m^3
Mass	2767 kg
Space margins	0.9m on all sides, see figure A.3
Efficiency	38-48%
Start-up time	<12 hours from 20 °C
Transient capabilities	5-6min to 50% H2 flow, 20min to 100% H2 flow
Power requirements	1.5 kW during operation, 4 kW during hot standby, 10 kW during cold start
Cooling	Up to 80 °C coolant outlet temperature
Lifetime	The system's target lifetime is 45,000 operational hours. Routine maintenance is conducted annually and an overhaul (replacement of metal membrane purifiers is estimated at 20-25,000 hours.

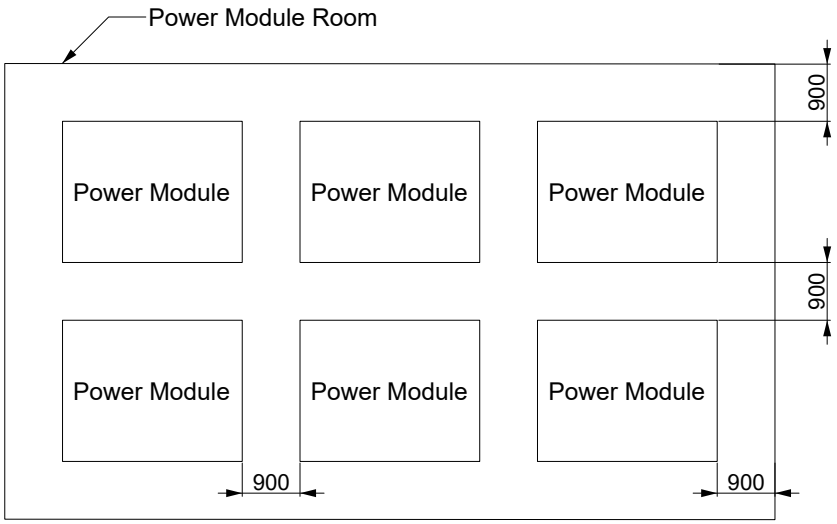

Figure A.3: Assumed space margins for positioning methanol power modules in ships. Dimensions are given in mm.

A.1.4. Internal Combustion Engine

In table A.4, the main specifications of the ICE as installed in de base case vessel are listed.

Table A.4: Specifications of the Wärtsilä 12V46DF engine.

Item	Specification
Total power output	13740 kW
Dimensions	11.12m L x 4.555m W x 5.29m H
Volume	268 m^3
Mass	184 tons
Efficiency	40% (assumption)

A.2. Fuel Storage

This section lists the relevant specifications of fuel tank types used in this thesis.

A.2.1. Type C Tanks

The specifications for the design of type C tanks are listed in table A.5.

Table A.5: Specifications for type-C cylindrical and bi-lobe tanks.

Item	Specification for LH2	Specification for NH3
Insulation thickness	0.5 m	0.18 m
Fuel storage temperature	-253 °C	-34 °C
Top margin	0.5 m	0.5 m
Bottom margin	0.1 m	0.1 m
Side margin	0.3 m	0.3 m
Max. filling limit	95% (few days), 69% (30 days)	95%
Min. filling limit	5%	0%
Fuel volumetric energy density	120 MJ/kg	18.6 MJ/kg
Fuel gravimetric energy density	8.5 GJ/m^3	12.7 GJ/m^3
Insulation density	48 kg/m^3	48 kg/m^3
Steel density (incl. welds)	8000 kg/m^3	8000 kg/m^3

A.2.2. Integrated Tanks

The specifications of integrated methanol tanks are listed in table A.6.

Table A.6: Specifications for integrated tanks.

Item	Specification for CH3OH
Max. filling limit	98%
Min. filling limit	2%
Fuel volumetric energy density	19.9 MJ/kg
Fuel gravimetric energy density	15.8 GJ/m^3
Cofferdams	0.9m cofferdams are required between the tank and other ship spaces/outside air above the lowest waterline; no cofferdams are required between the tank and seawater below the lowest waterline.

The positioning of cofferdams is further illustrated in figure A.4.

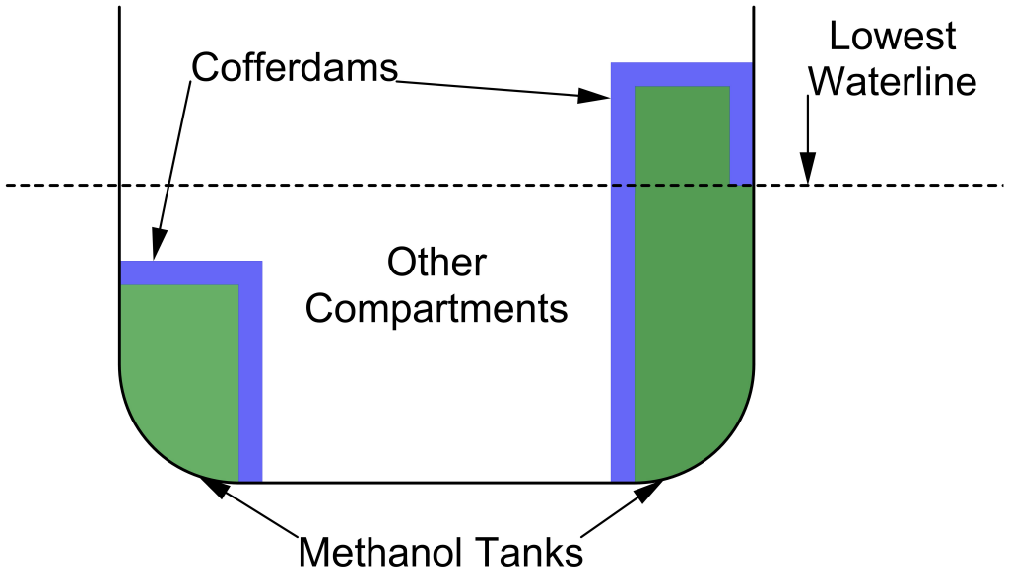

Figure A.4: Illustration of required locations for cofferdams on integrated methanol tanks.

A.3. Other Equipment

In this section, relevant specifications of other equipment is provided.

A.3.1. Batteries

The battery specifications are listed in table A.7.

Table A.7: Specifications of the Praxis GreenBattery-Power Rack 86 kWh (liquid cooled version).

Item	Specification
Storage capacity	86 kWh
Dimensions	2.8m L x 2.2m W x 2.3m H
Volume	0.79 m^3
Mass	1045 kg
Space margins	See figure A.5
Efficiency	90% (assumption)
SOC	10-90% (recommended), 5-95% (maximum)
Transient capabilities	5-6min to 50% H2 flow, 20min to 100% H2 flow
Ambient	IP66, 0-45 deg C charging, -20-45 deg C discharging
Cooling	<0.45 kW heat generation, water/glycol mixture, 4l/min, 5 deg C rise @3C, 15-35 deg C inlet temp. (22 deg C recommended)
Lifetime	See table below

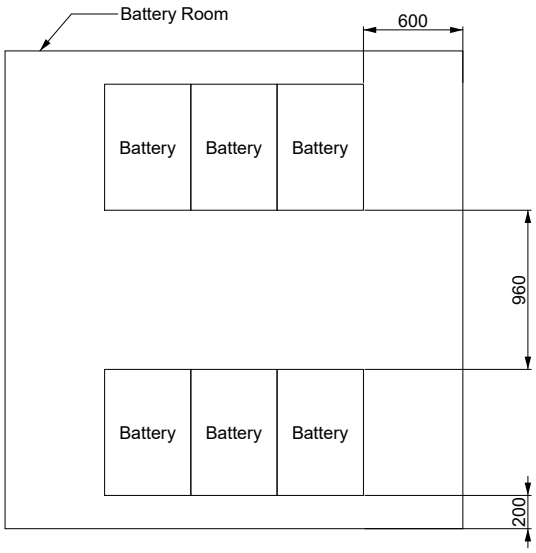

Figure A.5: Assumed space margins for positioning batteries in ships. Dimensions are given in mm.

A.3.2. Power Electronics

The specifications of the DC-DC converters are listed in table A.8.

Table A.8: Specifications of the Siemens 6RP0020-2AC32-5AA0 DC-DC converter.

Item	**Specification**
Total power output	250 kW 250 A at 1000 V DC continuous duty range: 0 - 1200 V DC, bidirectional
Dimensions	0.205m W x 0.5m D x 0.9m H
Volume	0.092 m^3
Mass	118 kg
Space margins	Mounting can be side-by-side, 250mm top and bottom margins for air circulation
Efficiency	>98%, maximum power loss 5800 W
Power requirements	24 V DC (18 V – 30V), IN = max. 20 A
Ambient	IP00, 0-40 deg C, humidity 5 % – 90 %, non-condensating
Cooling	Air, forced ventilation, flow rate 1200 m3/h, temperature-controlled fans

A.3.3. Ventilation requirements

Table A.9 lists the required amount of air changes per hour for various spaces onboard the vessel.

Table A.9: Amount of required air changes per hour for different compartments and other spaces onboard ships.

Space	Air changes per hour	Regulation Source	Comments
Nitrogen generation & storage rooms	6	[126, 154]	An independent mechanical extraction ventilation system is required.
Tank connection space	30	[126]	
ESD protected machinery spaces	30	[126]	15 air changes per hour is allowed when the system can increase to 30 air changes per hour if gas is detected.
Fuel preparation room	30	[126, 154]	An underpressure type mechanical ventilation system is required.
Ducts and double pipes containing fuel piping	30	[123, 126, 154]	An extraction type mechanical ventilation systemis required, the system may do less than 30 air changes per hour if the flow velocity is 3m/s or greater.
Permanent cargo spaces not normally entered	8	[123]	
Non-permanent cargo spaces not normally entered	16	[123]	
Entry spaces to fuel tanks & cofferdams	6	[154]	
Fuel hoses storage rooms	6	[154]	

B

Auxiliary Power Formula Derivation

B.1. Pump and Blower Power

To calculate the pump or blower power, the following definition of work (W) is used [155]:

$$W = \int_{V_0}^{V_1} p \, dV \tag{B.1}$$

In this formula, p represents pressure and V represents volume. Next, it is assumed that the volume of the medium stays approximately constant ($V_1 = V_0$). This leads to:

$$W = V \cdot \Delta p \tag{B.2}$$

When the work and volume are expressed as a flow per unit of time, equation B.2 changes to:

$$\dot{W} = \dot{V} \cdot \Delta p \tag{B.3}$$

The pressure that the pump or blower has to overcome is assumed to be equal to the pressure loss of the system [156]:

$$\Delta p = \sum \zeta \cdot \frac{1}{2} \cdot \rho \cdot v^2 \tag{B.4}$$

The term $\sum \zeta$ indicates the systems' resistance and ρ indicates the density of the medium. Substituting equation B.4 in equation B.3 leads to:

$$\dot{W} = \dot{V} \cdot \sum \zeta \cdot \frac{1}{2} \cdot \rho \cdot v^2 \tag{B.5}$$

Equation B.5 refers to a reversible process. To account for irreversibilities (losses), the equation is divided by an efficiency (η). This pump or blower efficiency accounts for losses that occur from the DC electrical grid to the desired pump or blower output. Using this definition, an expression for the pump or blower power is found:

$$P_{e,pump/blower} = \frac{\dot{V} \cdot \sum \zeta \cdot \frac{1}{2} \cdot \rho \cdot v^2}{\eta} \tag{B.6}$$

Using formula B.6, the pump or blower power for various purposes can be calculated. For each application, the volume flow, density of the medium, system resistance, flow velocity, and efficiency vary. In appendix H, the assumptions for the density of the medium, system resistance, flow velocity, and efficiency are given. The calculation of the volume flow is for cooling pumps, ventilation air blowers, and process air blowers is given in subsections B.1.1, B.1.2, B.1.3, and B.1.4.

B.1.1. Cooling Pumps

To calculate the total amount of heat ($\dot{Q}$) that should be transferred to cooling water, the following equation is used:

$$\dot{Q}_{cooling} = \frac{P_{PM}}{\eta_{PM}} \cdot (1 - \eta_{PM}) + \dot{Q}_{batteries} + \dot{Q}_{DC-DC} \tag{B.7}$$

In the above equation, η_{PM} relates to the efficiency of the power module. The heat flow from a mass flow ($\dot{m}$) can be expressed as [156]:

$$|\dot{Q}| = \dot{m} \cdot |\Delta h| \tag{B.8}$$

Δh indicates the specific enthalpy change. When constant specific heats are assumed, equation B.8 can be rewritten into:

$$|\dot{Q}| = \dot{m} \cdot c_p \cdot |\Delta T| \tag{B.9}$$

In the above equation, c_p represents the molar heat capacity. Using the general relation between mass, volume, and density, equation B.9 can be rewritten to:

$$\dot{V} = \frac{\dot{Q}_{cooling}}{\rho \cdot c_p \cdot |\Delta T|} \tag{B.10}$$

Inserting equation B.10 into equation B.6, yields:

$$P_{e,cooling} = \frac{\dot{Q}_{cooling} \cdot \sum \zeta \cdot \frac{1}{2} \cdot v^2}{c_p \cdot |\Delta T| \cdot \eta_{pump}} \tag{B.11}$$

B.1.2. Ventilation Air

To calculate the ventilation air supply requirement, the required amount of air changes per hour per room is multiplied by the volume of each respective room. The ventilation air volume flows per room are summed to obtain $\dot{V}_{ventilationair}$. Using equation B.6, the following expression for the ventilation air blower power demand is obtained:

$$P_{e,ventilation} = \frac{\dot{V}_{ventilationair} \cdot \sum \zeta \cdot \frac{1}{2} \cdot \rho_{air} \cdot v_{air}^2}{\eta_{blower}} \tag{B.12}$$

B.1.3. Fuel Pumps

Using the fuel volume flow required for the power modules or internal combustion engines and equation B.6, the following expression for the fuel pump power demand is obtained:

$$P_{e,fuelpump} = \frac{\dot{V}_{fuel} \cdot \sum \zeta \cdot \frac{1}{2} \cdot \rho_{fuel} \cdot v_{fuel}^2}{\eta_{pump}} \tag{B.13}$$

B.1.4. Process Air

To calculate the process air volume flow rate, the mass flow of process air is divided by the density of air:

$$\dot{V}_{processair} = \frac{\dot{m}_{processair}}{\rho_{air}} \tag{B.14}$$

The amount of process air is calculated using the mass flow of the fuel cell's hydrogen input, the mass ratio of hydrogen to air and an overdimensioning factor (a). To find the hydrogen mass flow rate, the following equation is used:

$$\dot{m}_{H2} = \frac{P_{PM}}{\eta_{FC} \cdot LHV_{H2}} \tag{B.15}$$

The term 'LHV_{H2}' refers to the lower heating value of hydrogen. The total reaction for an LT-PEMFC is:

$$2\,H_2 + O_2 \rightarrow 2\,H_2O \tag{B.16}$$

This results in a stoichiometric ratio of 2 moles of hydrogen per 1 mole of oxygen. Using the molar masses of oxygen (M_{O2}) and hydrogen (M_{H2}), the following mass balance holds:

$$\dot{m}_{O2} = \dot{m}_{H2} \cdot \frac{M_{O2}}{2 \cdot M_{H2}} \tag{B.17}$$

Substituting equation B.15 in equation B.17, gives:

$$\dot{m}_{O2} = \frac{P_{PM} \cdot M_{O2}}{\eta_{FC} \cdot LHV_{H2} \cdot 2 \cdot M_{H2}} \tag{B.18}$$

The relation between the mass flow of oxygen and the mass flow of outside air is defined as:

$$\dot{m}_{O2} = \dot{m}_{air} \cdot X_{O2} \tag{B.19}$$

Where X_{O2} is the oxygen mass fraction of outside air. Rewriting equation B.19 and substituting equation B.18 gives:

$$\dot{m}_{air} = \frac{P_{PM} \cdot M_{O2}}{\eta_{FC} \cdot LHV_{H2} \cdot 2 \cdot M_{H2} \cdot X_{O2}} \tag{B.20}$$

Substituting equations B.14 and B.20 in equation B.6, the following equation is obtained:

$$P_{e,processair} = \frac{P_{PM} \cdot M_{O2} \cdot \sum \zeta \cdot \frac{1}{2} \cdot v_{air}^2}{\eta_{FC} \cdot LHV_{H2} \cdot 2 \cdot M_{H2} \cdot x_{O2} \cdot \eta_{blower}} \tag{B.21}$$

Fuel cells require more process air to be supplied than is consumed based on the stoichiometric ratio. To account for this, the amount of process air flow is assumed to be two times the amount of air required according to the stoichiometric ratio. For power packs operating on NH3 and CH3OH, it is assumed that the fuel processing steps require the same amount of process air as the fuel cell. Considering these aspects, an overdimensioning factor (a) is introduced. This factor is 2 for power modules operating on H2 and 4 for power modules operating on NH3 and CH3OH. Inserting this definition in equation B.21, yields:

$$P_{e,processair} = \frac{a \cdot P_{PM} \cdot M_{O2} \cdot \sum \zeta \cdot \frac{1}{2} \cdot v_{air}^2}{\eta_{FC} \cdot LHV_{H2} \cdot 2 \cdot M_{H2} \cdot x_{O2} \cdot \eta_{blower}} \tag{B.22}$$

B.2. Compressor Power

The first law of thermodynamics states the following [157]:

$$\dot{W} = \dot{Q} + \dot{m} \cdot \left((h_0 - h_1) + \frac{v_0^2 - v_1^2}{2} + g \cdot (z_0 - z_1) \right) \tag{B.23}$$

For the compressor, the following is assumed:

- The compressor inlet is at approximately the same height as the outlet, therefore $z_1 = z_0$.
- Inlet and outlet velocities are approximately equal, therefore $v_1 = v_0$.
- The heat transfer between the heat transfer between the system and the surroundings is very limited, therefore $\dot{Q} = 0$.

This reduces equation B.23 to the following [157]:

$$\dot{W} = \dot{m} \cdot (h_0 - h_1) \tag{B.24}$$

For a perfect gas (constant c_p and c_v) and a constant mass, the following condition holds [157]:

$$H_1 - H_0 = m \cdot c_p \cdot (T_0 - T_1) \tag{B.25}$$

Where H indicates the enthalpy. Assuming the mass flow is constant, and the compressed medium behaves as a perfect gas, equation B.24 can be rewritten to:

$$\dot{W} = \dot{m} \cdot c_p \cdot (T_0 - T_1) \tag{B.26}$$

For a perfect gas, the following relation holds [155]:

$$\frac{T_1}{T_0} = PR^{\left(\frac{\gamma - 1}{\gamma}\right)} \tag{B.27}$$

Where γ indicates the heat capacity ratio and PR indicates the pressure ratio. Substituting equation B.27 in equation B.26 results in:

$$\dot{W} = \dot{m} \cdot c_p \cdot T_0 \cdot (PR^{\left(\frac{\gamma - 1}{\gamma}\right)} - 1) \tag{B.28}$$

Equation B.28 relates to an isentropic process. To account for the process not being isentropic, the work flow is divided by an isentropic compressor efficiency ($\eta_{is,comp}$). Equation B.28 also refers to a reversible process. To account for irreversibilities (losses), the equation is also divided by a compressor efficiency (η_{comp}). The compressor efficiency accounts for losses that occur from the DC electrical grid to the desired compressor output. Using these definitions, an expression for the compressor power is found:

$$P_{e,comp} = \frac{\dot{m} \cdot c_p \cdot T_0}{\eta_{isentropic} \cdot \eta_{comp}} \cdot \left(PR^{\left(\frac{\gamma - 1}{\gamma}\right)} - 1 \right) \tag{B.29}$$

C

Offshore Ship General Arrangement

This appendix shows the general arrangement of the lower decks for the vessel used in the case study.

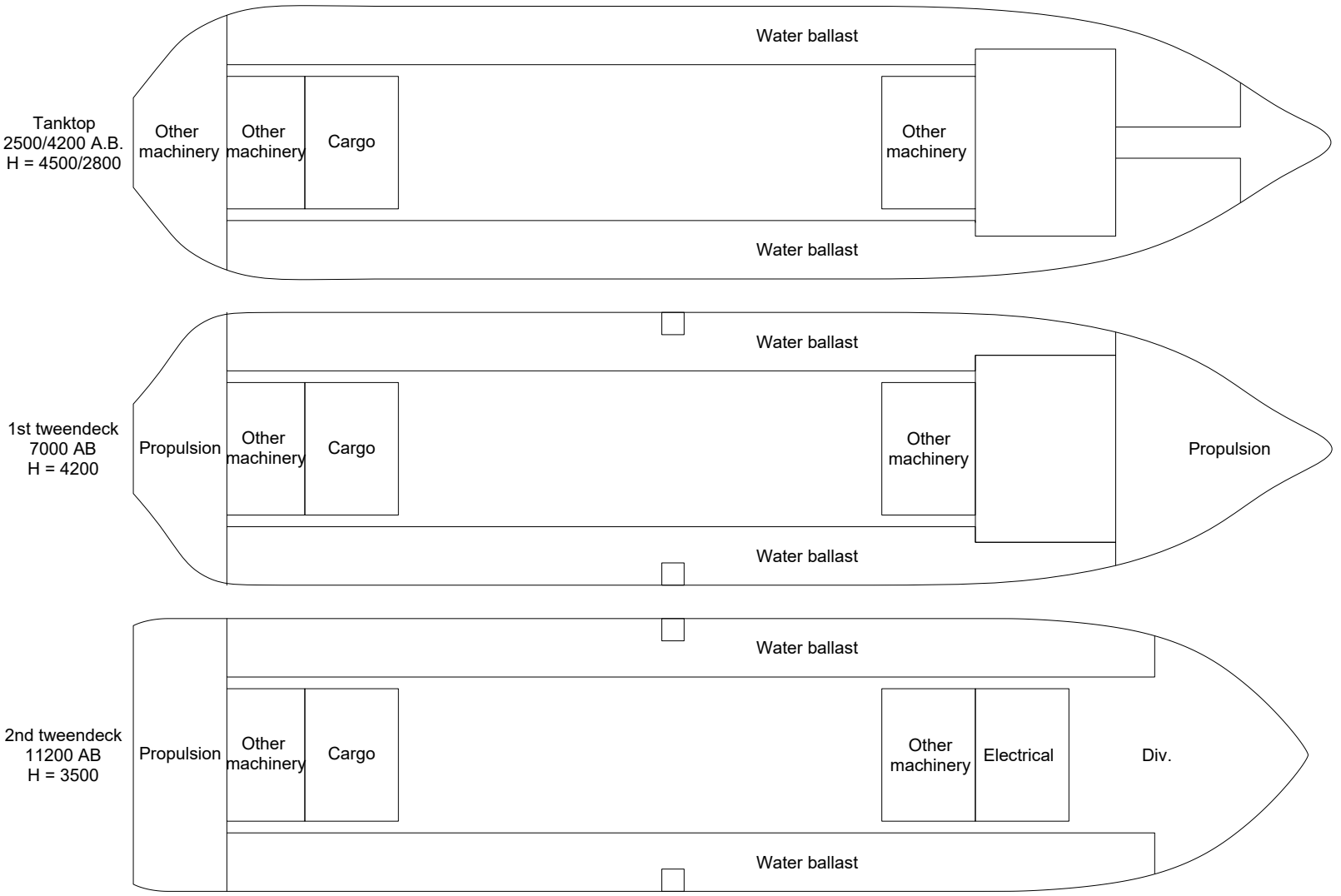

Figure C.1: General arrangement of the offshore ship used in the case study.

D

Power System Arrangement

The arrangements of the power generation systems for MDO, LH2, NH3 and CH3OH are shown in this appendix.

D.1. MDO

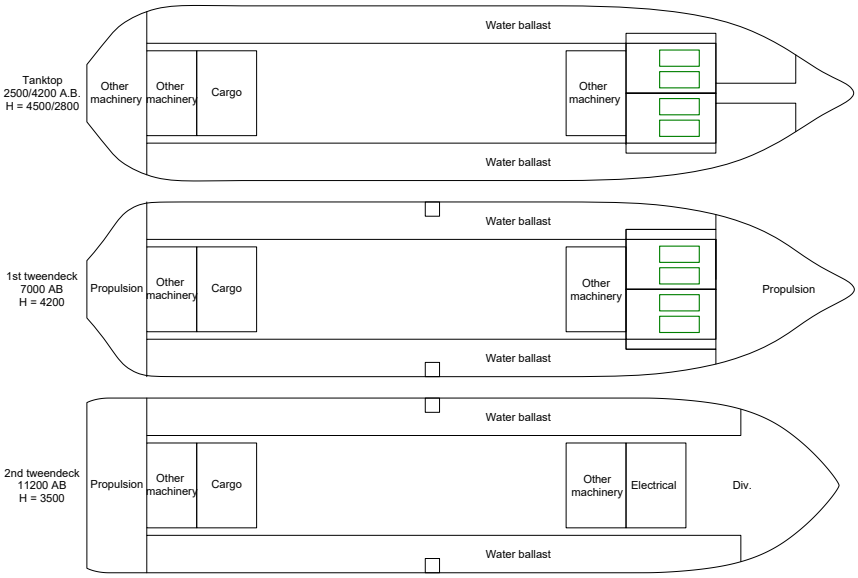

Figure D.1: MDO based power system arrangement. The internal combustion engines are indicated in green.

D.2. LH2

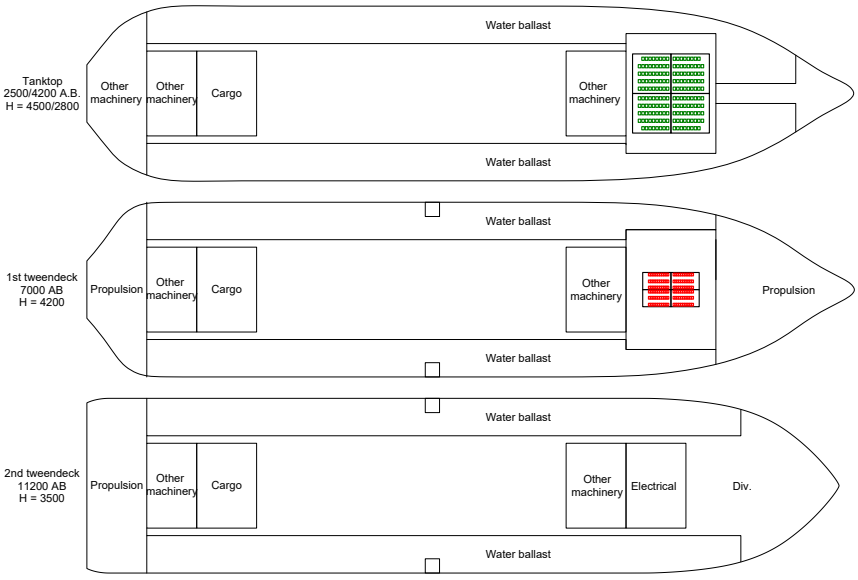

Figure D.2: LH2 based power system arrangement. The power modules are indicated in green and the batteries are indicated in red.

D.3. NH3

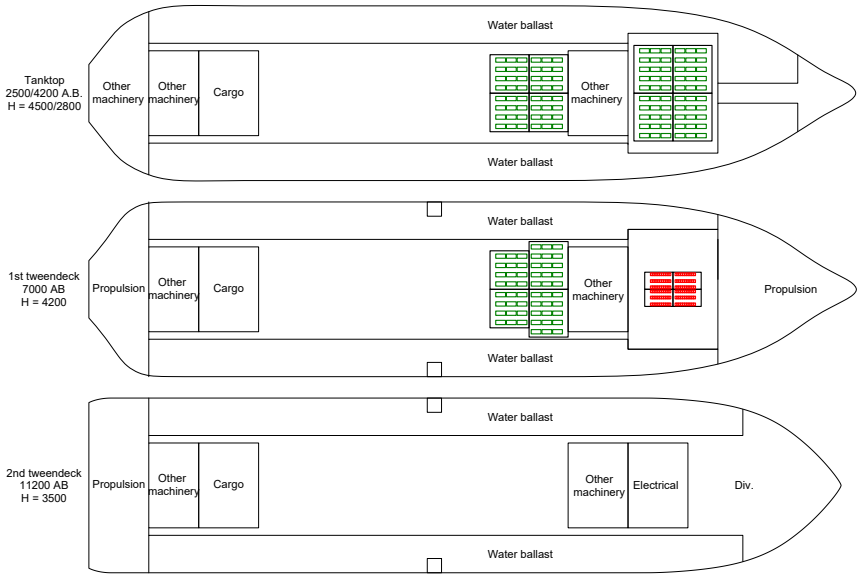

Figure D.3: NH3 based power system arrangement. The power modules are indicated in green and the batteries are indicated in red.

D.4. CH3OH

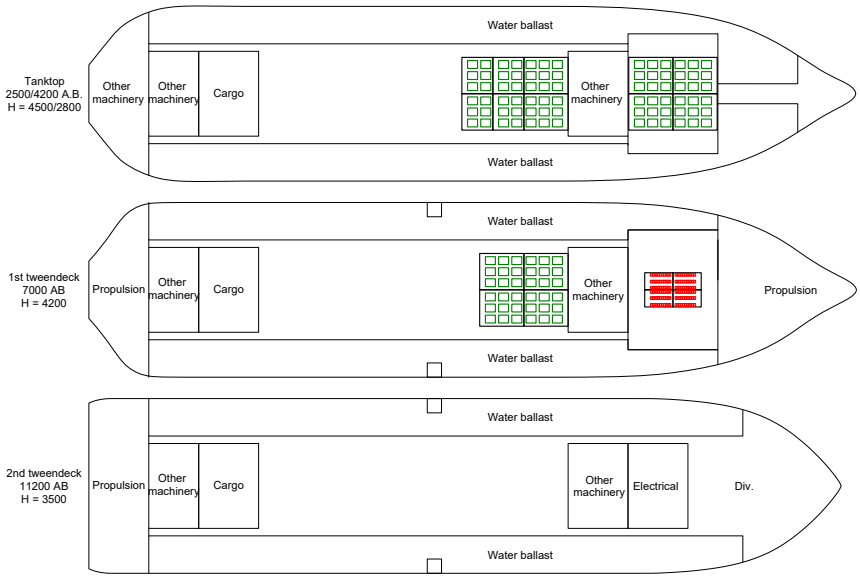

Figure D.4: CH3OH based power system arrangement. The power modules are indicated in green and the batteries are indicated in red.

E

Energy Storage System Arrangement

The arrangements of the energy storage systems for MDO, LH2, NH3 and CH3OH for autonomies of 7, 14, 21, 28, and 35 days are shown in this appendix.

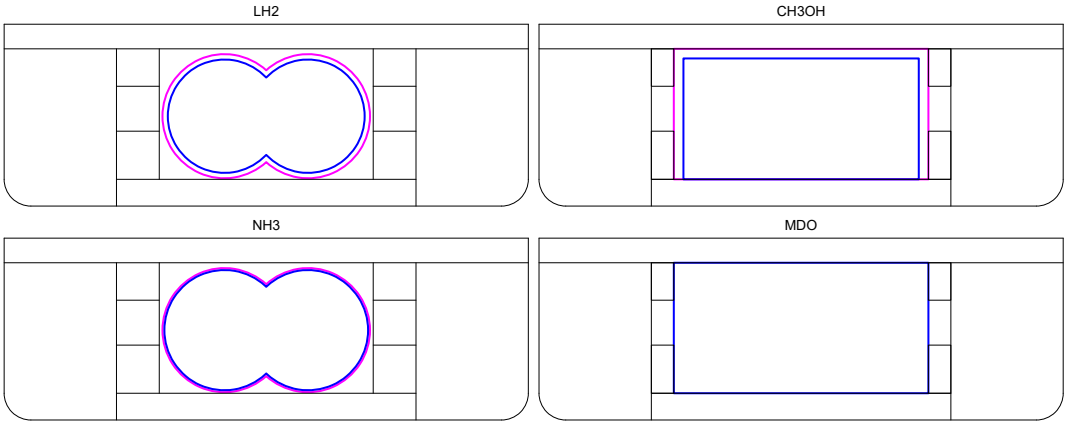

Figure E.1: Transverse views of the storage tanks for all considered fuels. The inner tank is indicated in blue, and the outer tank is indicated in magenta.

E.1. 7 Days

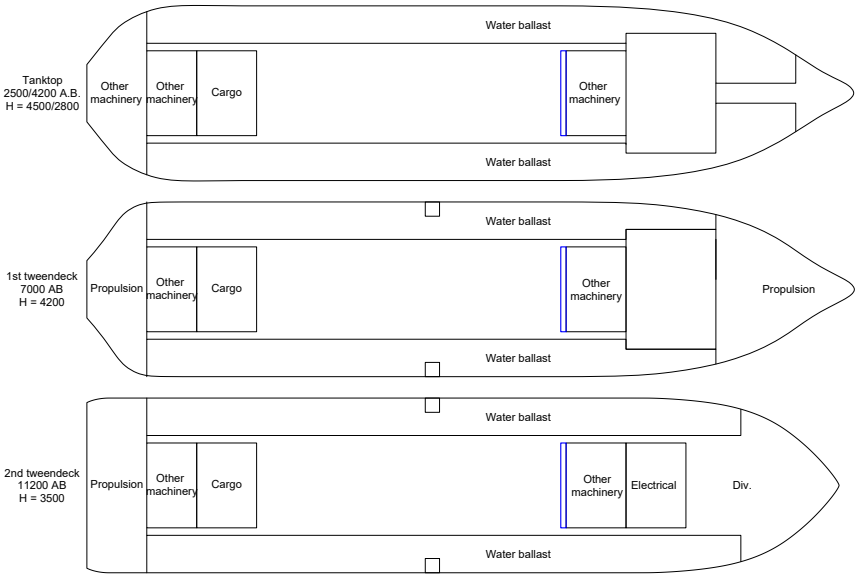

Figure E.2: MDO storage system for an autonomy of 7 days. The tank is indicated in blue.

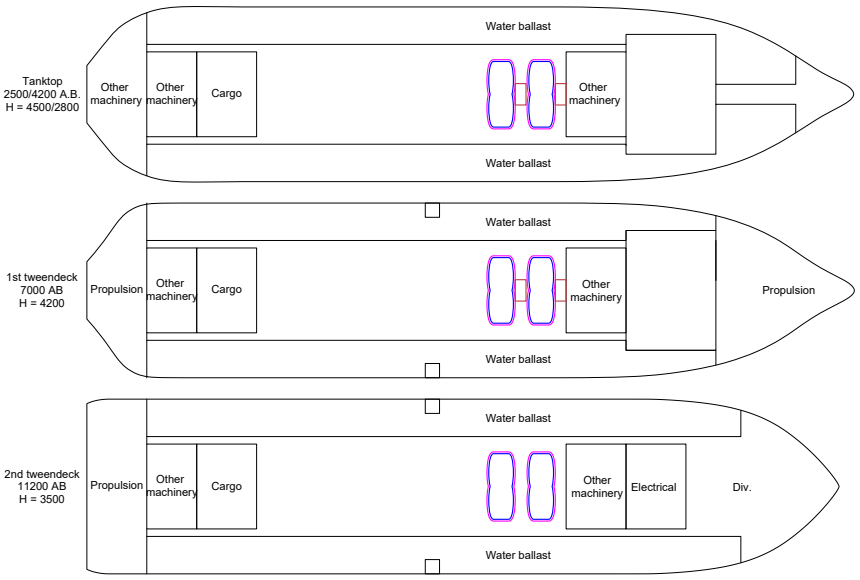

Figure E.3: LH2 storage system for an autonomy of 7 days. The inner tank is indicated in blue, the outer tank is indicated in magenta, the TCS is indicated in brown.

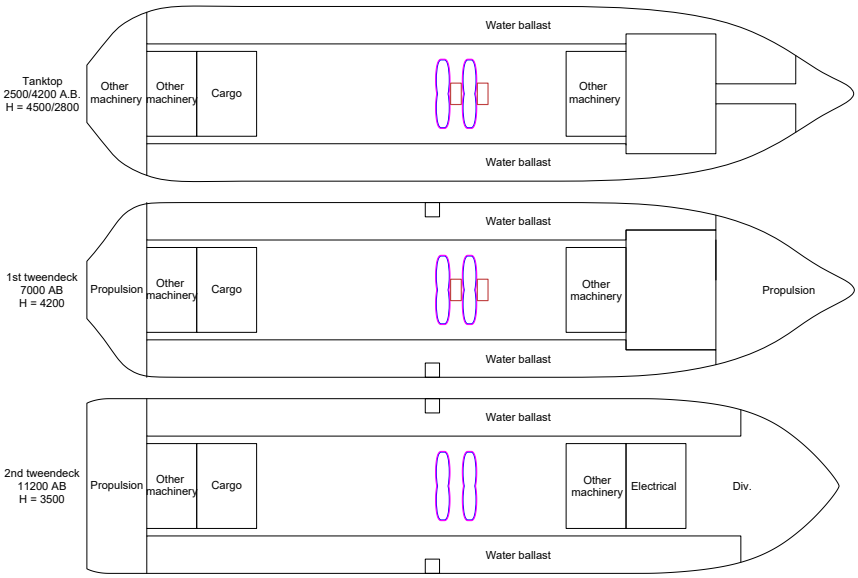

Figure E.4: NH3 storage system for an autonomy of 7 days. The inner tank is indicated in blue, the outer tank is indicated in magenta, the TCS is indicated in brown.

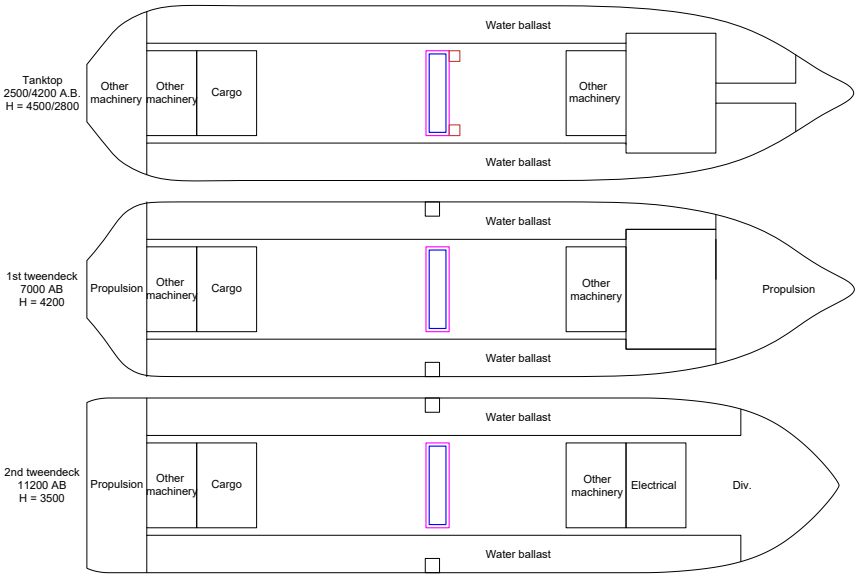

Figure E.5: CH3OH storage system for an autonomy of 7 days. The inner tank is indicated in blue, the outer shell of the cofferdam is indicated in magenta, the TCS is indicated in brown.

E.2. 14 Days

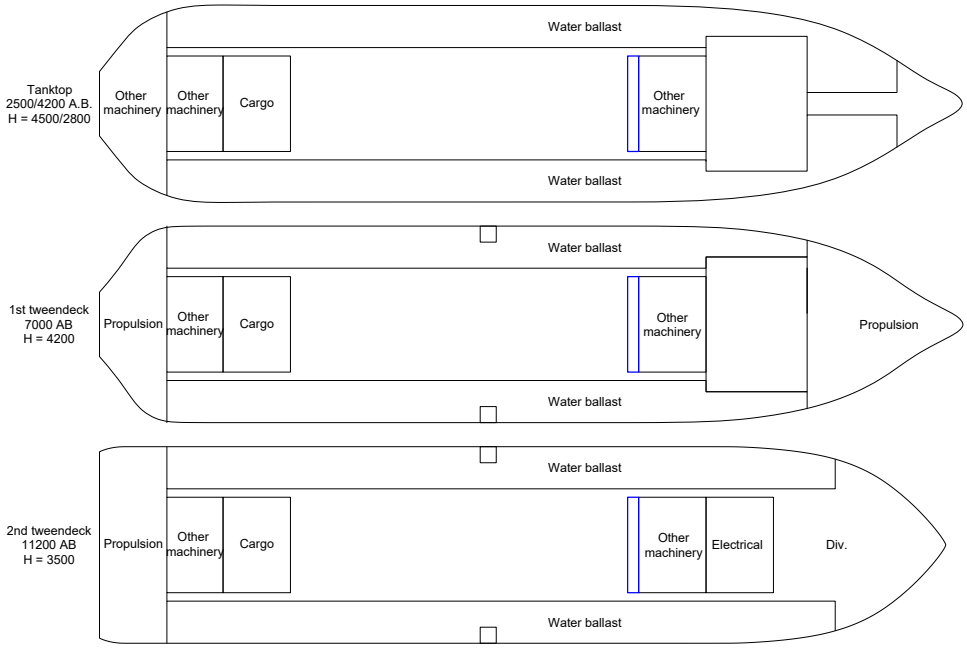

Figure E.6: MDO storage system for an autonomy of 14 days. The tank is indicated in blue.

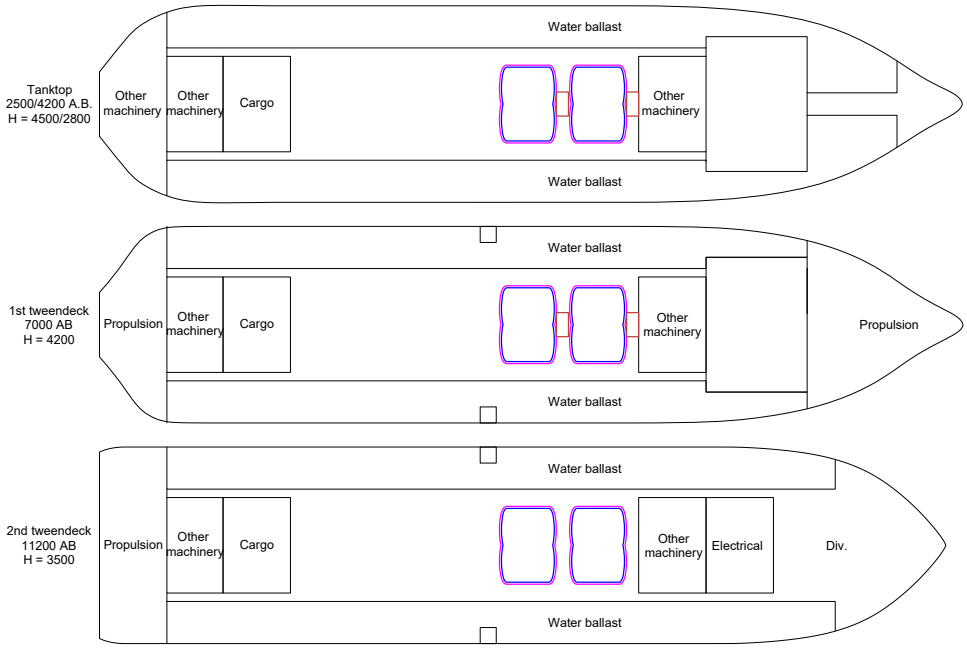

Figure E.7: LH2 storage system for an autonomy of 14 days. The inner tank is indicated in blue, the outer tank is indicated in magenta, the TCS is indicated in brown.

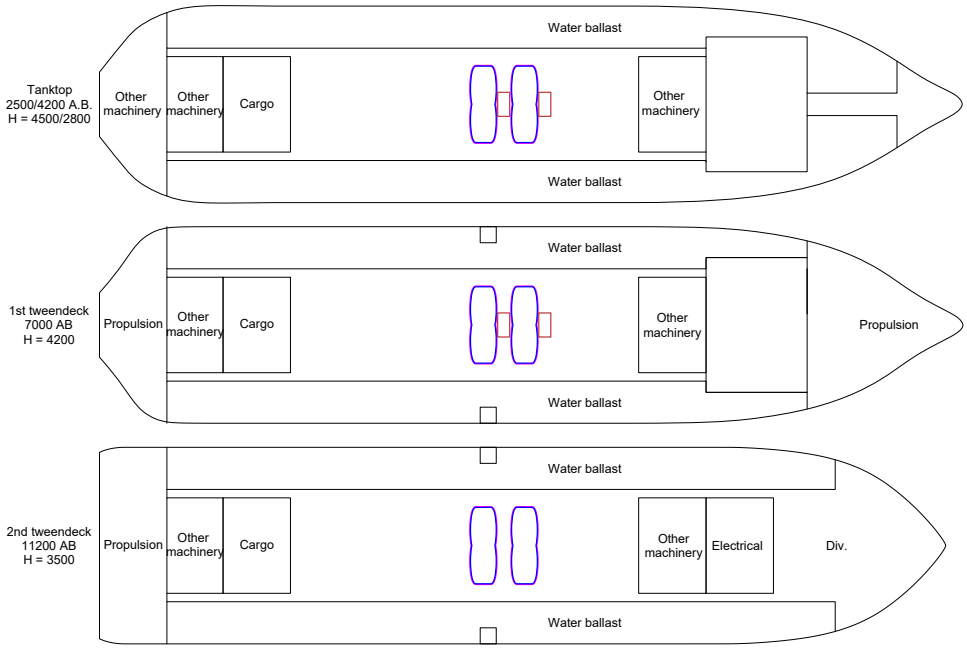

Figure E.8: NH3 storage system for an autonomy of 14 days. The inner tank is indicated in blue, the outer tank is indicated in magenta, the TCS is indicated in brown.

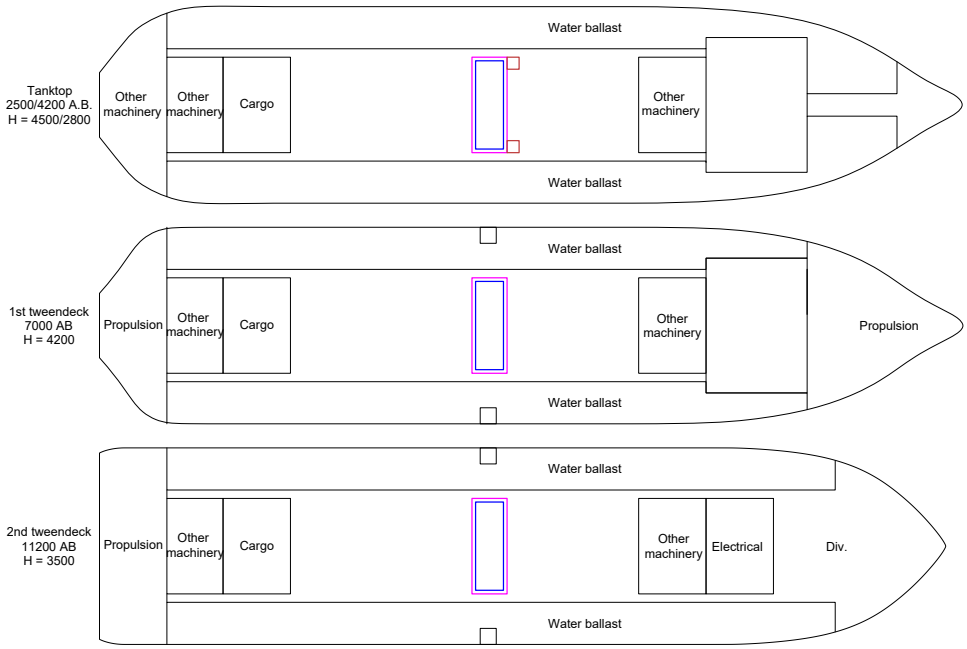

Figure E.9: CH3OH storage system for an autonomy of 14 days. The inner tank is indicated in blue, the outer shell of the cofferdam is indicated in magenta, the TCS is indicated in brown.

E.3. 21 Days

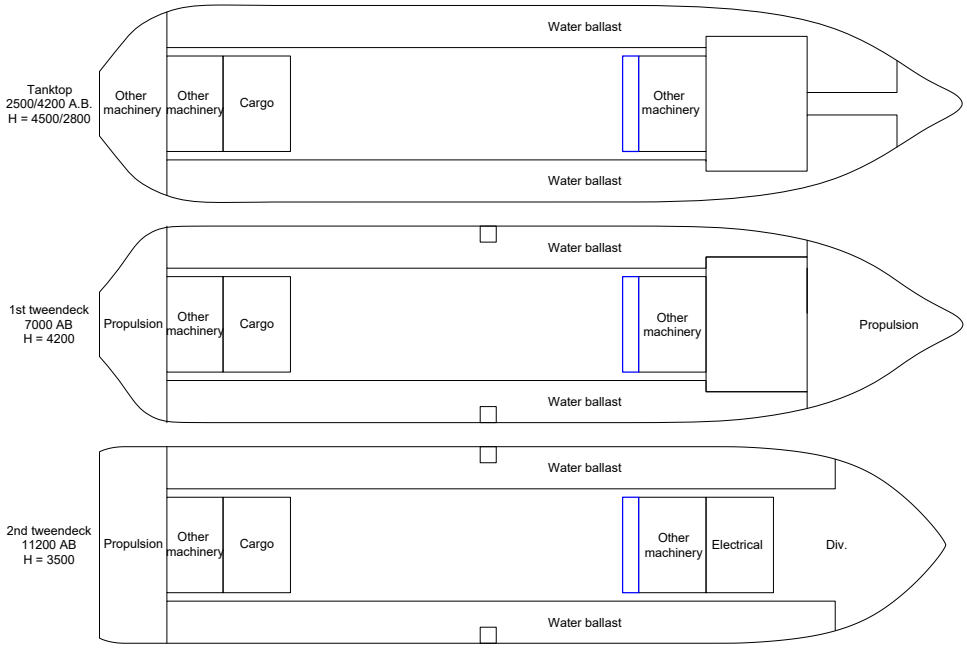

Figure E.10: MDO storage system for an autonomy of 21 days. The tank is indicated in blue.

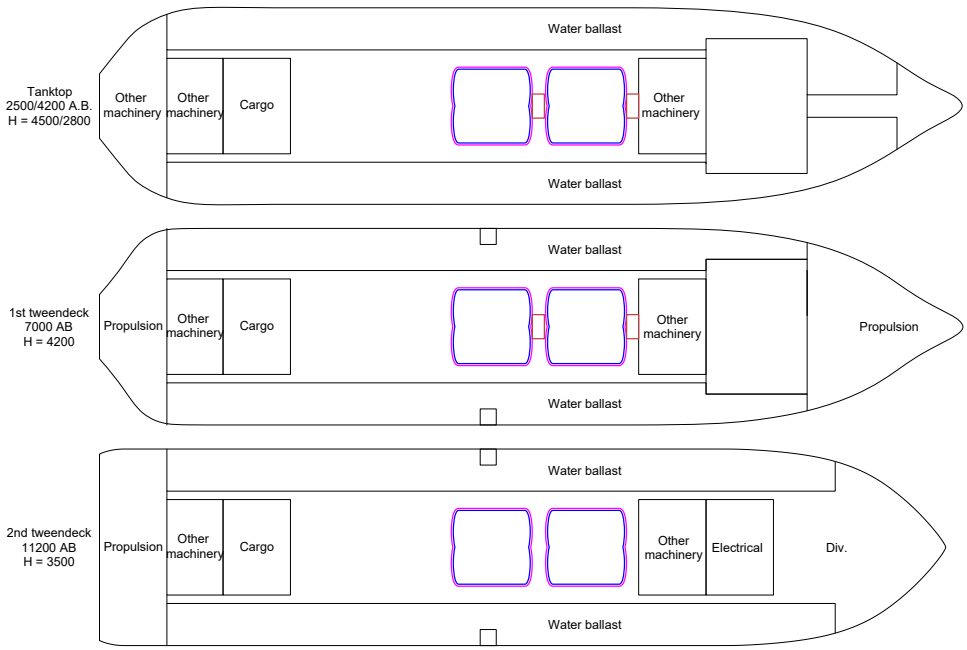

Figure E.11: LH2 storage system for an autonomy of 21 days. The inner tank is indicated in blue, the outer tank is indicated in magenta, the TCS is indicated in brown.

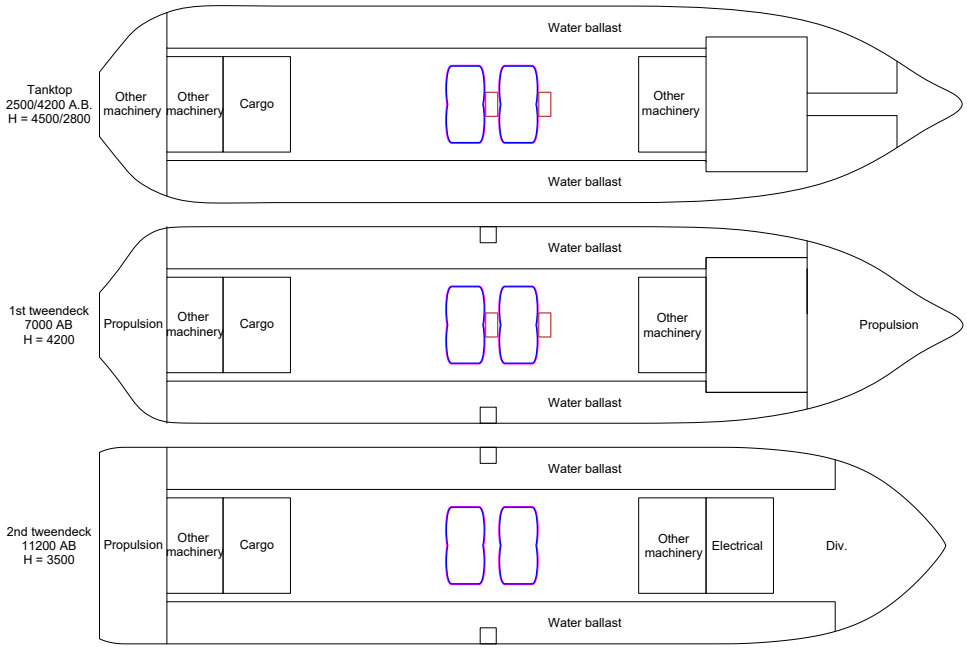

Figure E.12: NH3 storage system for an autonomy of 21 days. The inner tank is indicated in blue, the outer tank is indicated in magenta, the TCS is indicated in brown.

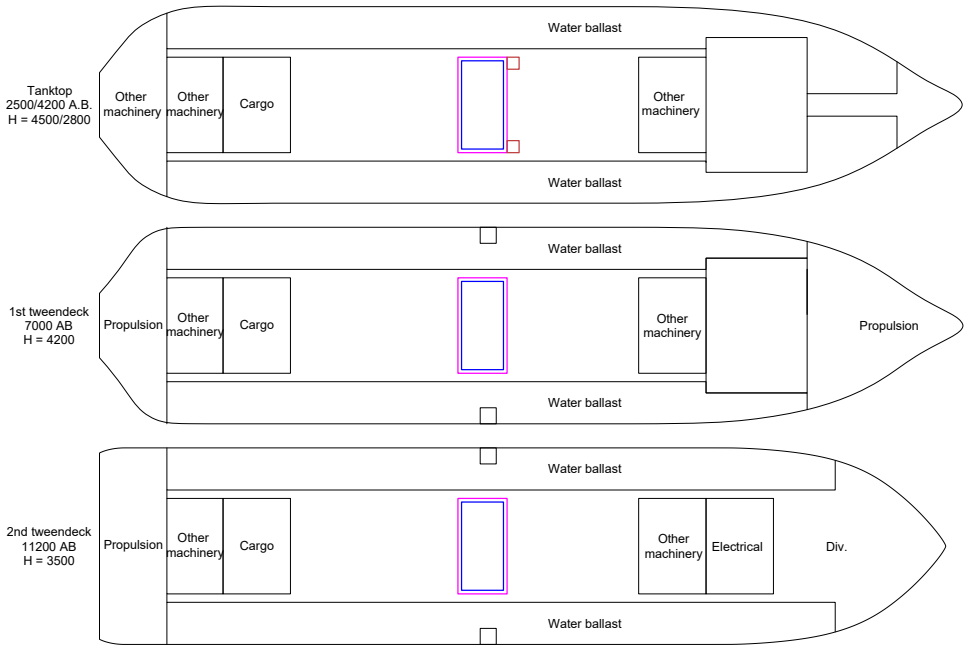

Figure E.13: CH3OH storage system for an autonomy of 21 days. The inner tank is indicated in blue, the outer shell of the cofferdam is indicated in magenta, the TCS is indicated in brown.

E.4. 28 Days

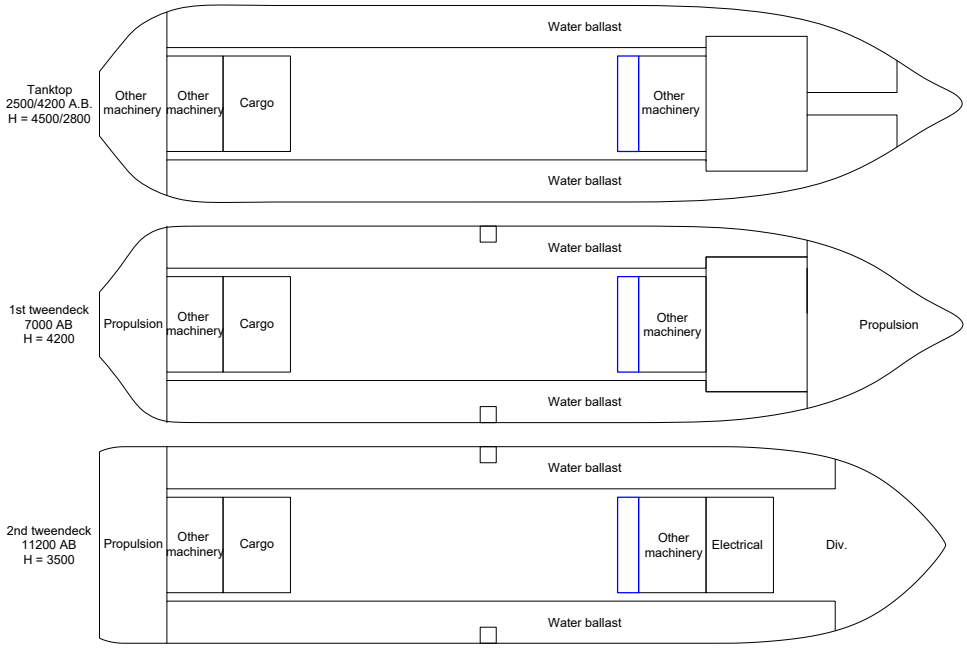

Figure E.14: MDO storage system for an autonomy of 28 days. The tank is indicated in blue.

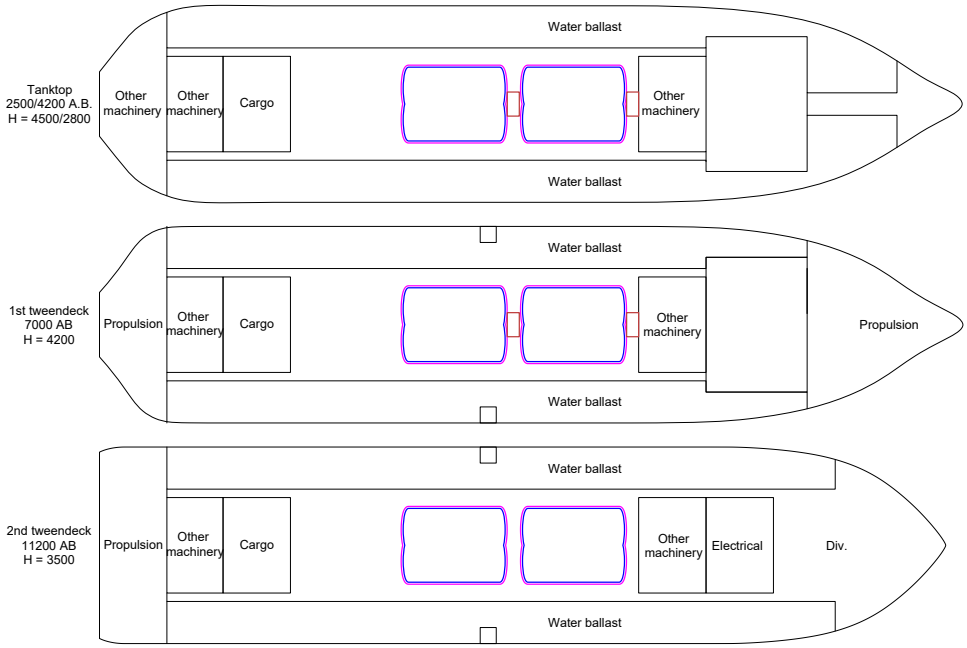

Figure E.15: LH2 storage system for an autonomy of 28 days. The inner tank is indicated in blue, the outer tank is indicated in magenta, the TCS is indicated in brown.

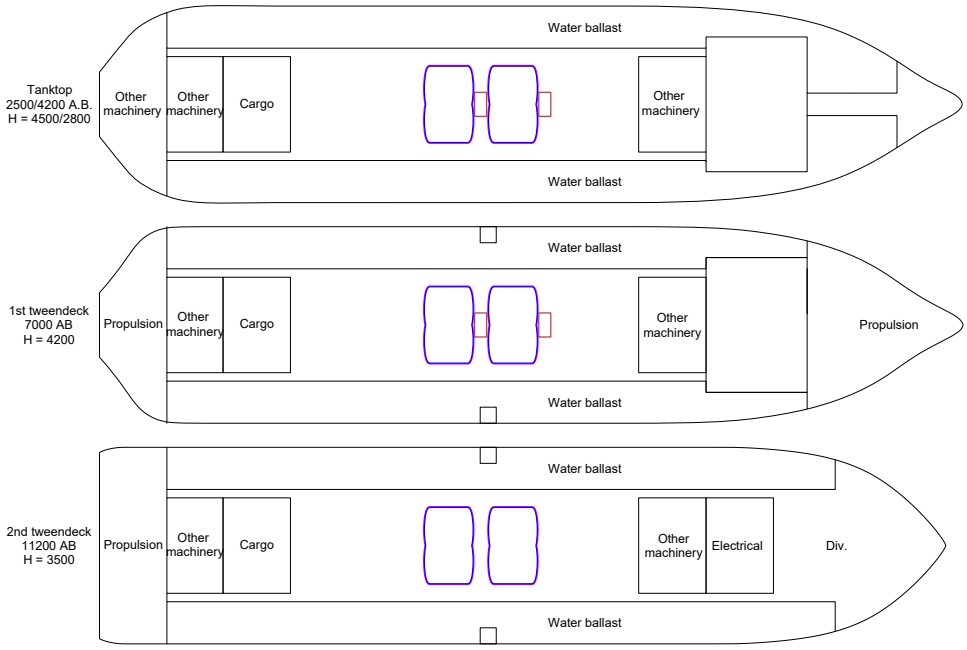

Figure E.16: NH3 storage system for an autonomy of 28 days. The inner tank is indicated in blue, the outer tank is indicated in magenta, the TCS is indicated in brown.

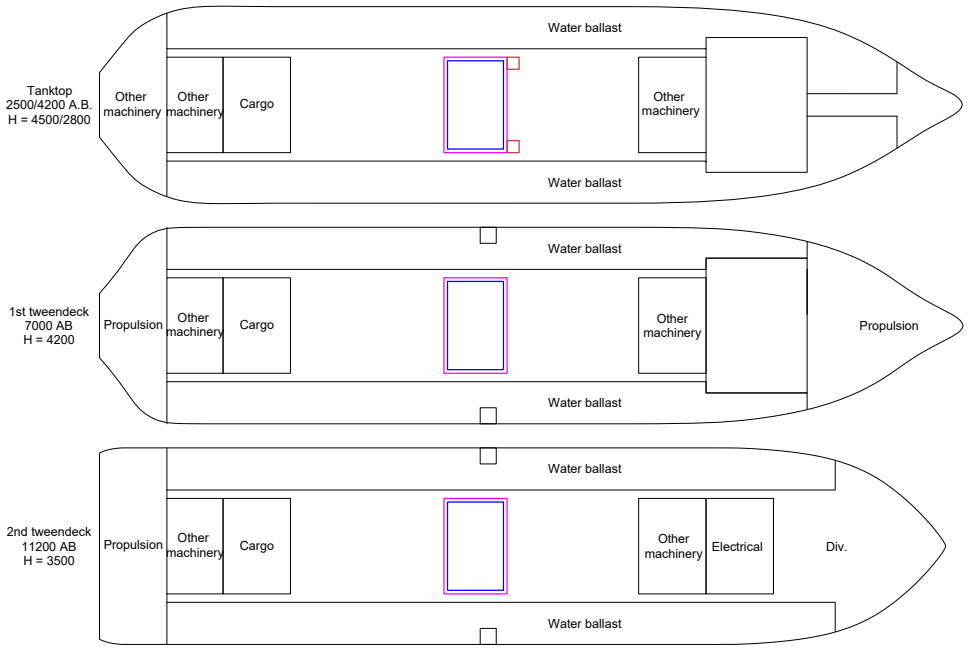

Figure E.17: CH3OH storage system for an autonomy of 28 days. The inner tank is indicated in blue, the outer shell of the cofferdam is indicated in magenta, the TCS is indicated in brown.

E.5. 35 Days

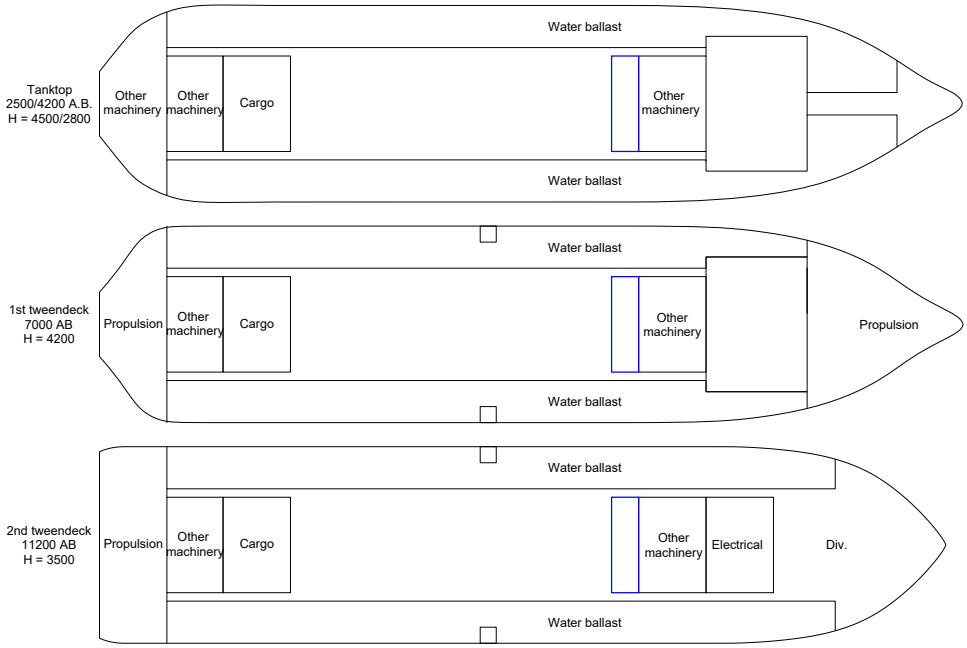

Figure E.18: MDO storage system for an autonomy of 35 days. The tank is indicated in blue.

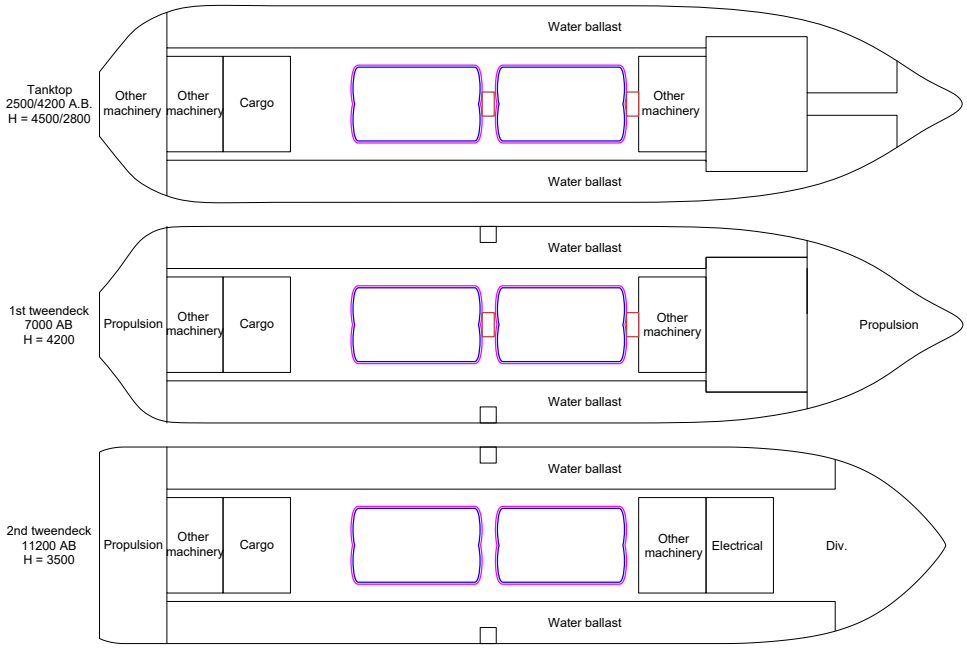

Figure E.19: LH2 storage system for an autonomy of 35 days. The inner tank is indicated in blue, the outer tank is indicated in magenta, the TCS is indicated in brown.

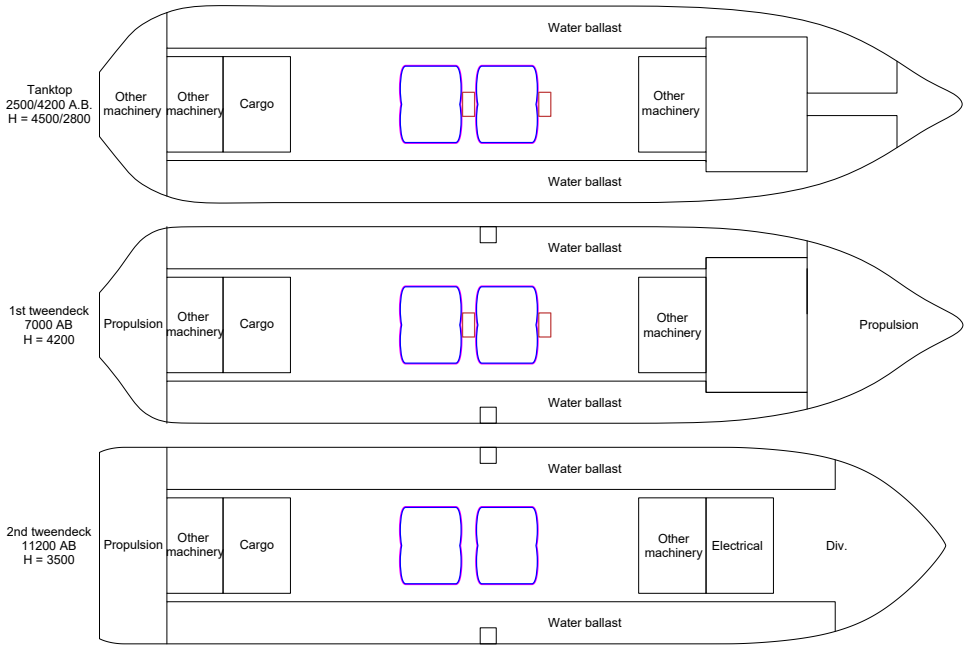

Figure E.20: NH3 storage system for an autonomy of 35 days. The inner tank is indicated in blue, the outer tank is indicated in magenta, the TCS is indicated in brown.

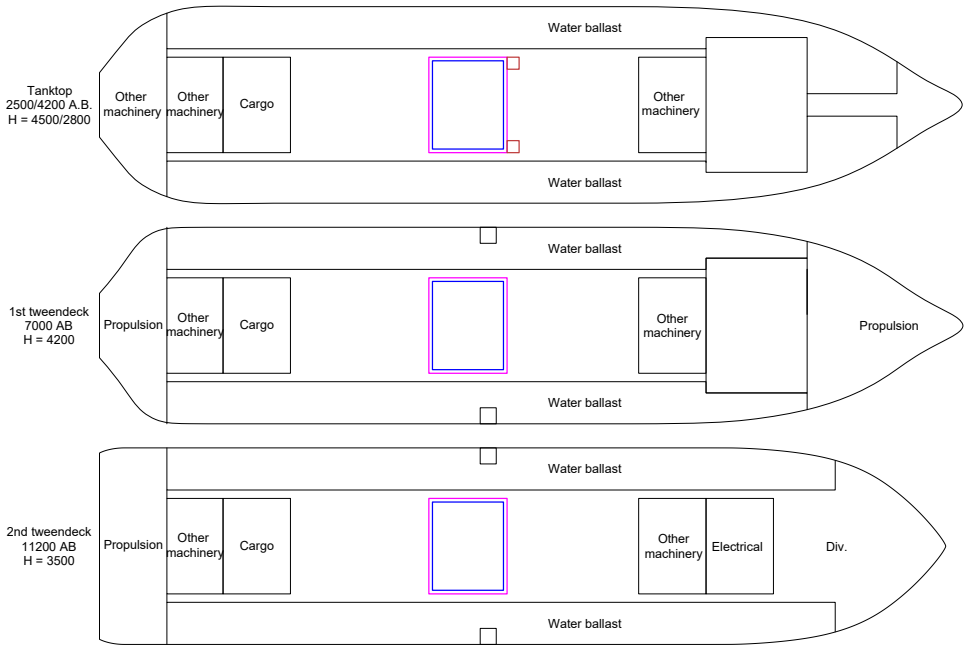

Figure E.21: CH3OH storage system for an autonomy of 35 days. The inner tank is indicated in blue, the outer shell of the cofferdam is indicated in magenta, the TCS is indicated in brown.

F

Routing of Piping & Ducting

F.1. Process Flow Diagram

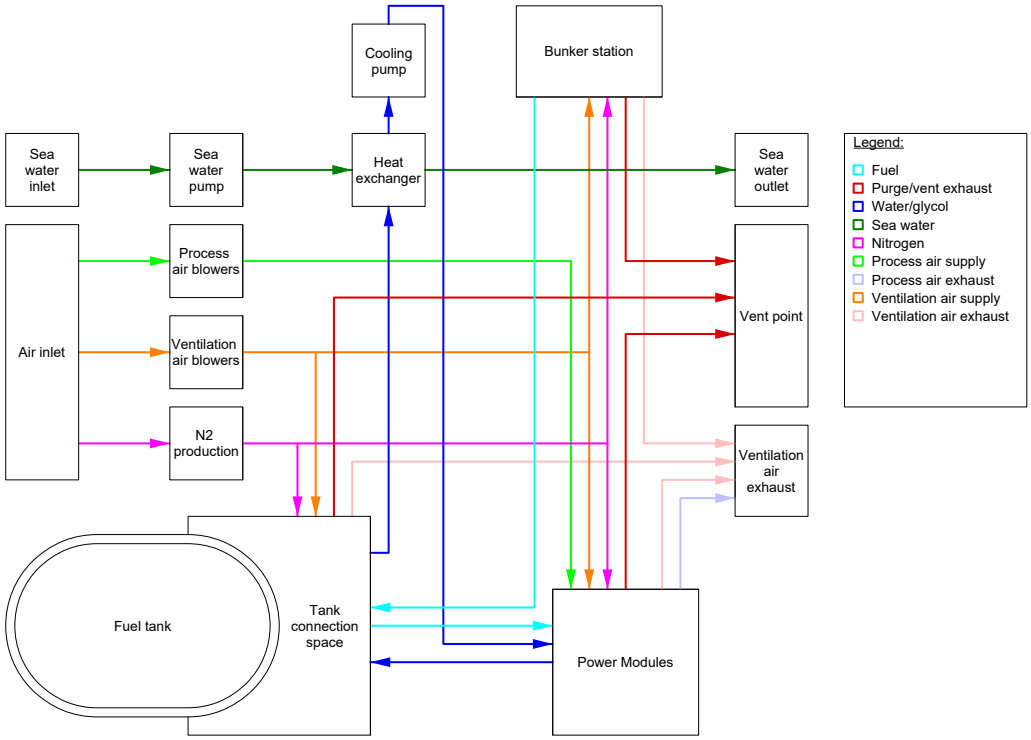

Figure F.1: Piping and instrumentation diagram showing the connections between various components onboard the vessel.

F.2. LH2 Routing

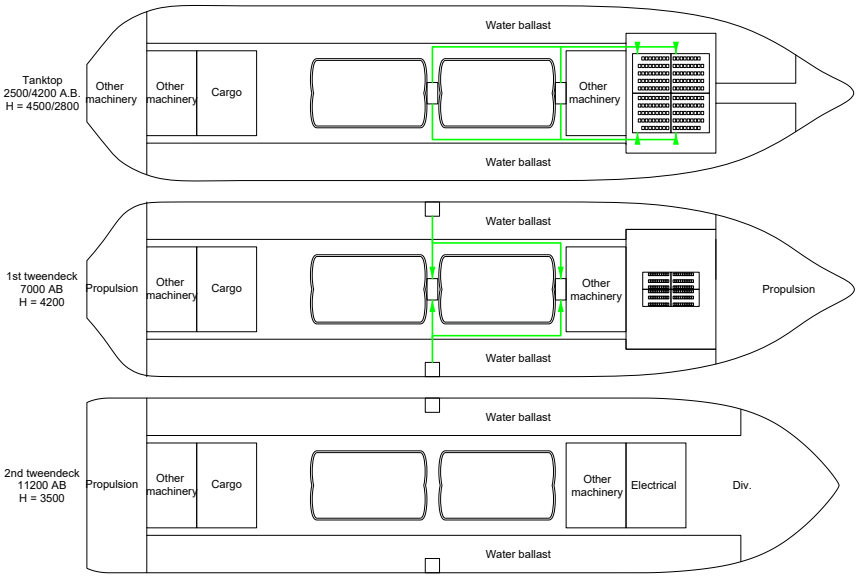

Figure F.2: Diagram showing the routing of fuel lines within the vessel for the LH2 case.

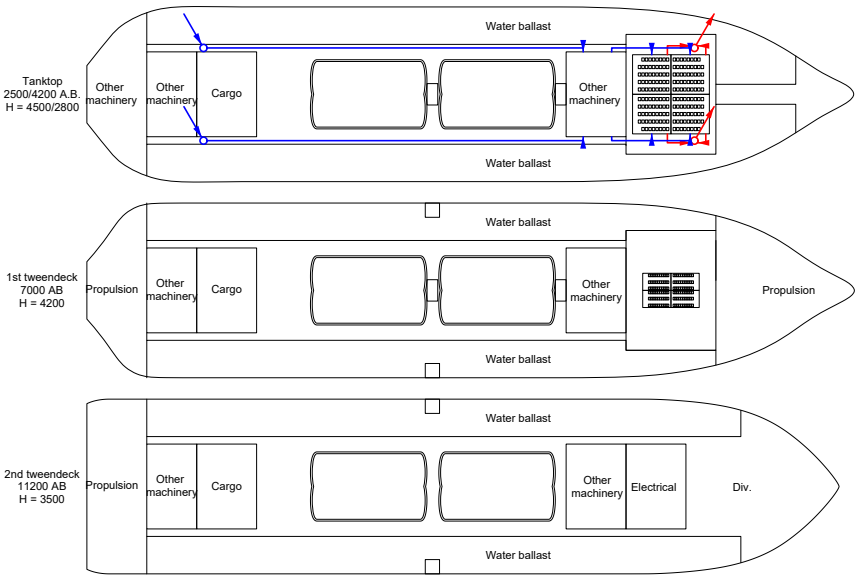

Figure F.3: Diagram showing the routing of process air ducts within the vessel for the LH2 case. Process air supply is indicated in blue; process air exhausts are indicated in red.

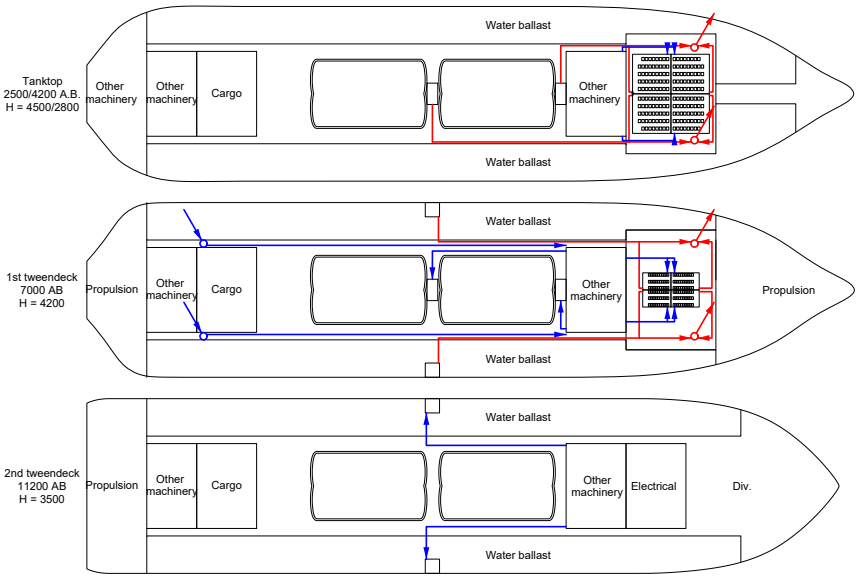

Figure F.4: Diagram showing the routing of ventilation air ducts within the vessel for the LH2 case. Process air supply is indicated in blue; process air exhausts are indicated in red.

F.3. NH3 Routing

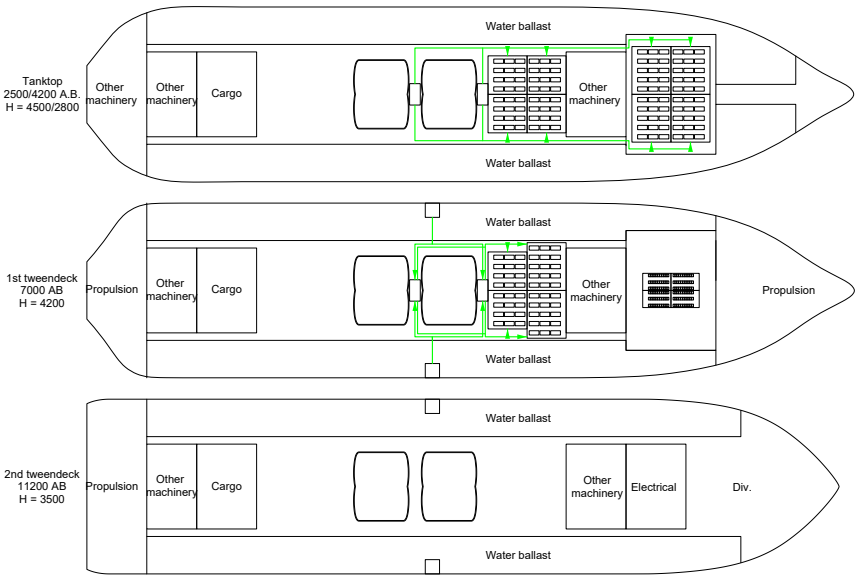

Figure F.5: Diagram showing the routing of fuel lines within the vessel for the NH3 case.

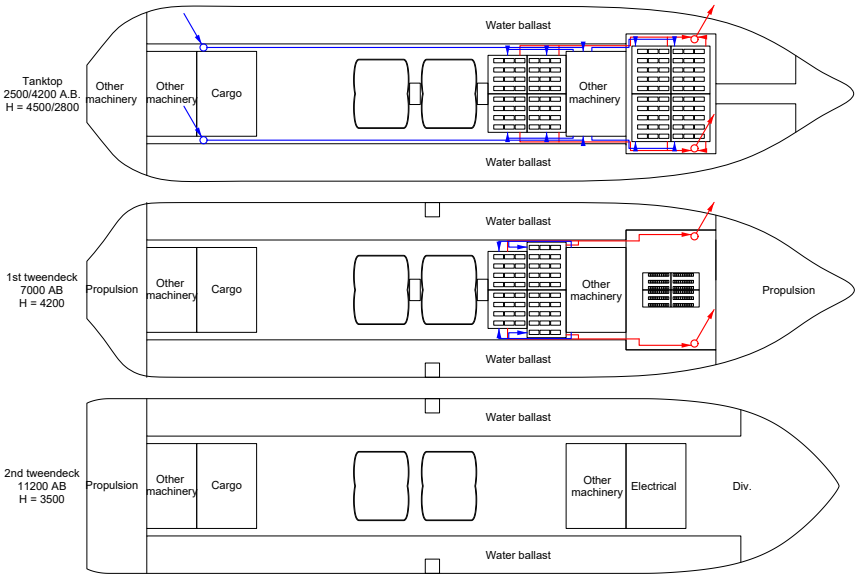

Figure F.6: Diagram showing the routing of process air ducts within the vessel for the NH3 case. Process air supply is indicated in blue; process air exhausts are indicated in red.

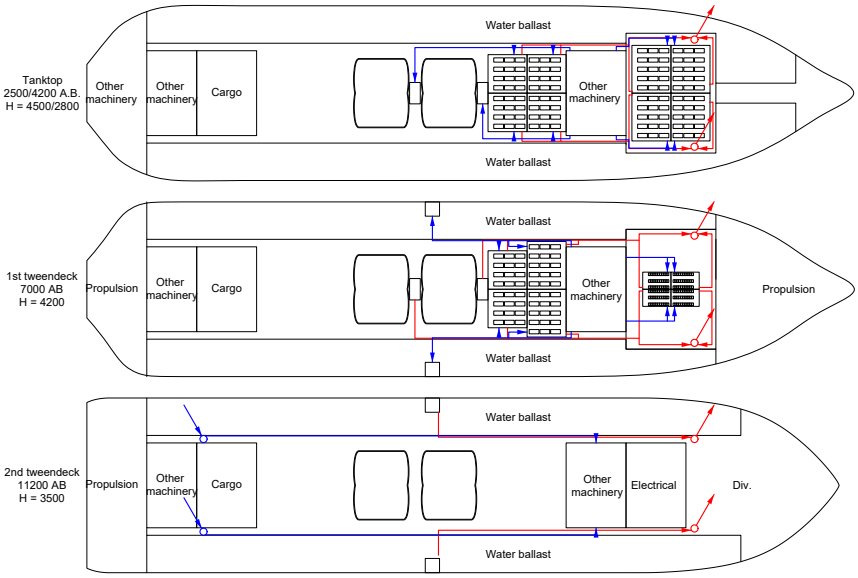

Figure F.7: Diagram showing the routing of ventilation air ducts within the vessel for the NH3 case. Process air supply is indicated in blue; process air exhausts are indicated in red.

F.4. CH3OH Routing

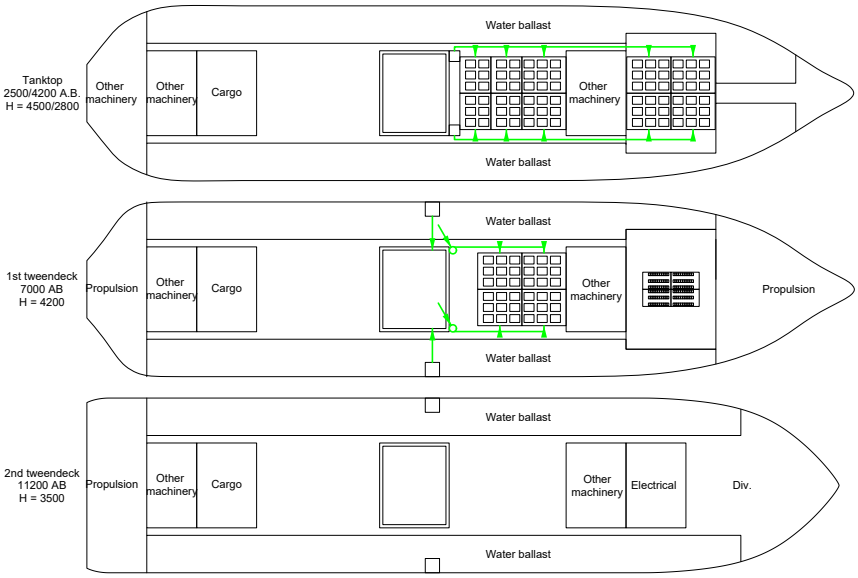

Figure F.8: Diagram showing the routing of fuel lines within the vessel for the CH3OH case.

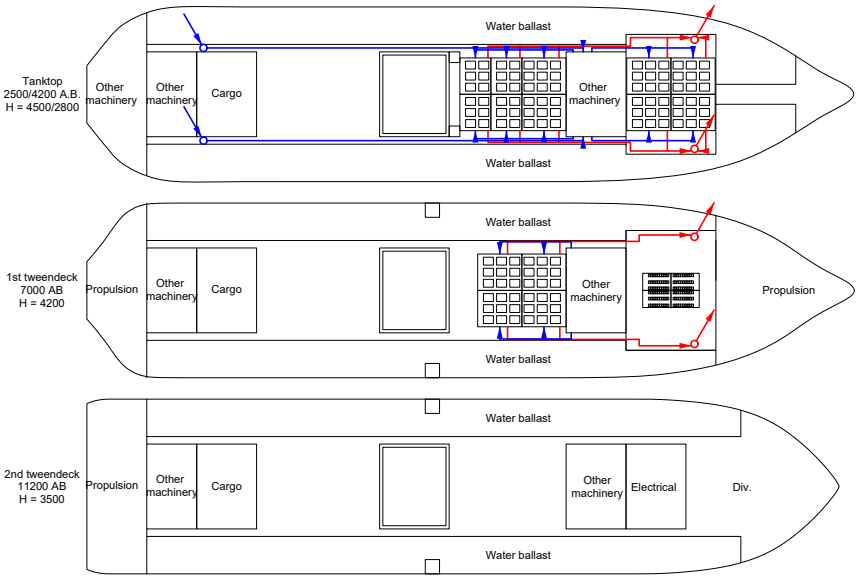

Figure F.9: Diagram showing the routing of process air ducts within the vessel for the CH3OH case. Process air supply is indicated in blue; process air exhausts are indicated in red.

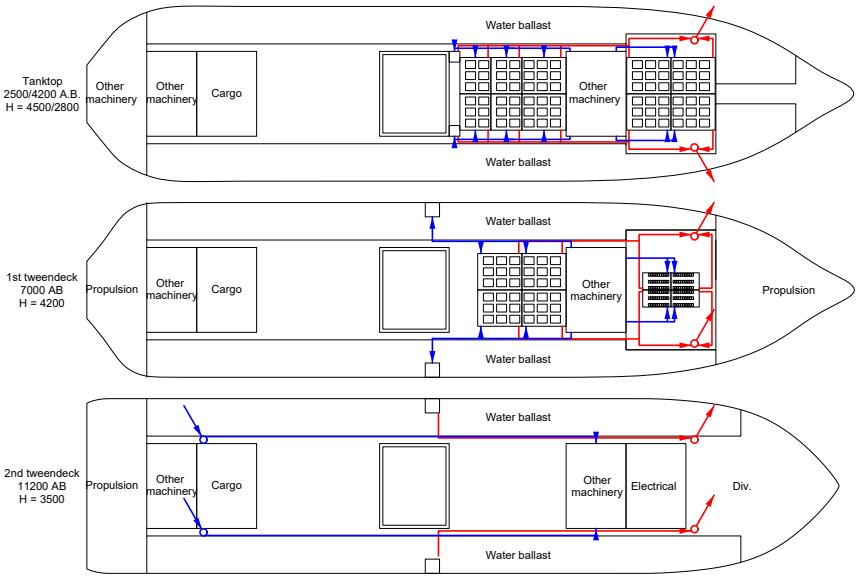

Figure F.10: Diagram showing the routing of ventilation air ducts within the vessel for the CH3OH case. Process air supply is indicated in blue; process air exhausts are indicated in red.

G

Energy Storage System Energy Densities

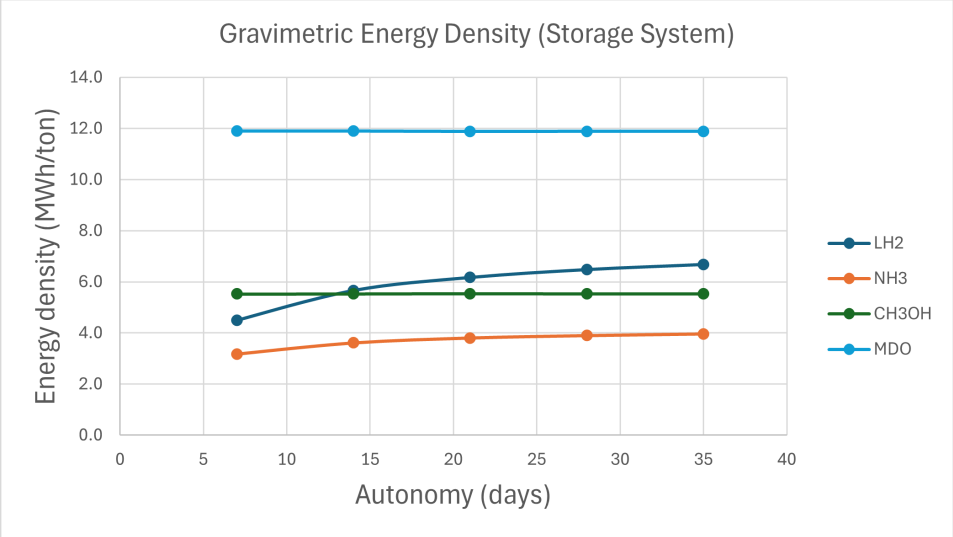

Figure G.1: Energy storage system gravimetric energy density per fuel and autonomy.

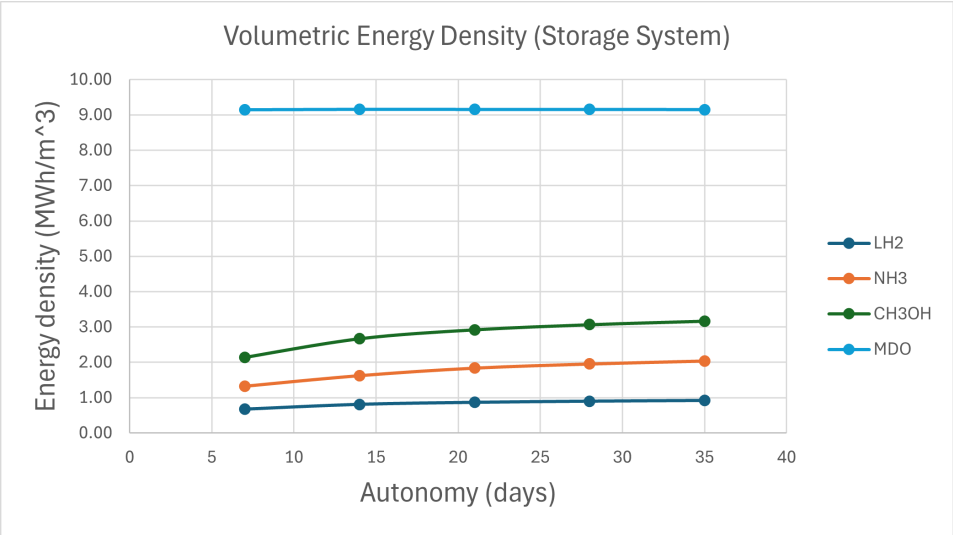

Figure G.2: Energy storage system volumetric energy density per fuel and autonomy.

H

Data for Calculations

The values listed below are used for all calculations in this thesis.

Quantity	Value	Unit
ρ_{air}	1.225	kg/m^3
ρ_{SW}	1025	kg/m^3
ρ_{FW}	1000	kg/m^3
$\rho_{N2,gas}$	1.2506	kg/m^3
ρ_{LH2}	71	kg/m^3
$\rho_{NH3,liq}$	682.8	kg/m^3
ρ_{CH3OH}	792	kg/m^3
ρ_{LNG}	428	kg/m^3
ρ_{MDO}	855	kg/m^3
$\rho_{deionizedwater}$	998.23	kg/m^3
ρ_{steel}	8000	kg/m^3
H2 PM efficiency	0.48	-
NH3 PM efficiency	0.4065	-
CH3OH PM efficiency	0.4	-
MDO ICE efficiency	0.4	-
$c_{p,air}$	1.006	$kJ/(kg \cdot K)$
$c_{p,SW}$	4.007	$kJ/(kg \cdot K)$
$c_{p,FW}$	4.194	$kJ/(kg \cdot K)$
$c_{p,N2}$	1.042	$kJ/(kg \cdot K)$
γ_{air}	1.4	-
γ_{N2}	1.4	-
$T_{air,outside}$	35	°C
$T_{SW,inlet}$	30	°C
$T_{SW,outlet}$	40	°C
$T_{coolant,H}$	65	°C
$T_{coolant,C}$	45	°C
air fraction N2	0.78	-
air fraction O2	0.21	-
molar mass H2	2.016	g/mol
molar mass O2	31.999	g/mol
LHV H2	120	MJ/kg
LHV NH3	18.6	MJ/kg
LHV CH3OH	19.9	MJ/kg
LHV LNG	48.6	MJ/kg
LHV LFO	42.8	MJ/kg

Quantity	Value	Unit
η_{DC-DC}	0.98	-
η_{bus}	0.98	-
η_{inv}	0.97	-
η_{batt}	0.97	-
η_{blower}	0.6305	-
η_{pump}	0.6305	-
$\eta_{is,comp}$	0.75	-
η_{comp}	0.1	-
LH2 tank insulation thickness	0.5	m
NH3 tank insulation thickness	0.18	m
cofferdam thickness	0.9	m
LH2 tank steel tickness	0.02	m
NH3 tank steel tickness	0.02	m
space margin tank top side	0.5	m
space margin tank bottom	0.1	m
space margin tank sides	0.3	m
H2 PM width	0.73	m
NH3 PM width	2.75	m
CH3OH PM width	2.8	m
H2 PM depth	0.9	m
NH3 PM depth	1.2	m
CH3OH PM depth	2.2	m
H2 PM height	2.2	m
NH3 PM height	2.2	m
CH3OH PM height	2.3	m
piping diameter	0.2	m
flow rate air	8	m/s
flow rate process air	5	m/s
flow rate water	2.5	m/s
flow rate fuel	2.5	m/s
$P_{gross,PM,H2}$	200	kW
$P_{gross,PM,NH3}$	200	kW
$P_{gross,PM,CH3OH}$	250	kW
$P_{cons,PM,H2}$	5	kW
$P_{cons,PM,NH3}$	30	kW
$P_{cons,PM,CH3OH}$	4	kW
$P_{cons,batt}$	0.5	kW
$P_{cons,DC-DC}$	0.48	kW
E_{batt}	86	kWh
battery C-rate charging	3	-
battery C-rate discharging	3	-
$\zeta_{ventilation,air}$	35	-
$\zeta_{process,air}$	100	-
ζ_{CW}	40	-
ζ_{SW}	30	-
$\zeta_{fuel,NH3}$	100	-
$\zeta_{fuel,CH3OH}$	100	-
$\zeta_{fuel,LFO}$	100	-
$\zeta_{deionized,water}$	100	-
battery heat output	0.45	kW
DC-DC converter heat output	5.8	kW
n batteries installed	132	-
n batteries operational	99	-

Quantity	Value	Unit
autonomy	35	days
purging volume LH2 PM	0.39	m^3
purging volume NH3 PM	0.39	m^3
purging volume CH3OH PM	0.39	m^3
purging volume vent mast	2.20	m^3
purging volume piping	31.42	m^3
overcapacity N2 production	0.2	-
pressure ratio air compressor	3.5	-
pressure ratio N2 compressor #1	3	-
pressure ratio N2 compressor #2	3.5	-